Mem. R. astr. Soc. (1977) **84**, 61–99

Observations of 104 extragalactic radio sources with the Cambridge 5-km telescope at 5 GHz

C. J. Jenkins, G. G. Pooley and J. M. Riley *Mullard Radio Astronomy Observatory, Cavendish Laboratory, Cambridge CB3 0HE*

Received 1976 December 7

Summary. One hundred and four radio sources from the 3C and 4C catalogues have been mapped with a resolution of 2 arcsec in RA and 2 cosec δ arcsec in dec. The results are presented here as contour maps and in tabular form, with accurate measurements of the positions of optical objects in the fields.

1 Introduction

We present the results of observations with the 5-km telescope (Ryle 1972) of 104 extragalactic radio sources at 5 GHz. These form part of a continuing study of such objects at the Mullard Radio Astronomy Observatory. Most of the sources described here are in the 3CR catalogue and make up part of a complete sample of 3CR sources all but one of which have now been observed with the 5-km telescope at 5 GHz; the constitution of the complete sample is discussed in Section 5. Eight 4C sources are also included, six of which are identified with quasars of redshift greater than 1.5 in the sample of Lynds & Wills (1972). The positions of the optical objects associated with or in the fields of all these sources have been measured from the prints of the National Geographic Society–Palomar Observatory Sky Survey (PSS prints) to an accuracy better than 0.75 arcsec.

2 The observations

The observing technique was essentially that described by Pooley & Henbest (1974) with the modifications discussed by Riley & Pooley (1976). Each source has been mapped with a resolution of 2 arcsec in RA and 2 cosec δ arcsec in dec; for a map with n 12-hr observations, that is $16n$ ($=N$) interferometer spacings, the first grating response of the instrument is an ellipse of semi-axes ($42n$) arcsec in RA and ($42n$ cosec δ) arcsec in dec. For accurate mapping of the large-scale structure, the overall angular size of a source should not exceed about half this value; there are several cases in which this condition is not satisfied and the largescale structure should then be derived from the lower resolution maps to be found in Macdonald, Kenderdine & Neville (1968, hereafter MKN), Mackay (1969) and Branson *et al.* (1972, hereafter BEPR). The noise level on the maps is about $3n^{-1/2}$ mJy, and the flux density scale is based on an assumed value of 8.2 Jy for 3C 147.

3 The results

The results are presented as contour maps in Figs 1–26 and in Table 1; 1950.0 coordinates are used throughout. As the observations were made with feeds having the E vector in pa 90°, each contour map represents the distribution of the Stokes parameters $I–Q$ across the source; it has been found by Pooley & Henbest (1974) that the polarization seldom exceeds 10 per cent in such sources so that an $I–Q$ map is, in general, a reasonable representation of the distribution of the total intensity I. Each map is plotted with equal scales in RA and dec,

Plate 1

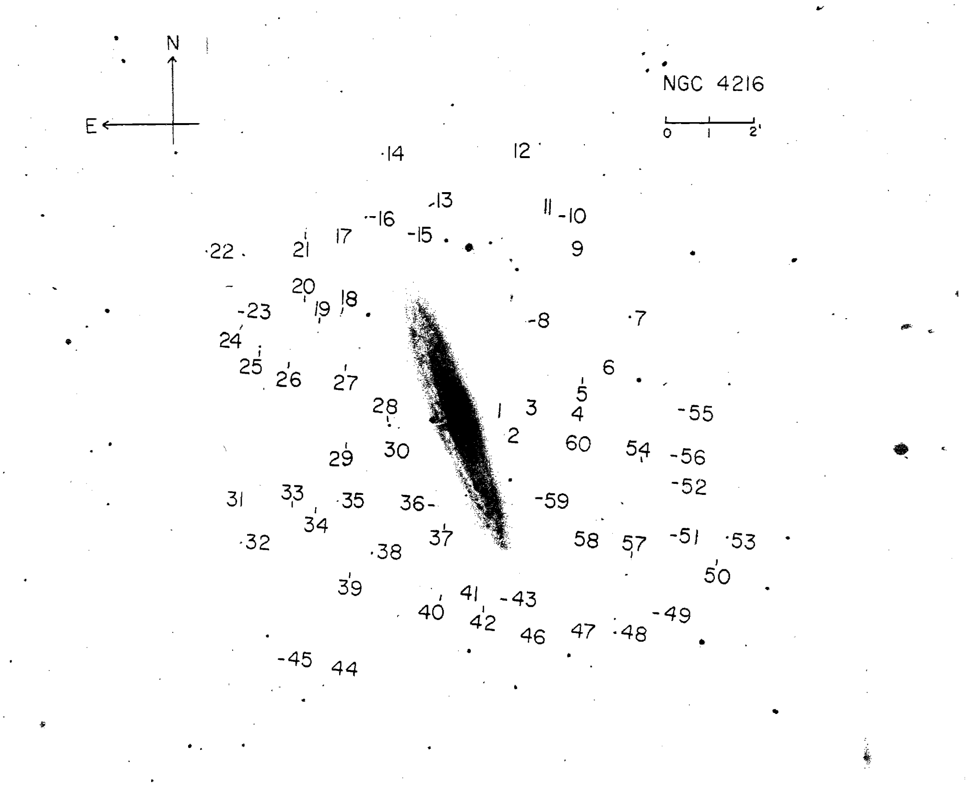

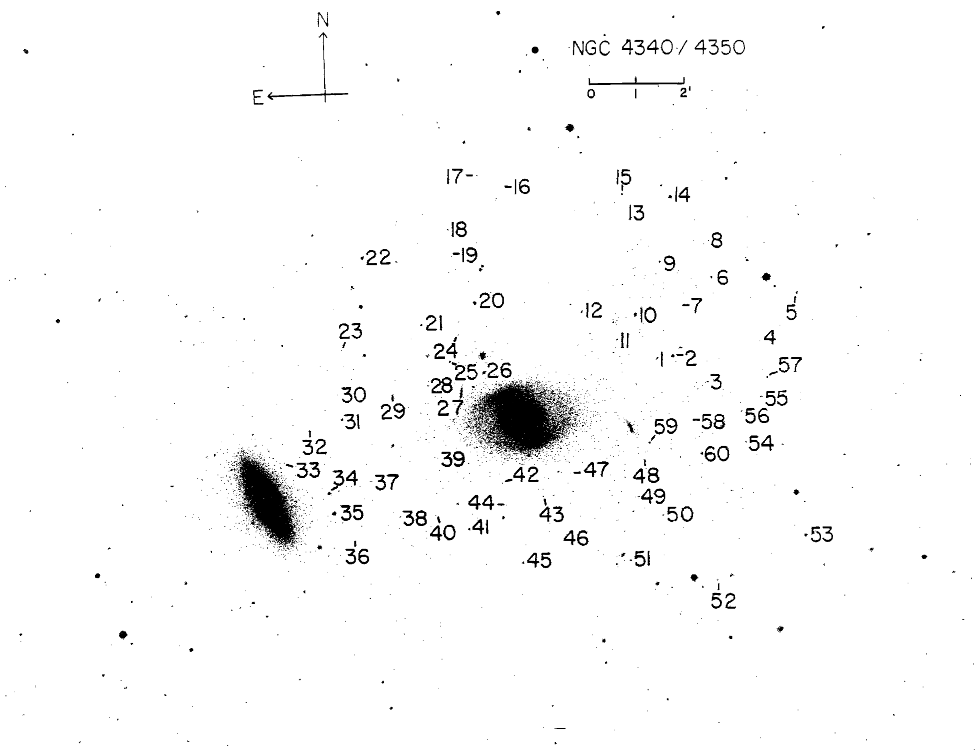

Plate 2

Plate 1

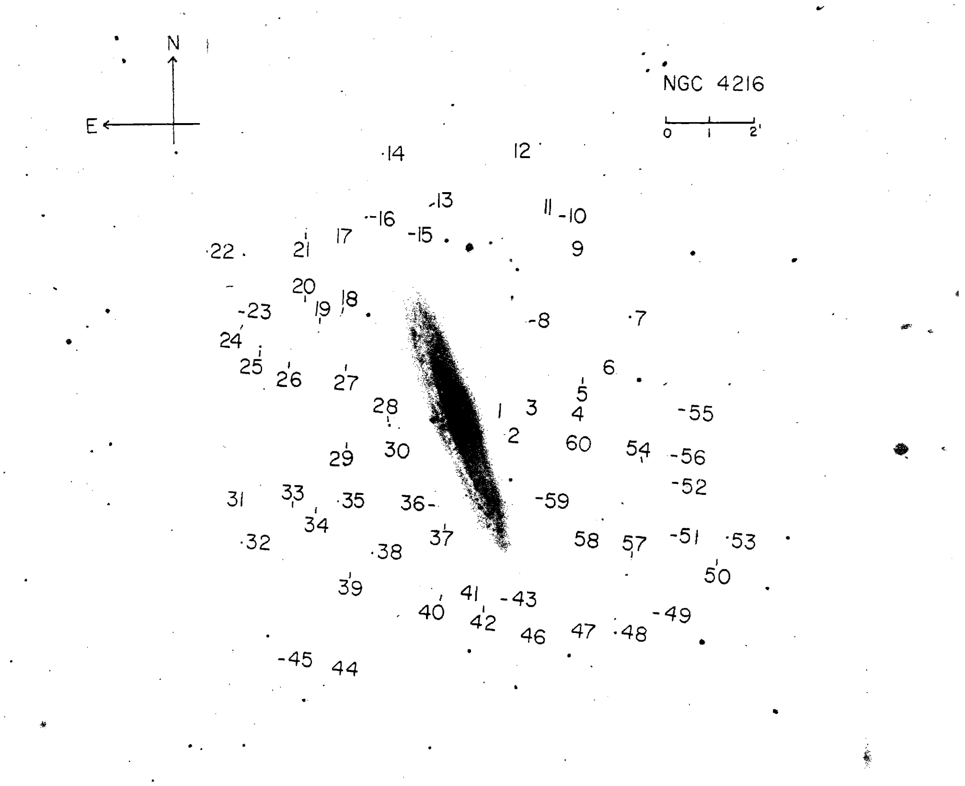

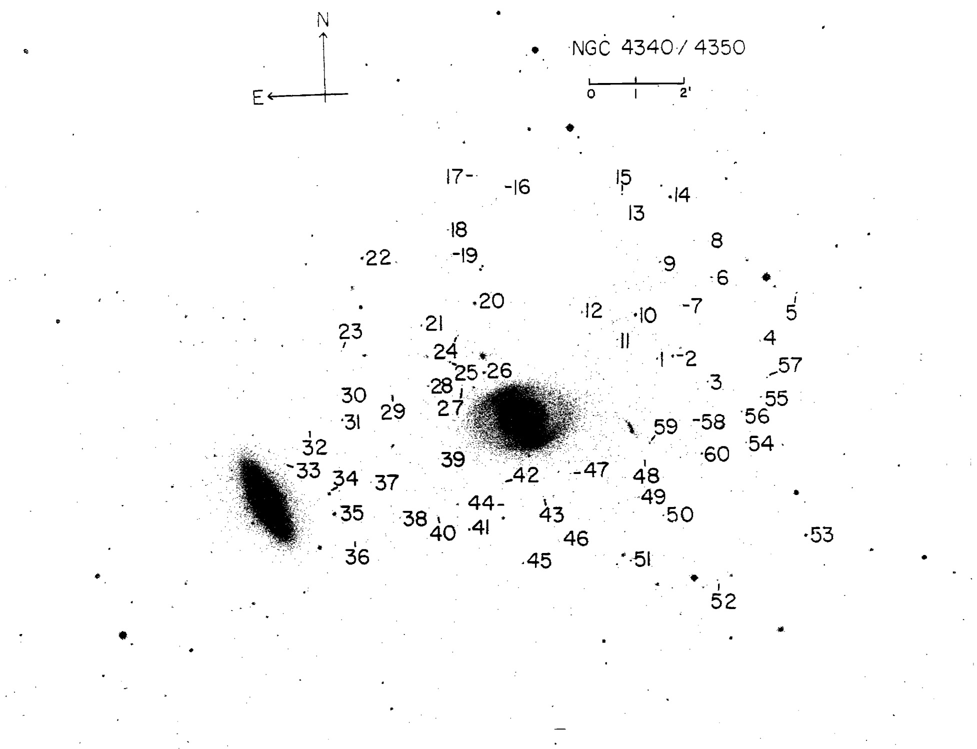

Plate 2

Plate 3

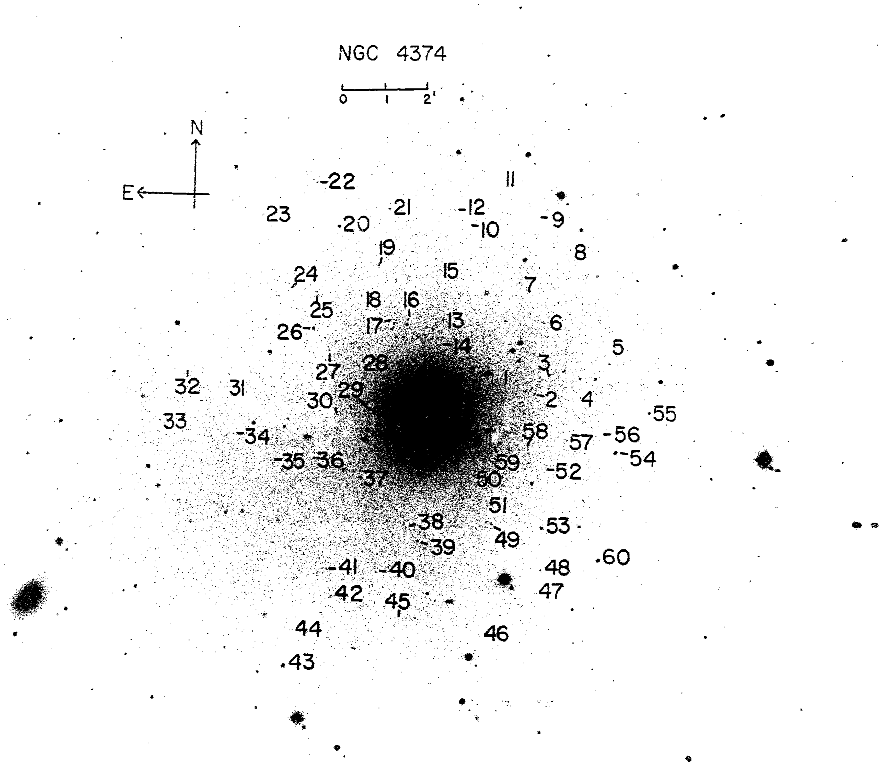

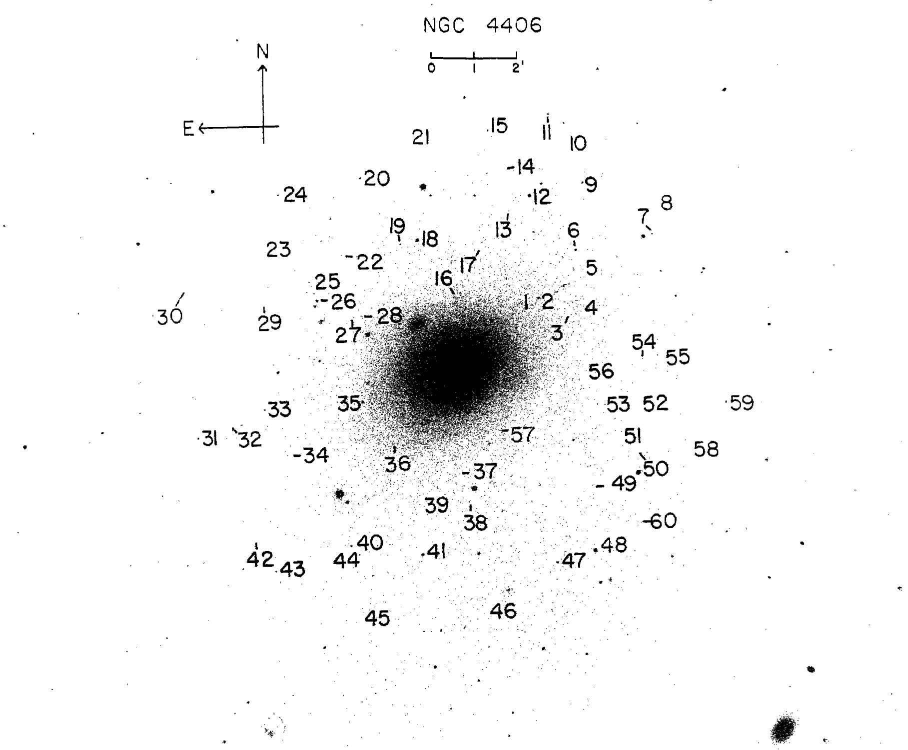

Plate 4

Plate 3

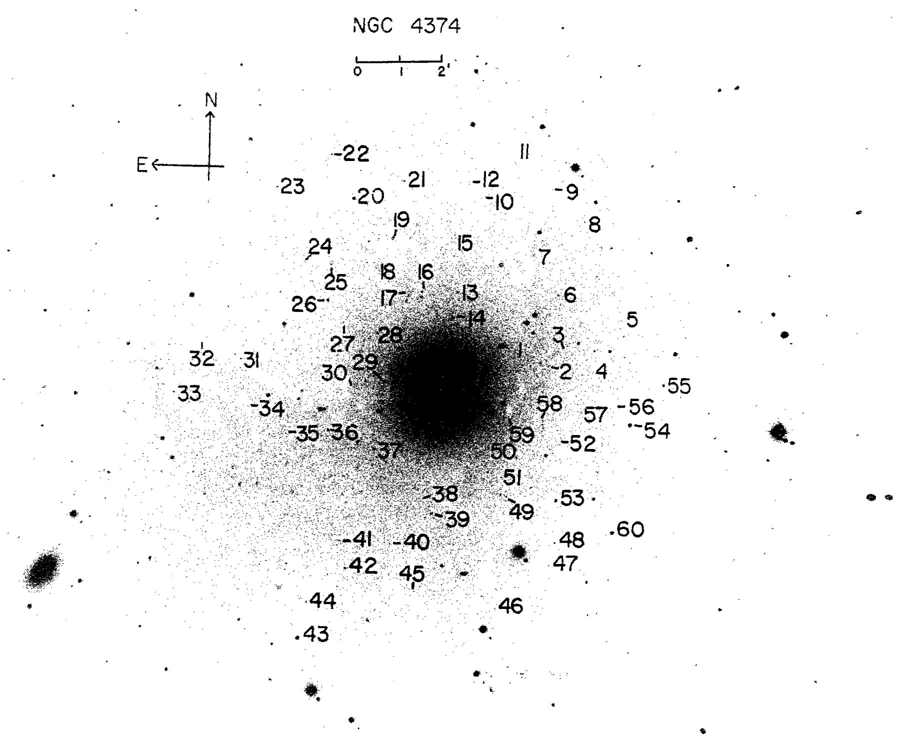

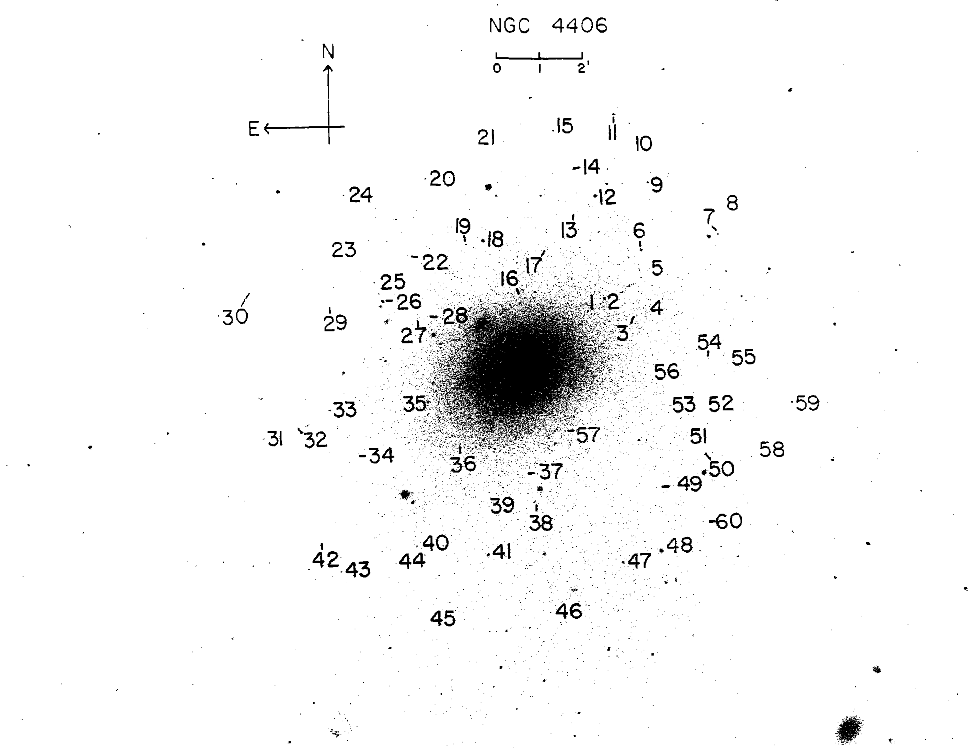

Plate 4

Plate 5

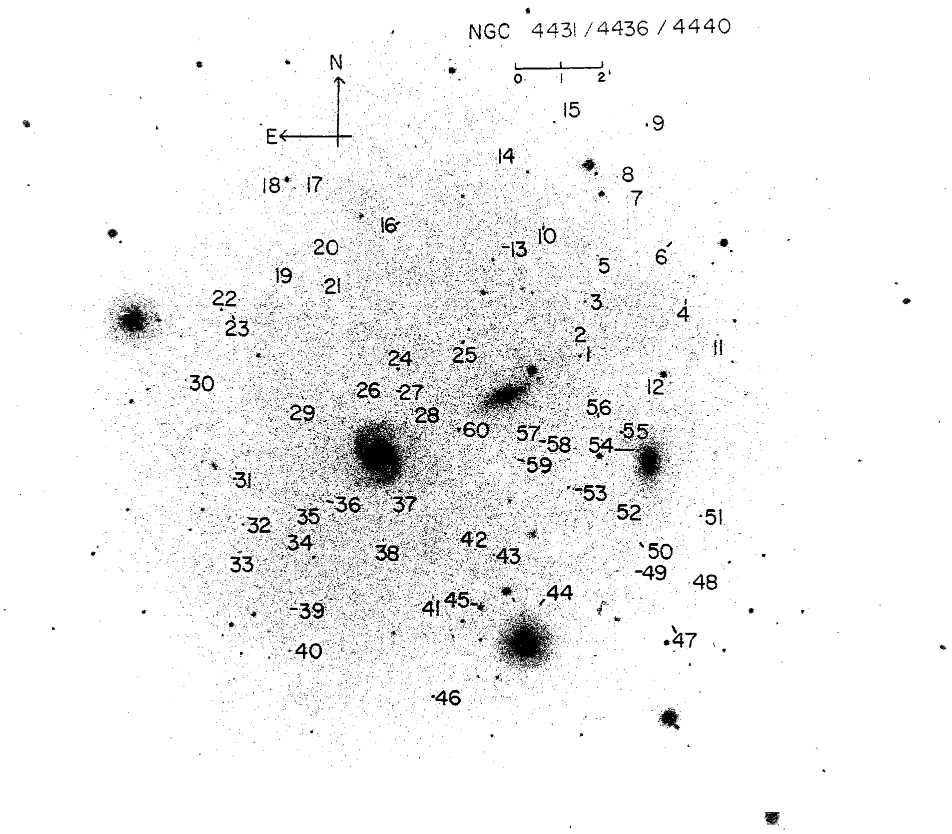

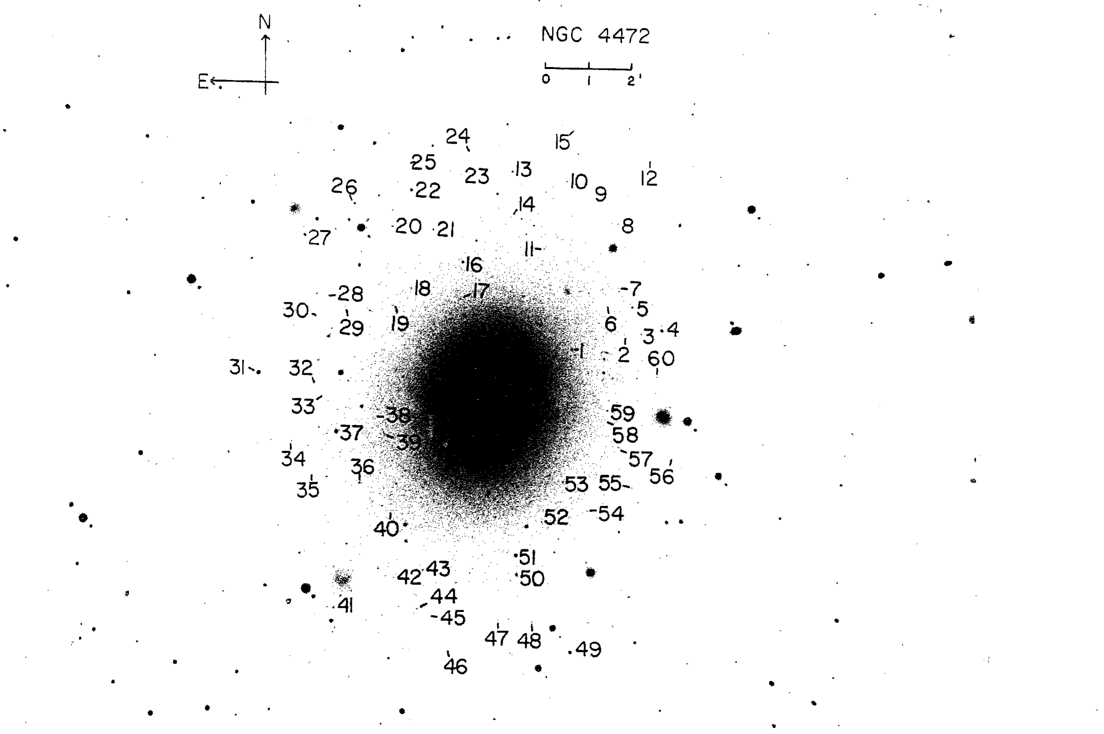

Plate 6

Plate 5

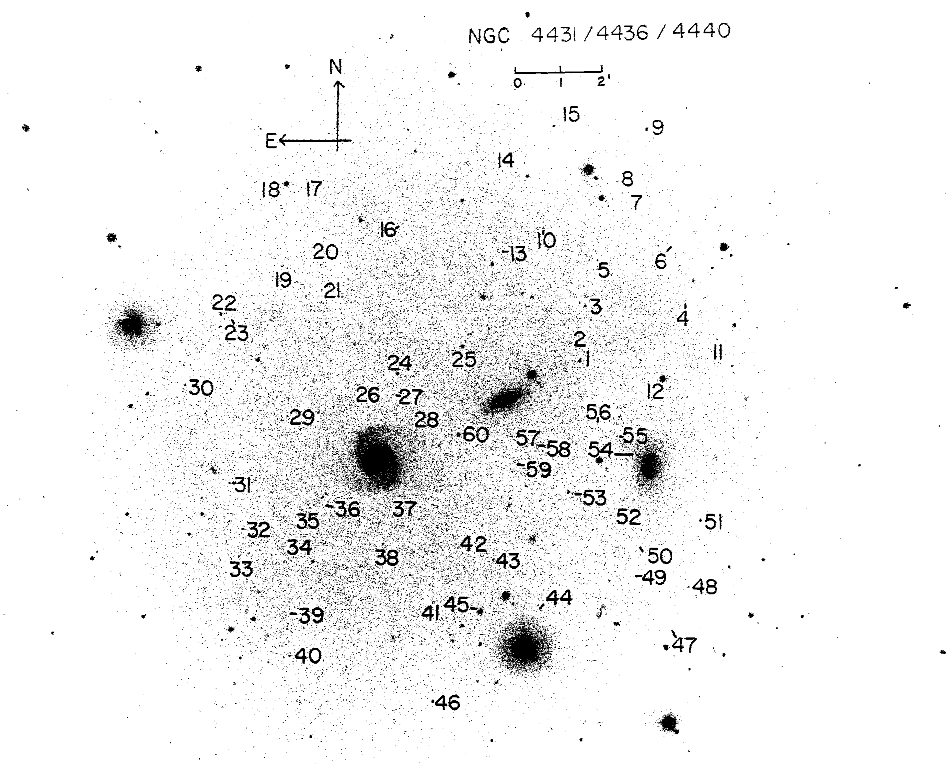

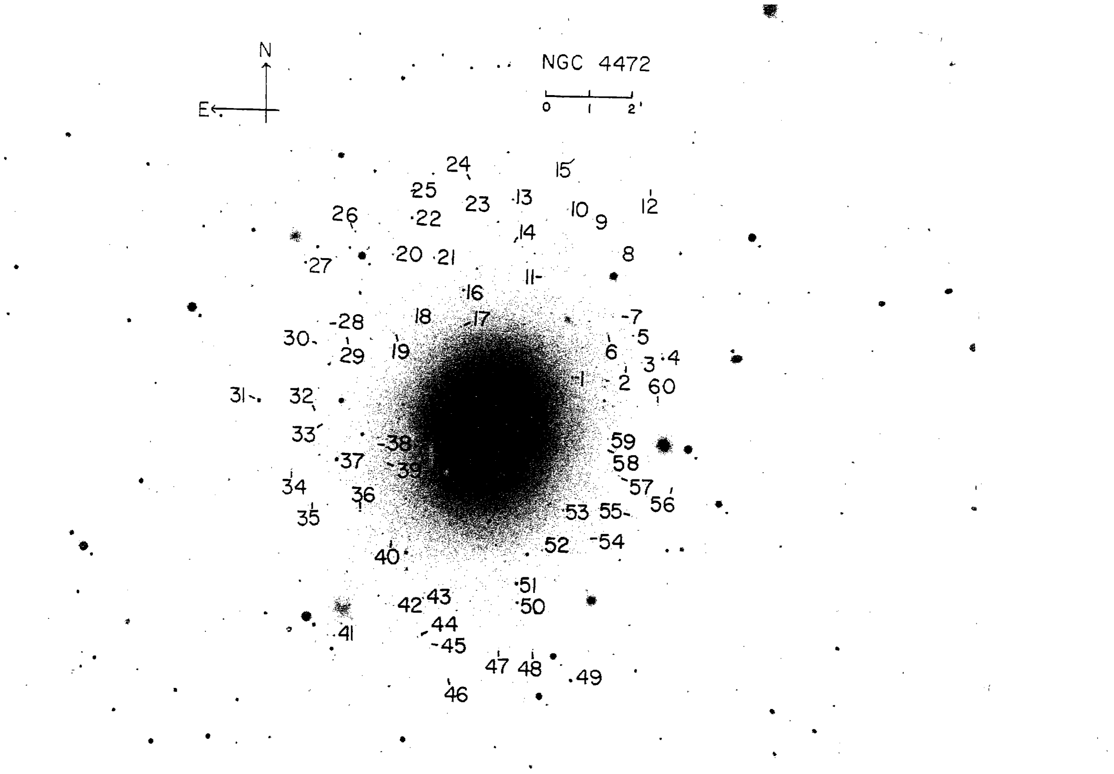

Plate 6

Plate 7

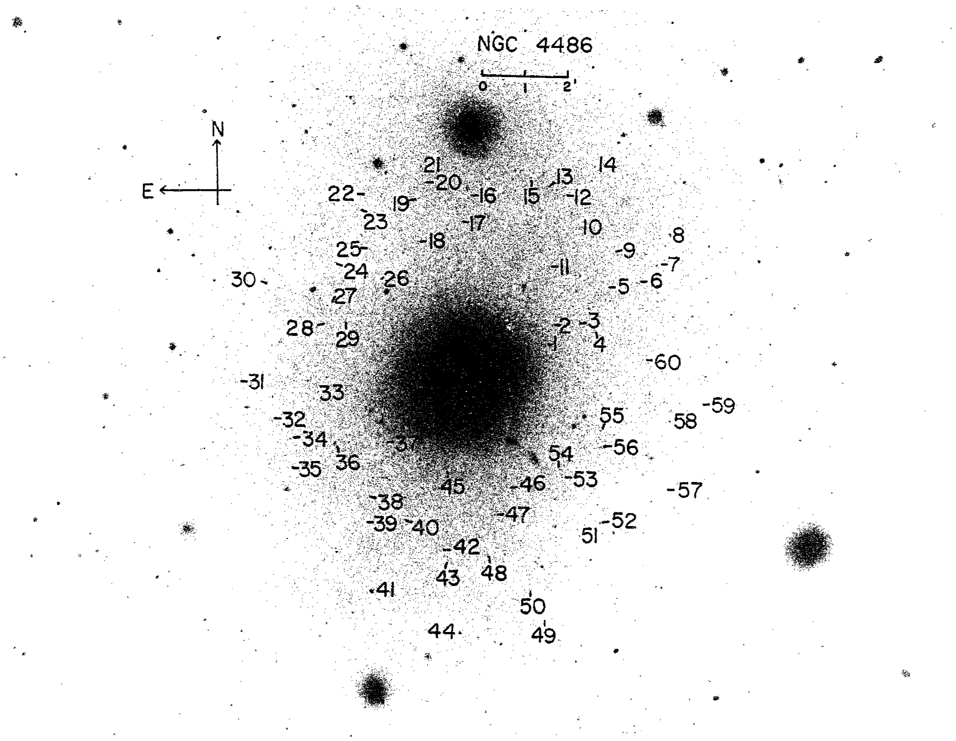

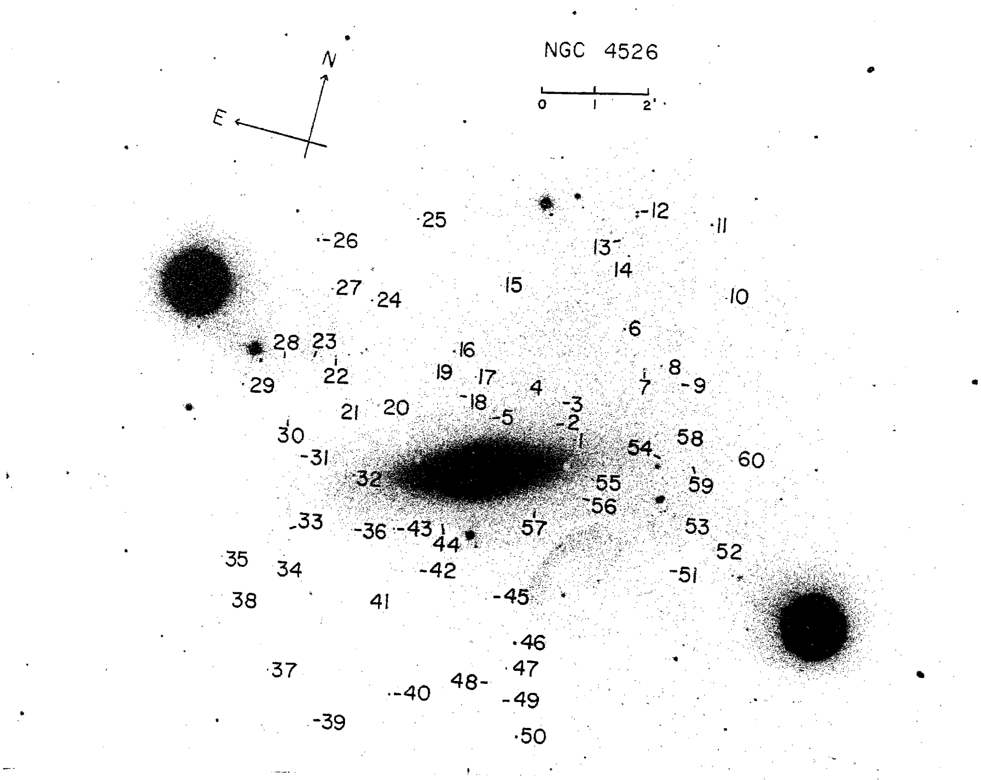

Plate 8

Plate 7

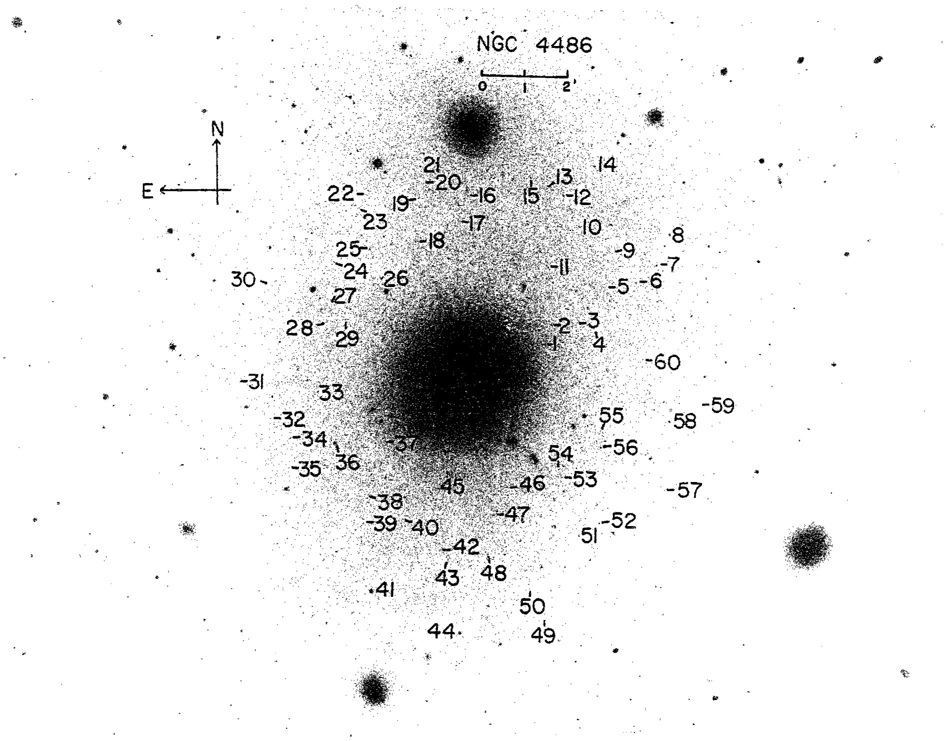

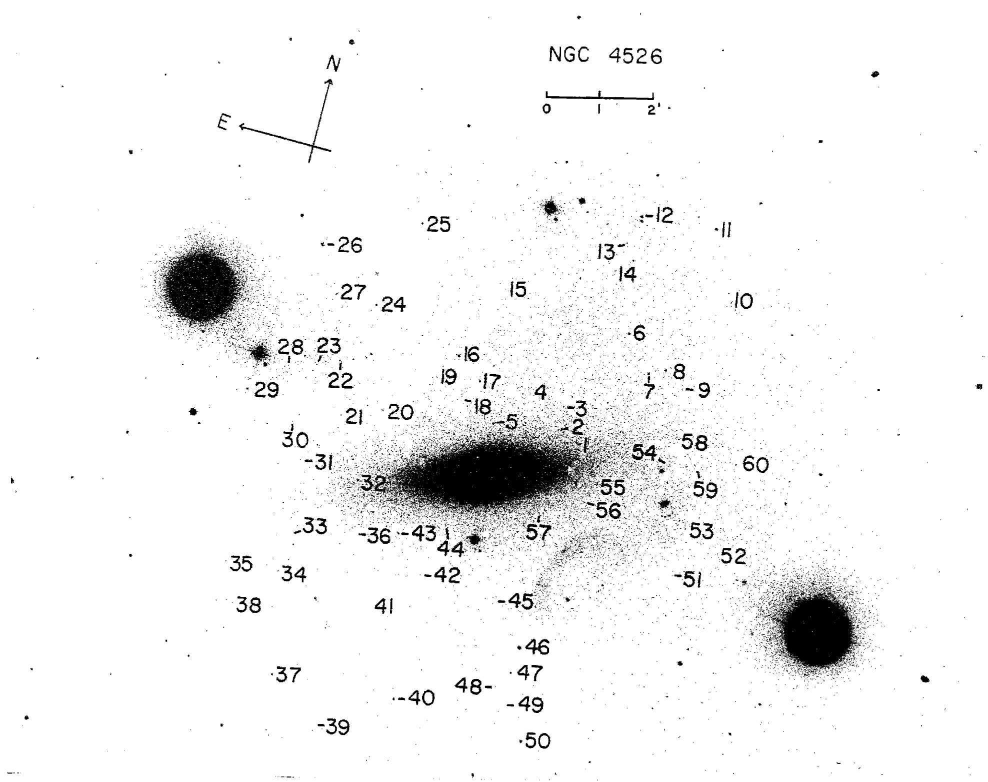

Plate 8

Plate 9

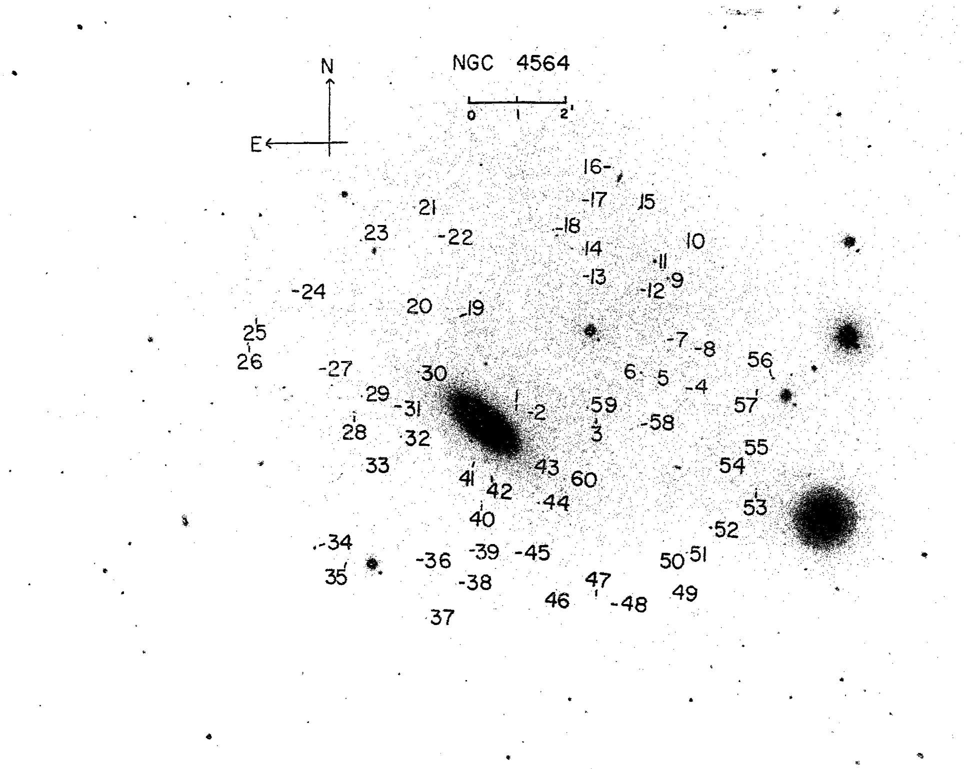

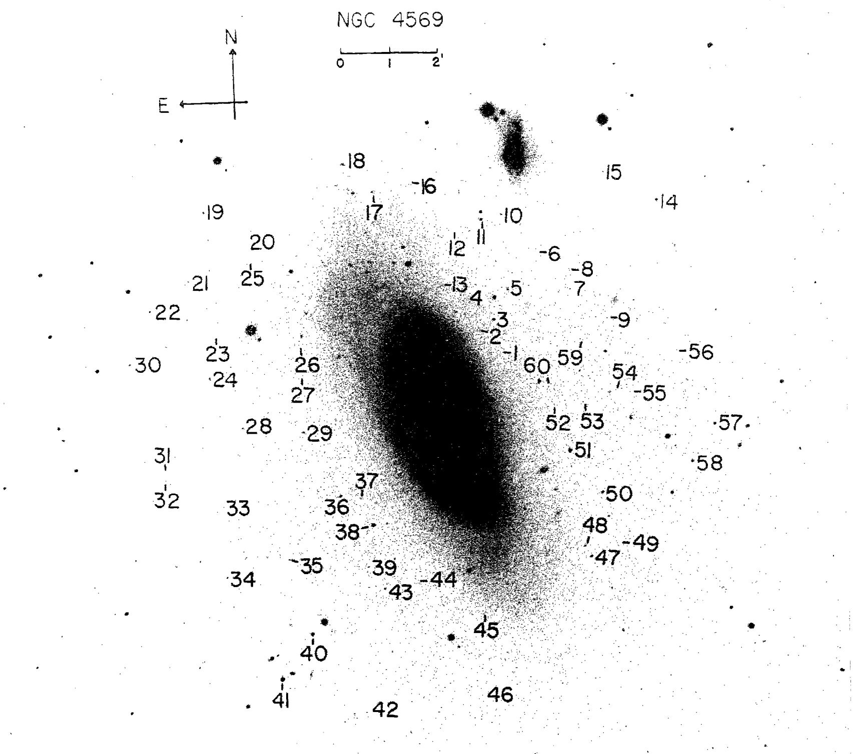

Plate 10

Plate 9

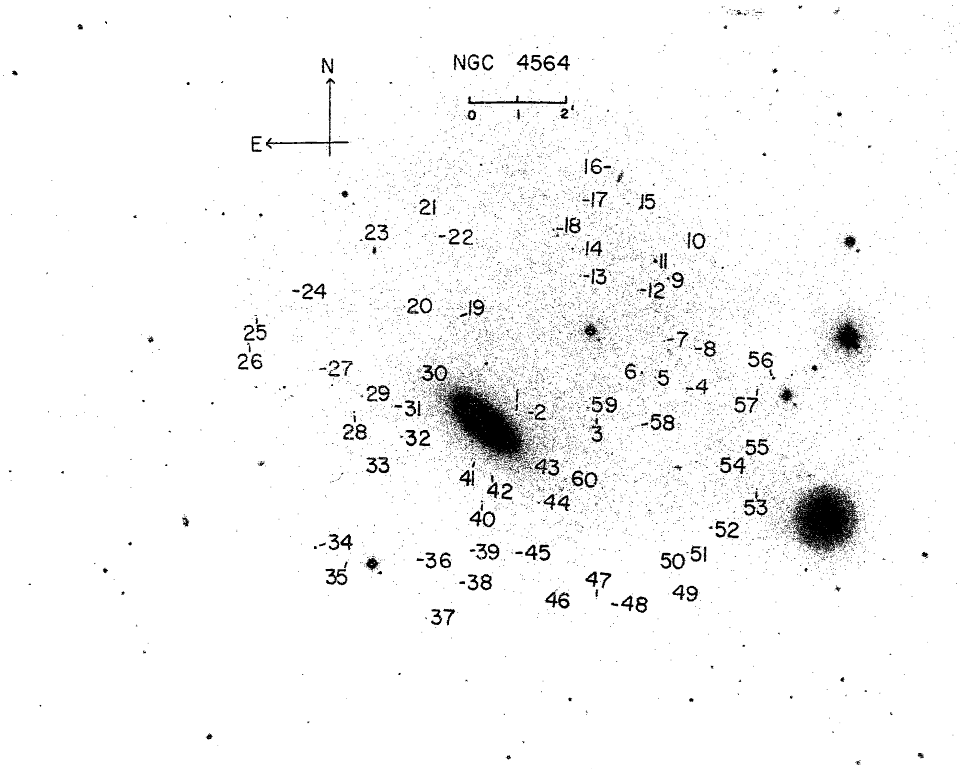

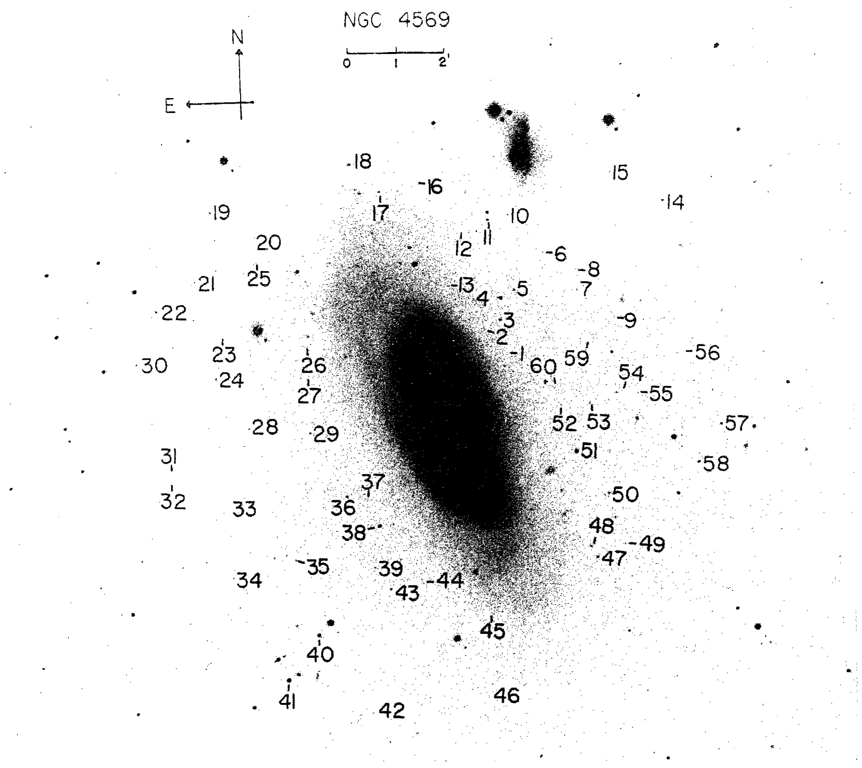

Plate 10

Plate 11

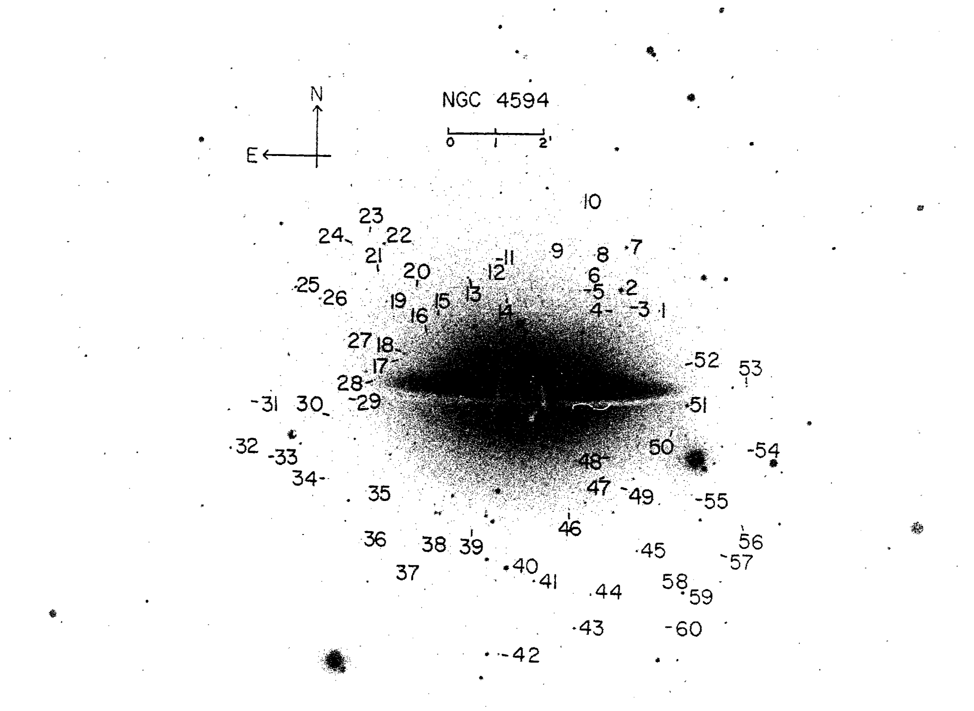

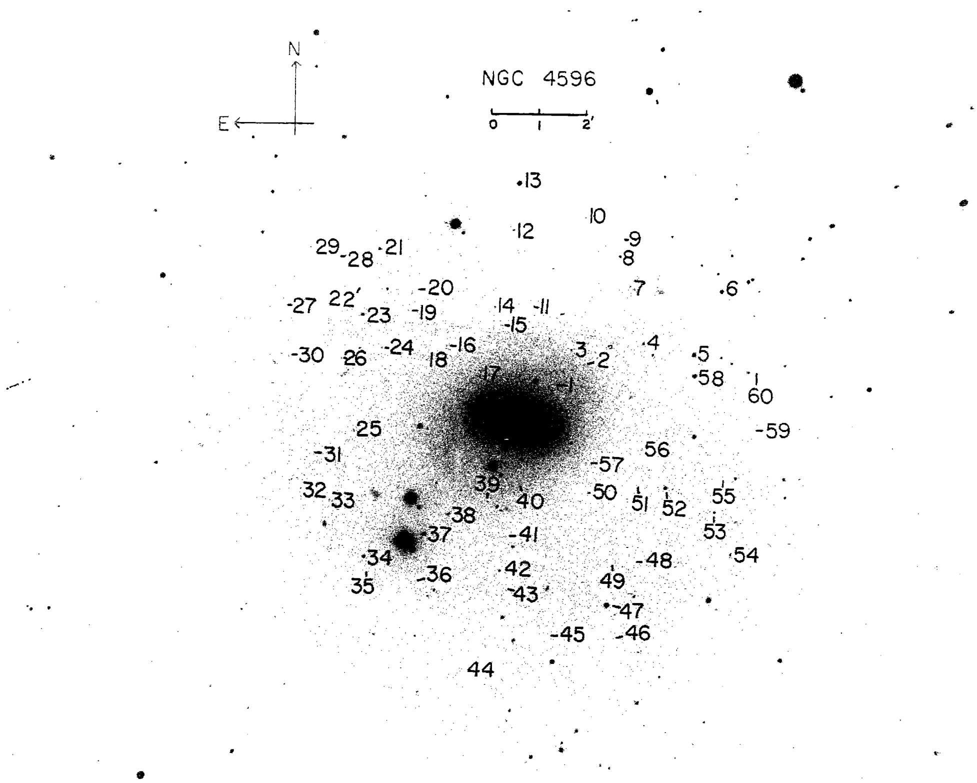

Plate 12

Plate 11

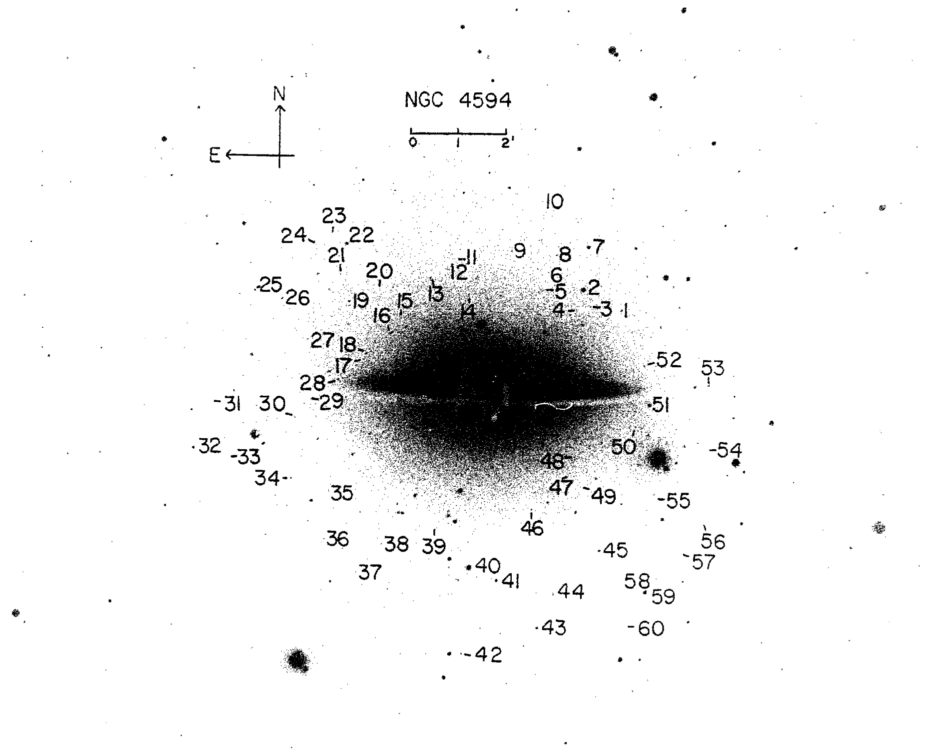

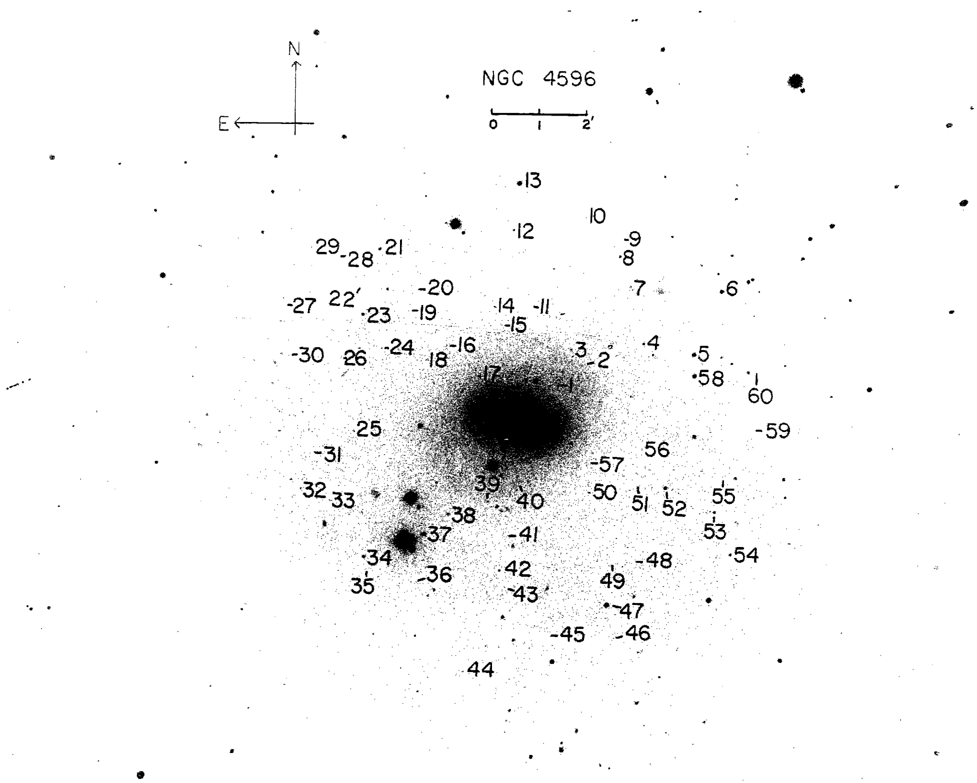

Plate 12

Plate 13

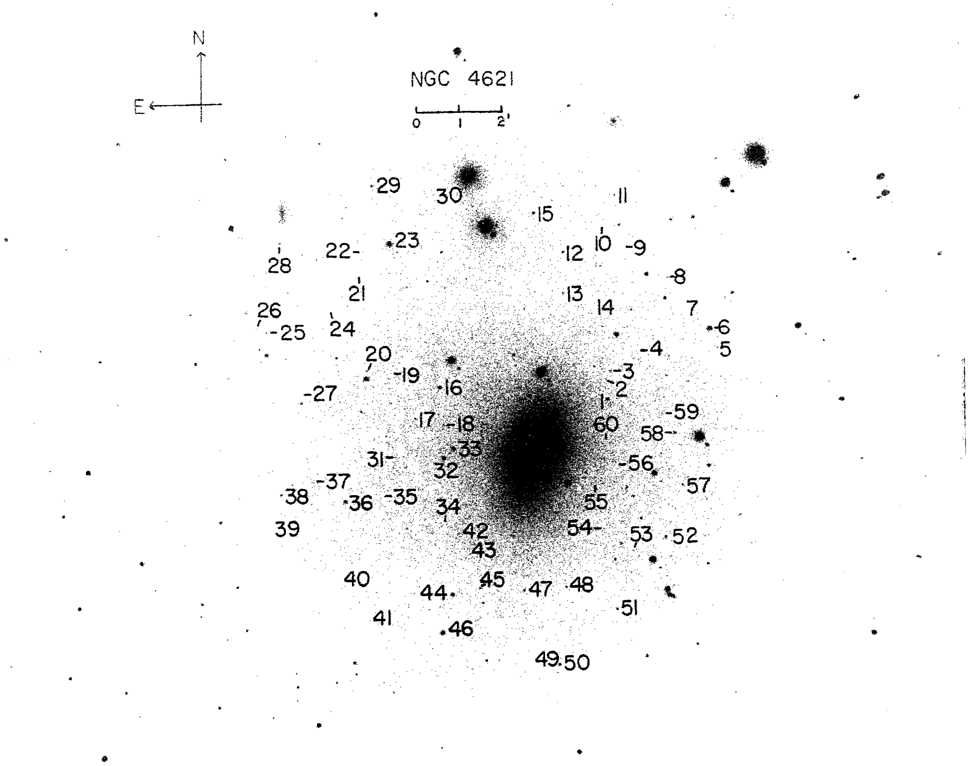

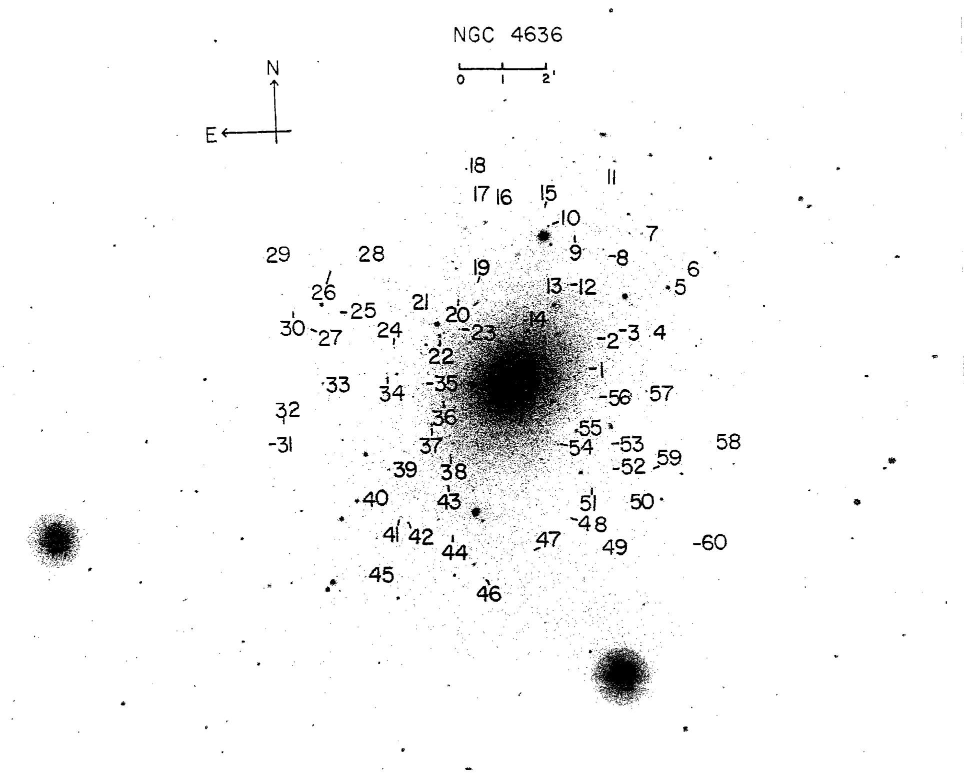

Plate 14

Plate 13

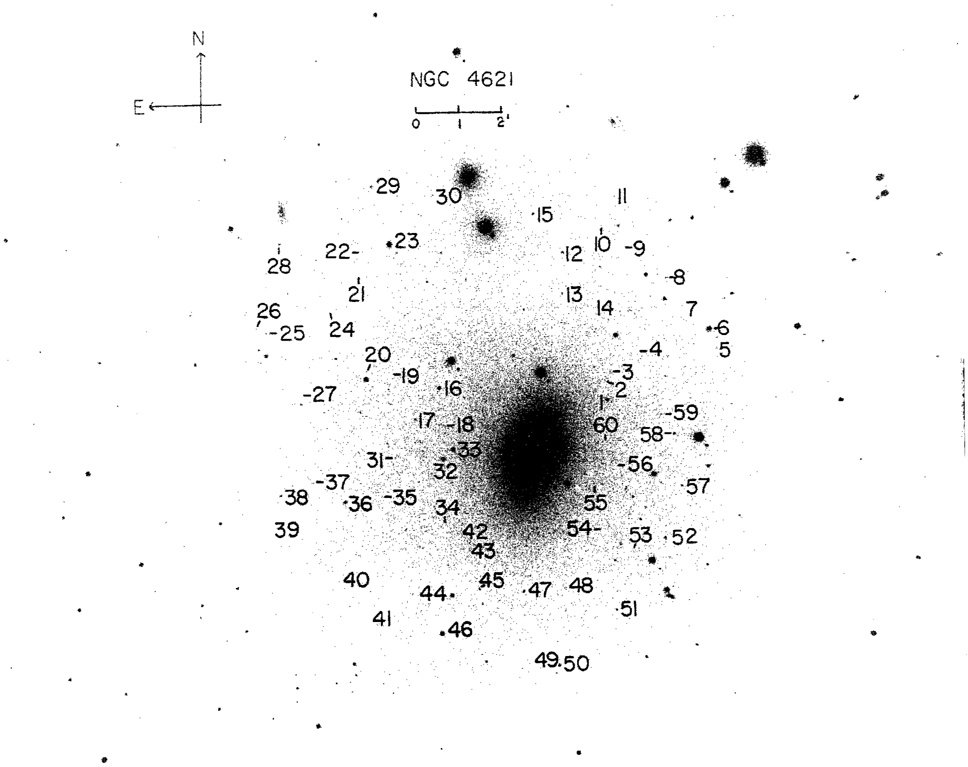

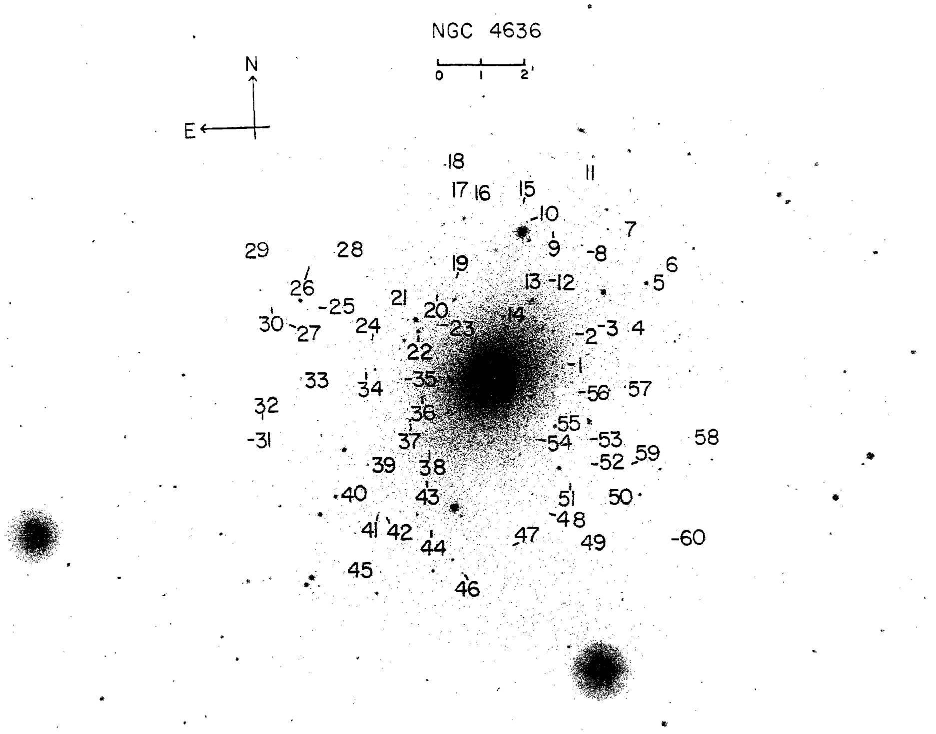

Plate 14

Plate 15

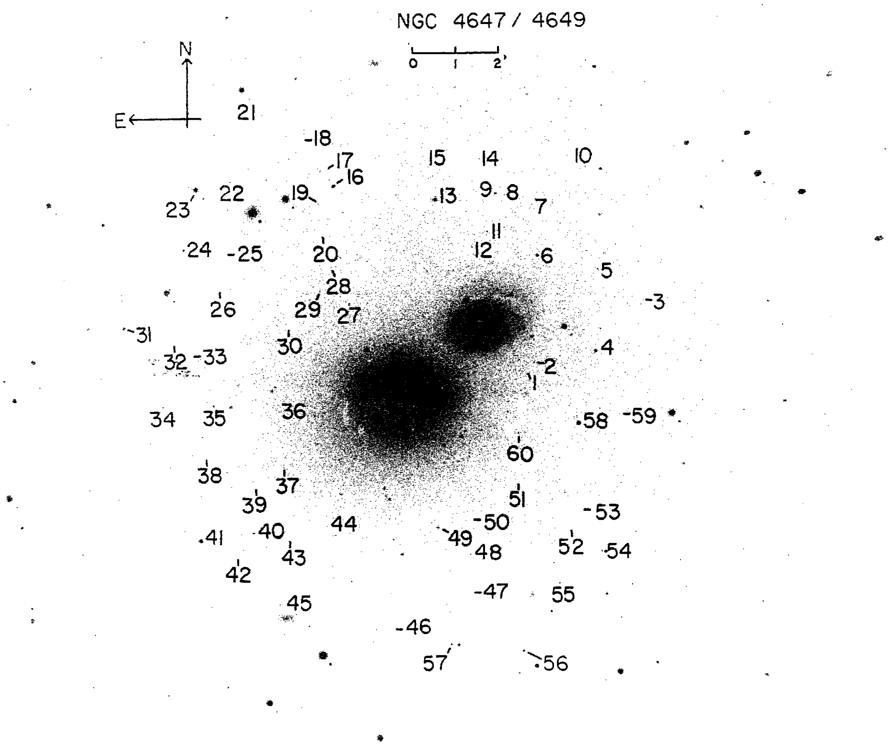

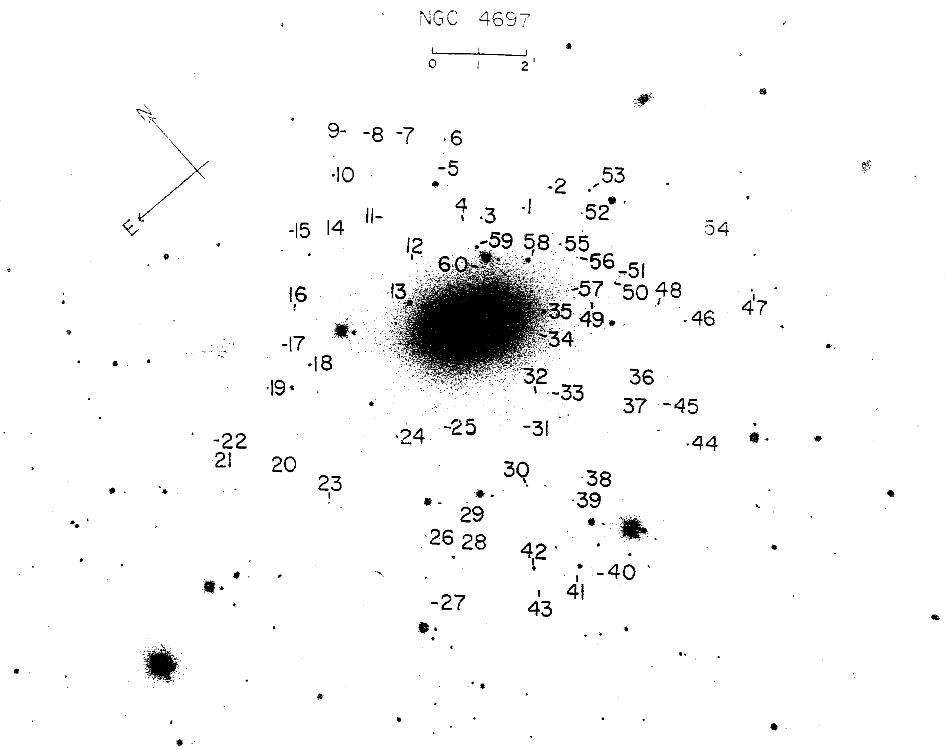

Plate 16

Plate 15

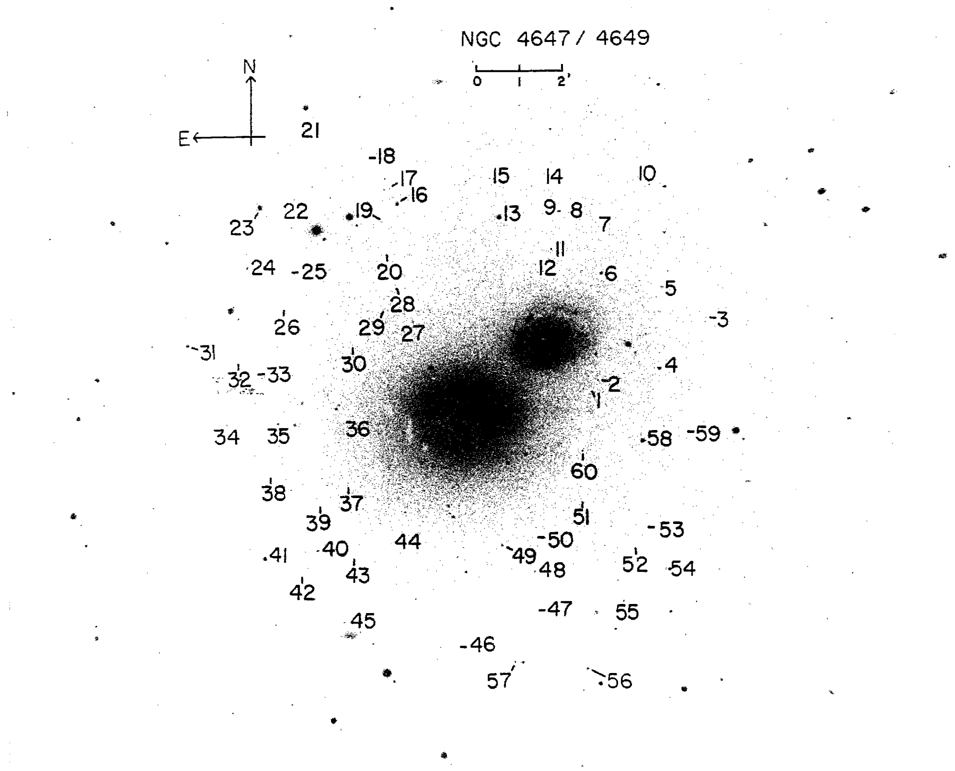

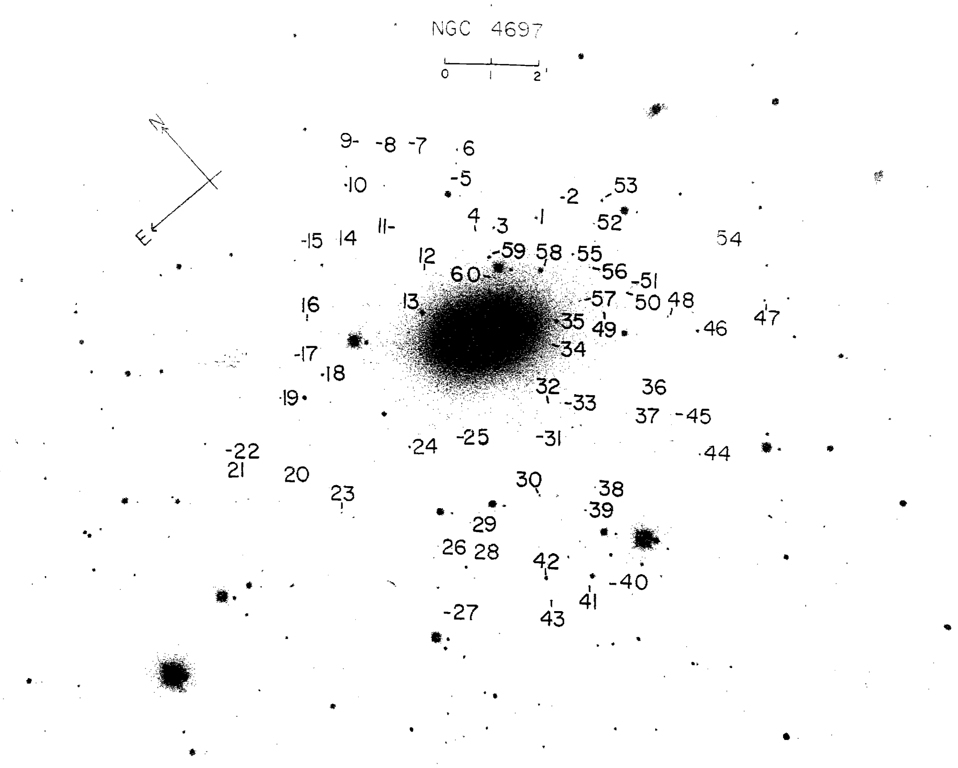

Plate 16

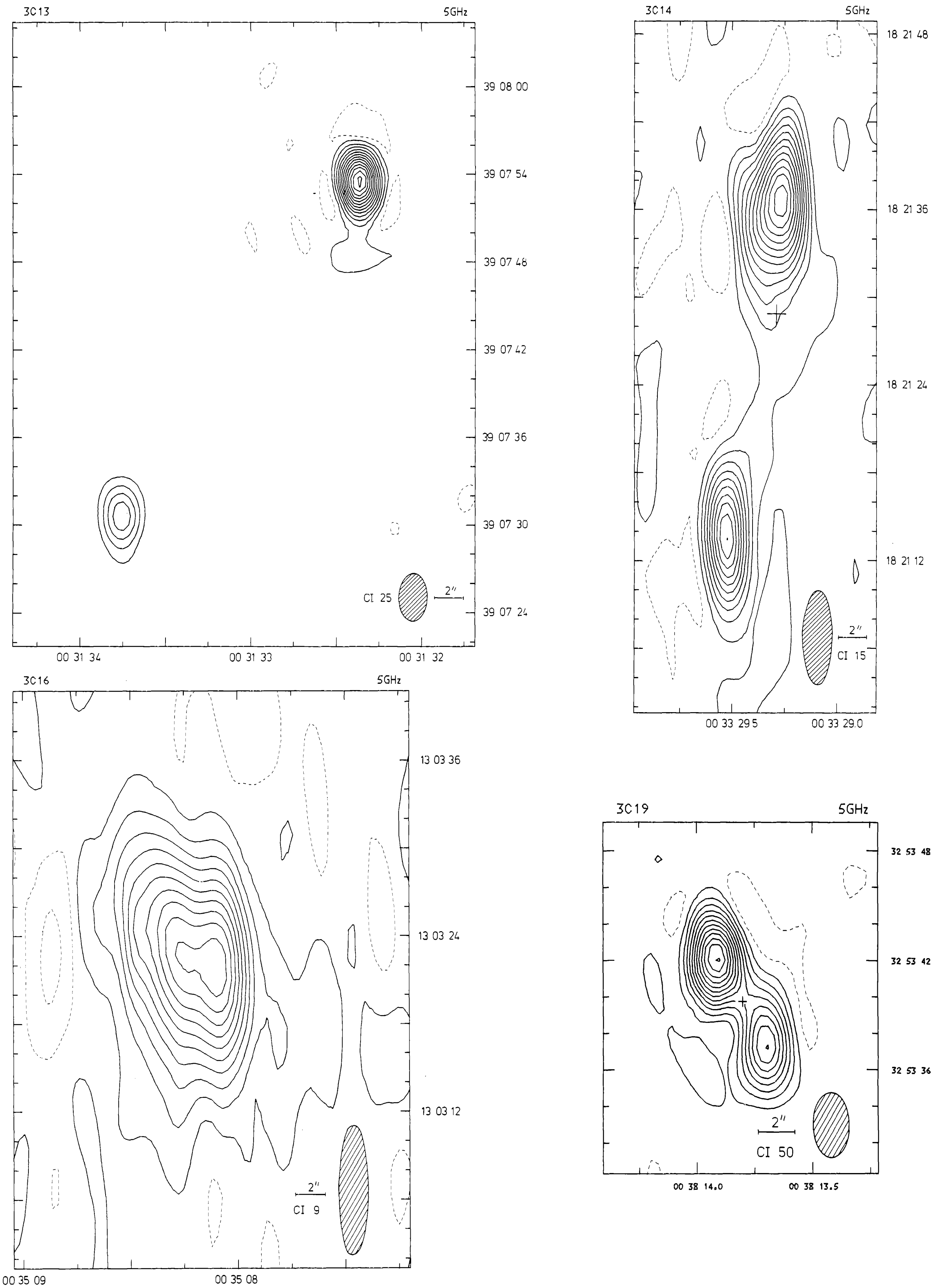

Figure 1. *3C13*. There are no objects visible on the PSS prints near the radio source, but Smith, Burbidge & Spinrad (1976) suggest that it is identified with a 21 mag object.
3C 14. The position of the 20 mag object was measured by KSK; its nature is uncertain.
3C 16. This source has not been identified.
3C 19. The position of the 20 mag galaxy in a cluster was measured by KSK.

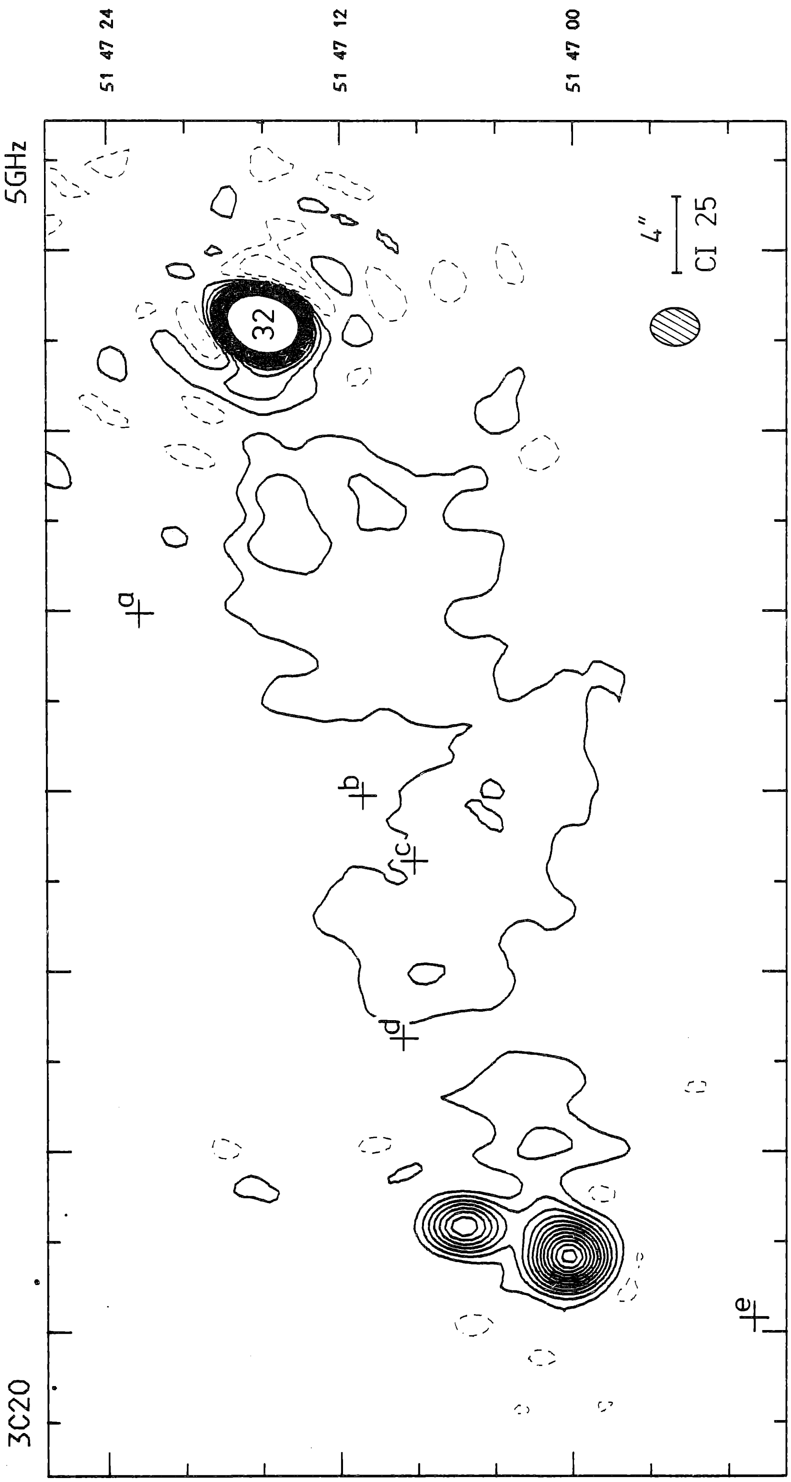

Figure 2. *3C 20.* Objects b, c and e are 19 mag red galaxies; a and d are 18 mag slightly red objects.

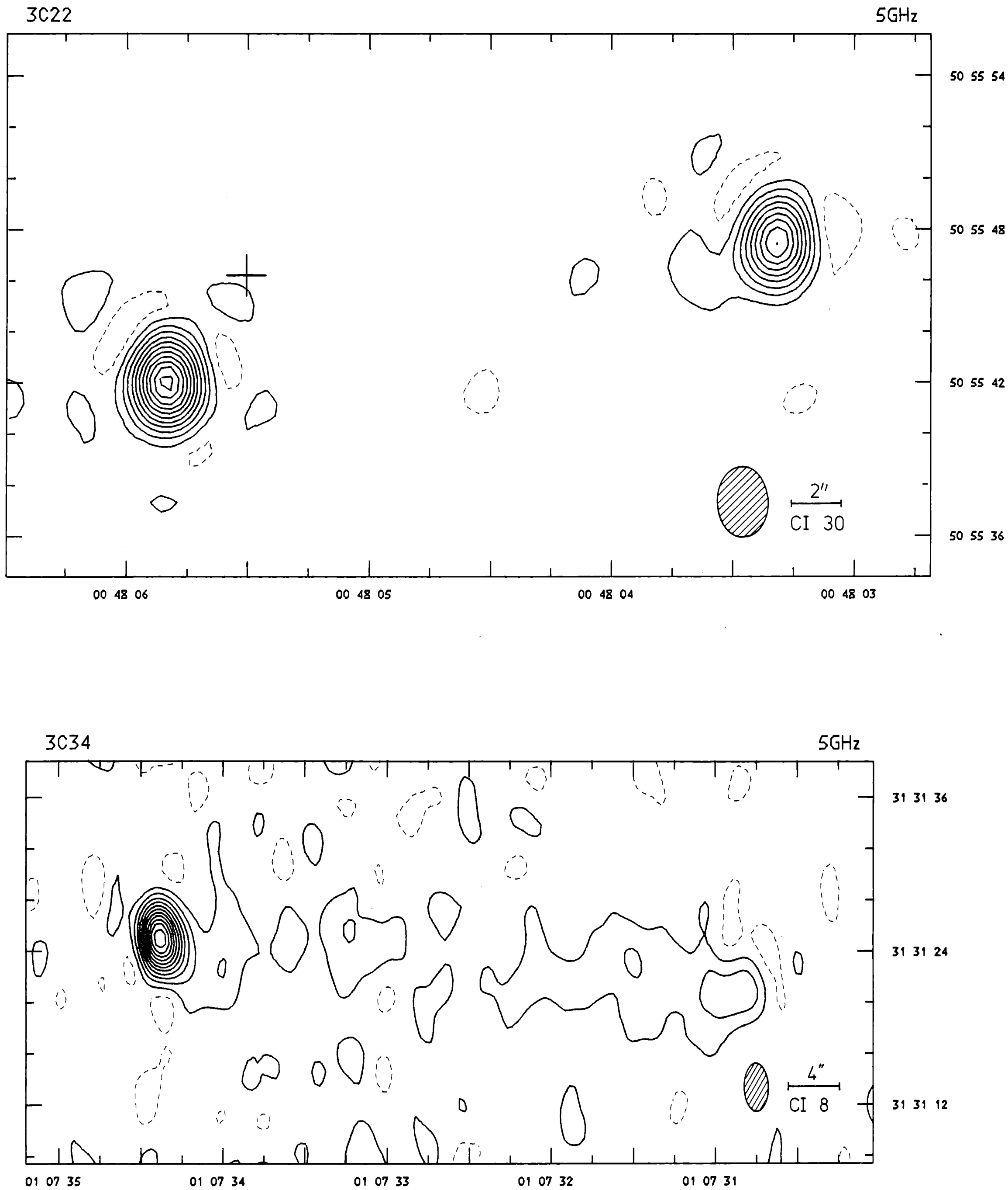

Figure 3. *3C 22.* The cross marks the position of a 19 mag neutral coloured object.
3C 34. This source has not been identified.

1977MmRAS..84...61J

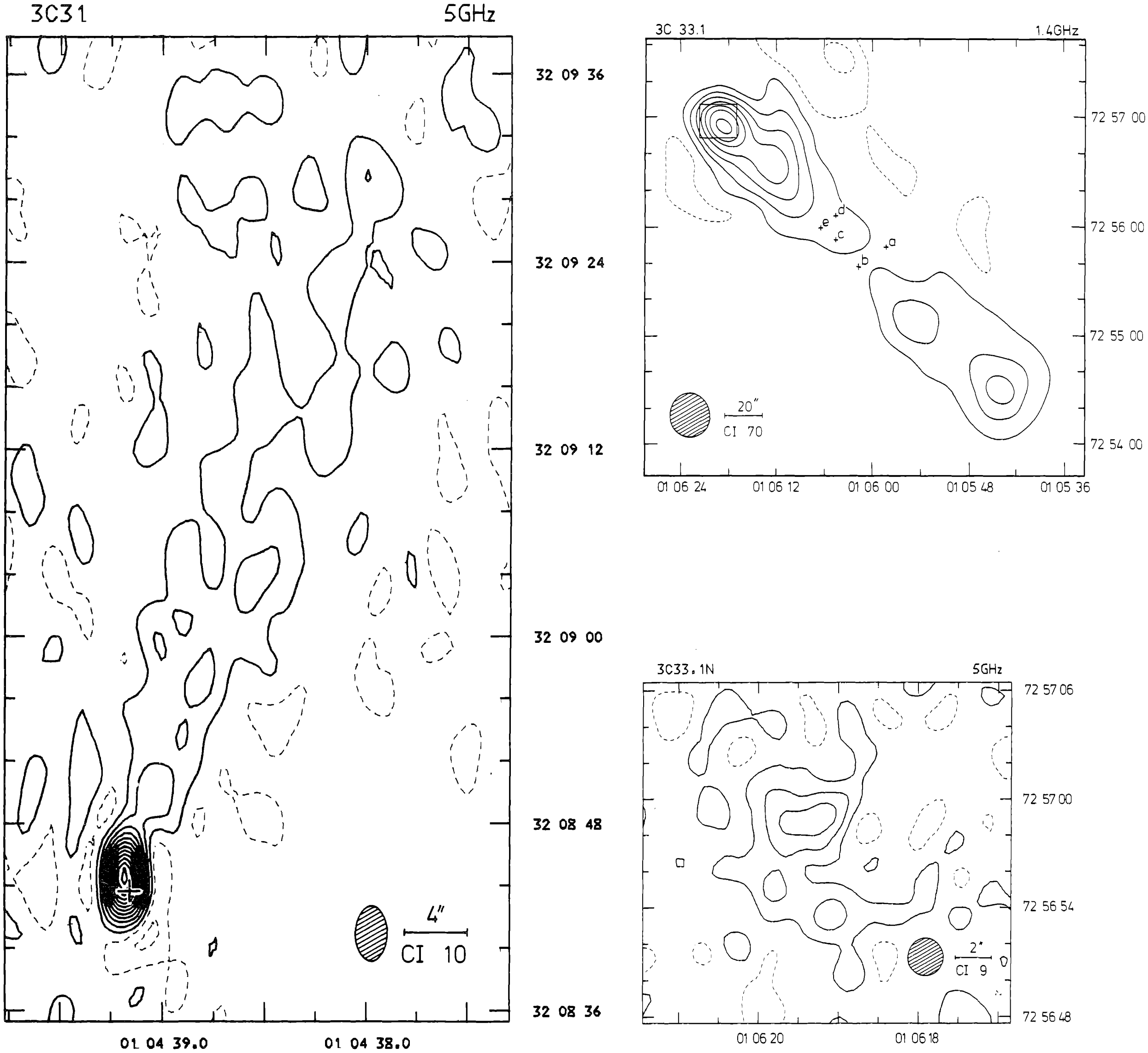

Figure 4. *3C 31.* The cross marks the position of the 12 mag galaxy NGC 383. There is no emission at 5 GHz exceeding 10 mJy/beam area from the other eight galaxies in the region of the source, whose positions are given in Table 1. A low-resolution map of this source at 408 MHz is shown in MKN. The source is discussed in detail by Burch (1977).

3C 33.1. The overall structure of the source is shown on the 1.4 GHz map from MKN; the crosses mark the positions of (a), (b) and (c) 18.5 mag stellar objects, (d) 19.5 mag galaxy and (e) 19 mag double galaxy (LG) with a redshift of 0.173 (Sargent, private communication). The high-resolution map of the northern component is shown separately; there is no other unresolved structure brighter than 10 mJy.

1977MmRAS..84...61J

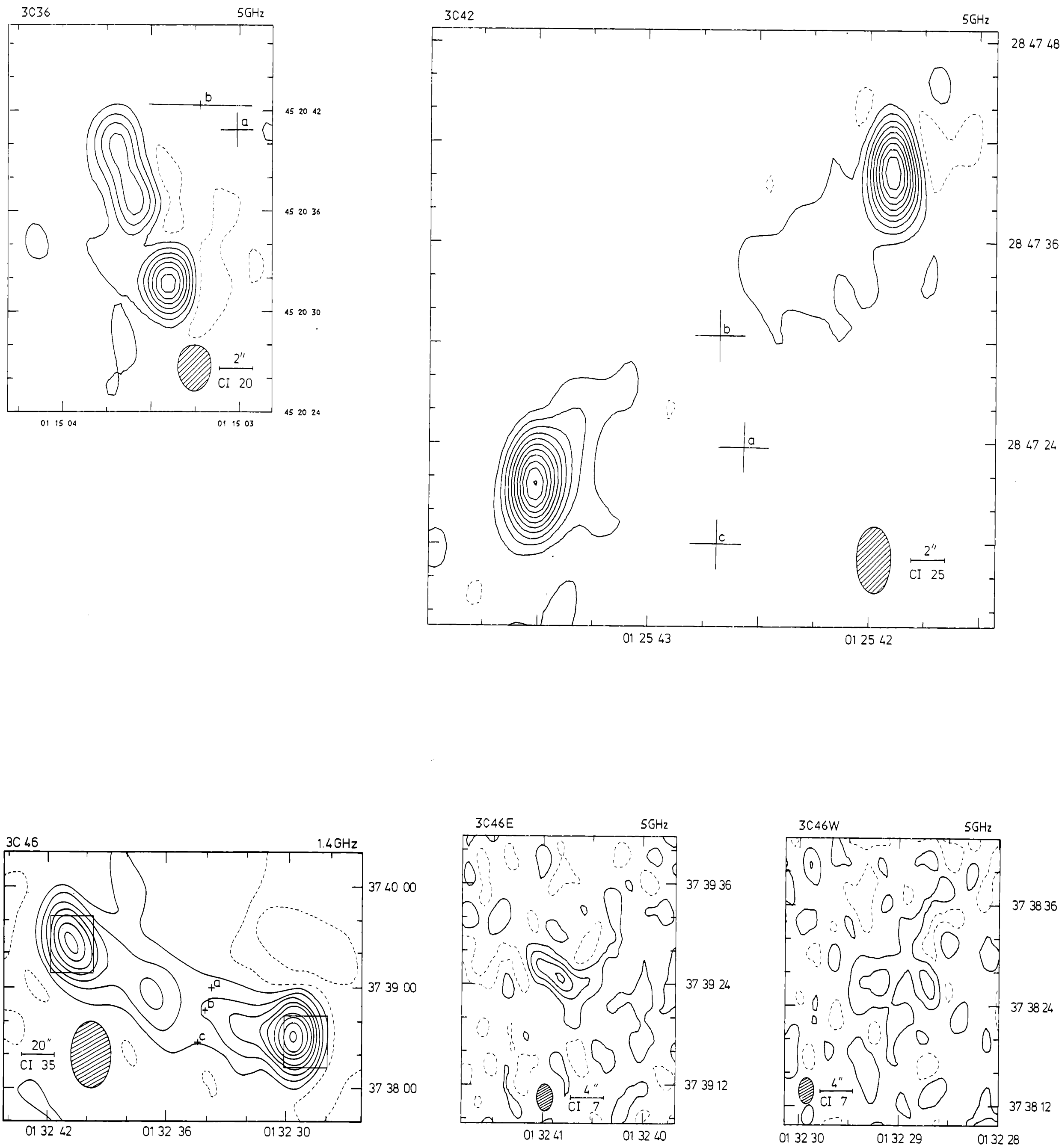

Figure 5. *3C 36.* The cross (a) marks the position of an object at the limit of the blue PSS print and not visible on the red; the cross (b) marks the position given by KSK of a possible quasar. It seems probable that these are the same object but unlikely that this object is related to the radio source.

3C42. The positions of the objects marked were measured on the plate taken by LG; object b is a 20 mag galaxy and objects a and c are 21 mag galaxies.

3C 46. The overall structure of the source is shown on the 1.4 GHz map from MKN; the crosses mark the positions of (a) 18.5 mag stellar object, (b) 19.5 mag galaxy (LG) and (c) 19.5 mag red object. 5-GHz maps of the outer components are shown separately.

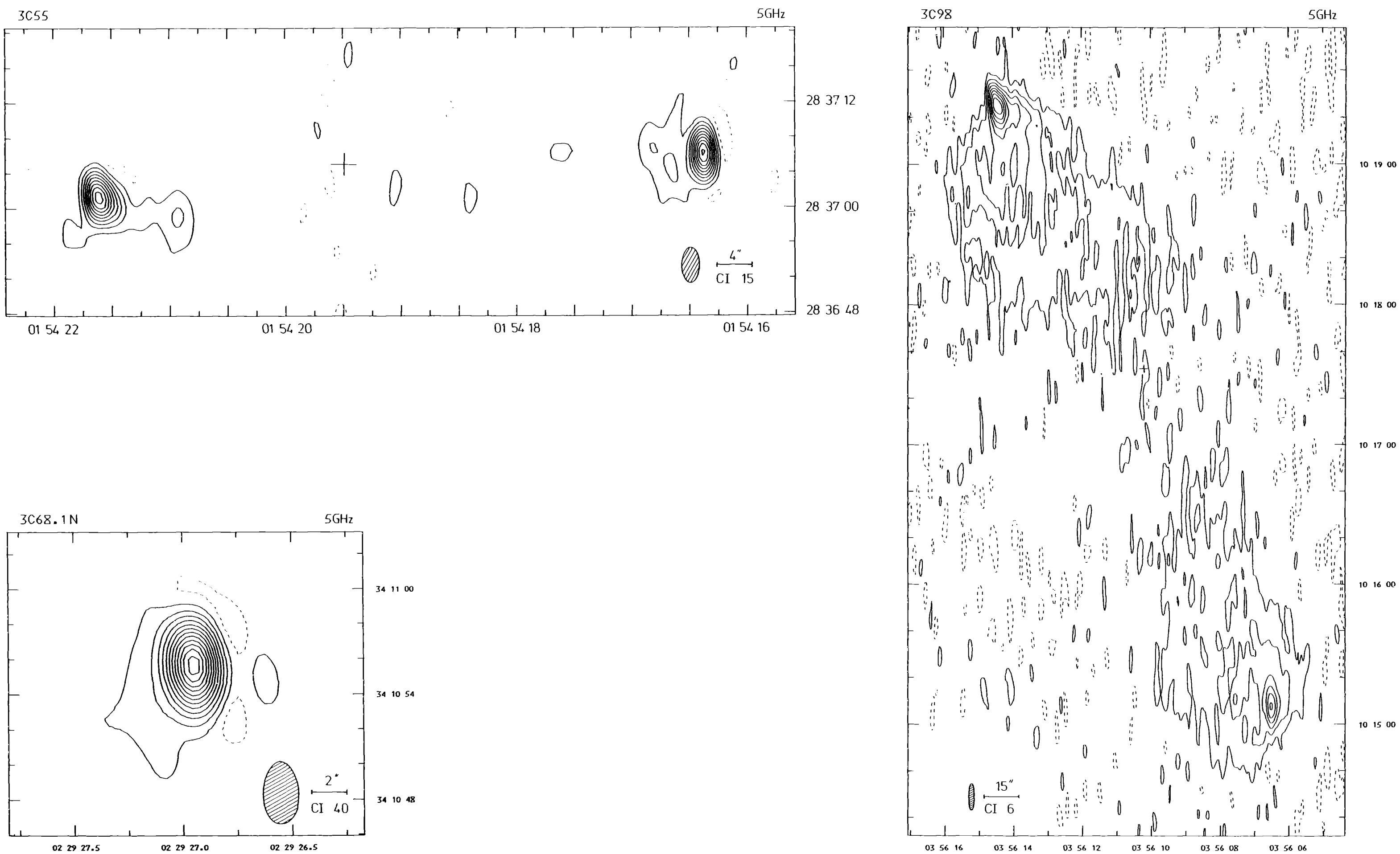

Figure 6. *3C55.* The position of the 20 mag galaxy was measured on the plate taken by LG.
3C68.1. There is a very faint radio component 46 arcsec south of the component shown (MKN); a 19.8 mag quasar lies between these two components.
3C98. The cross marks the position of a 14.5 mag ED3 galaxy; the position of this galaxy has also been measured by Griffin (1963).

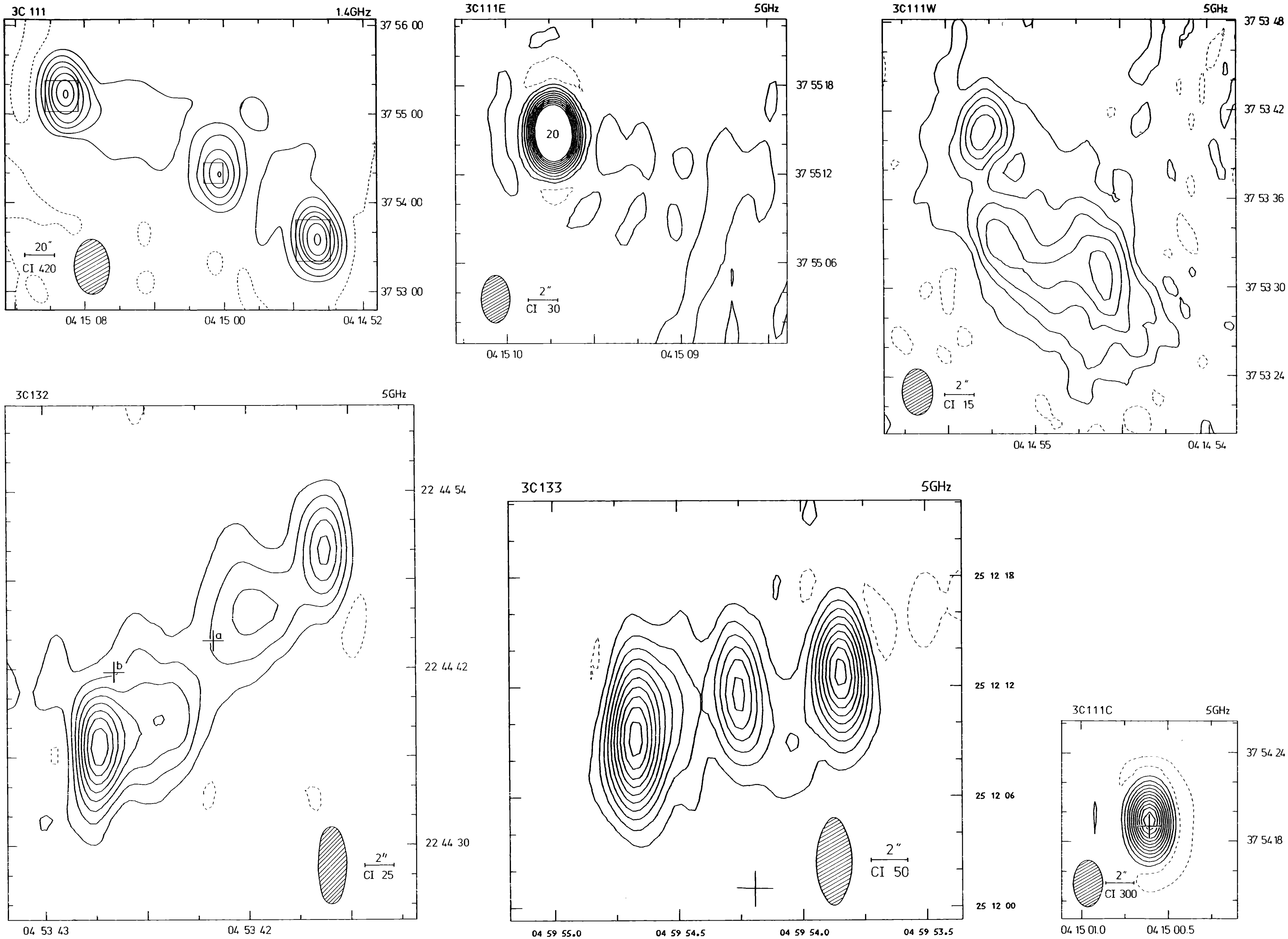

Figure 7. *3C111.* The overall structure of the source is shown on the 1.4-GHz map (Mackay 1969); the cross marks the position of an 18 mag very compact galaxy. The 5-GHz maps of the outer components and the highly variable central component are shown separately; these observations were made in 1975 October–November.
3C132. Object a is a 19 mag red galaxy; object b is a 17 mag stellar object.
3C133. Optically, this region is obscured; the cross marks the position of an 18 mag red stellar object, probably unrelated to the source. The other optical positions listed in Table 1 are of a 17 mag red stellar object and a 19 mag red stellar object.

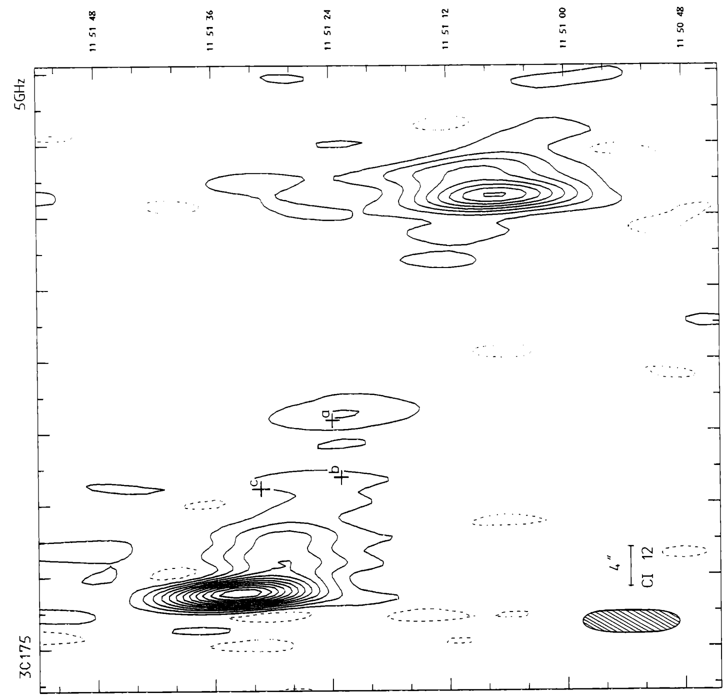

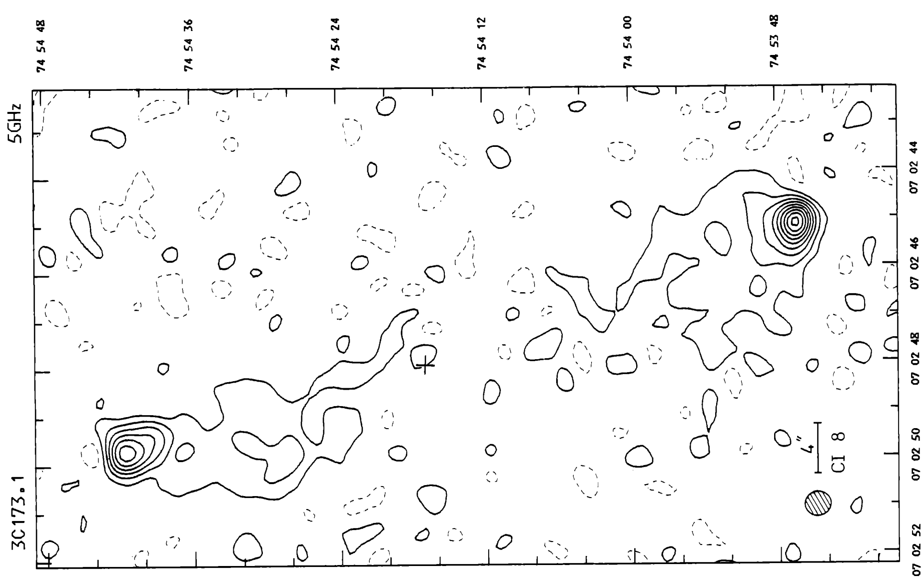

Figure 8. *3C 173.1.* The cross marks the position of an 18 mag galaxy. *3C 175.* Object a is a 17 mag quasar; objects b and c are stars.

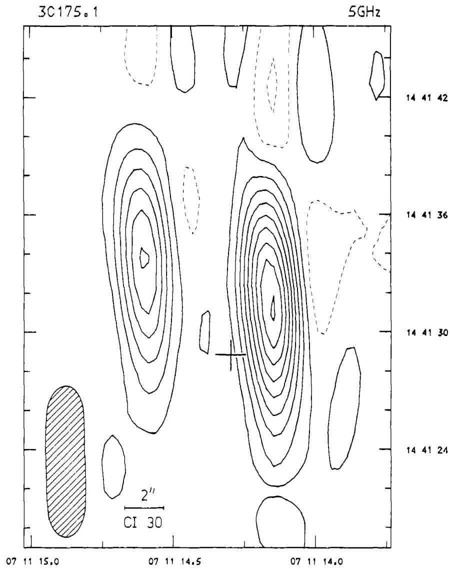

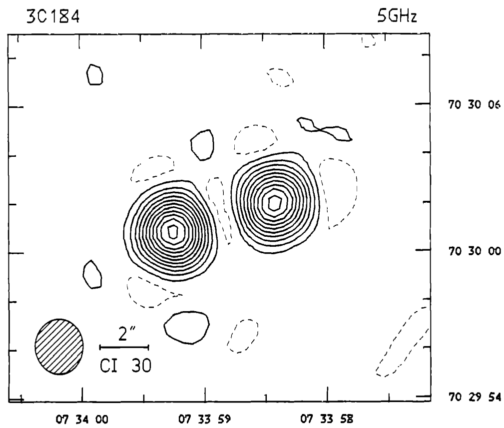

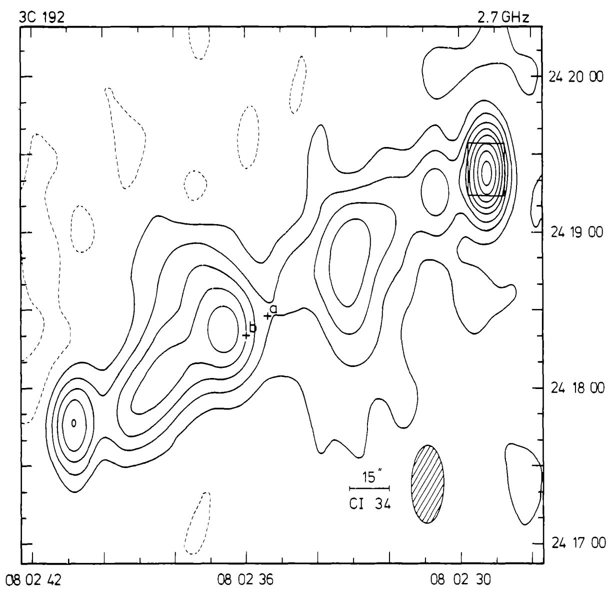

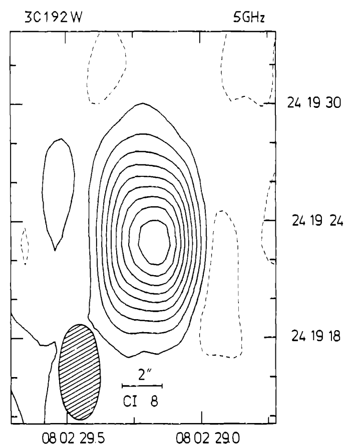

Figure 9. *3C 175.1.* The object marked is a star; the field of the source is otherwise empty (KSK).
3C 184. This source has not been identified.
3C 192. The crosses on the 2.7-GHz map (Harris 1973) mark the positions of (a) a 15 mag galaxy with $z = 0.0597$ and (b) a 14 mag stellar object. The high-resolution map is of the western component only; the eastern component is resolved with a maximum surface brightness of 20 mJy/beam area.

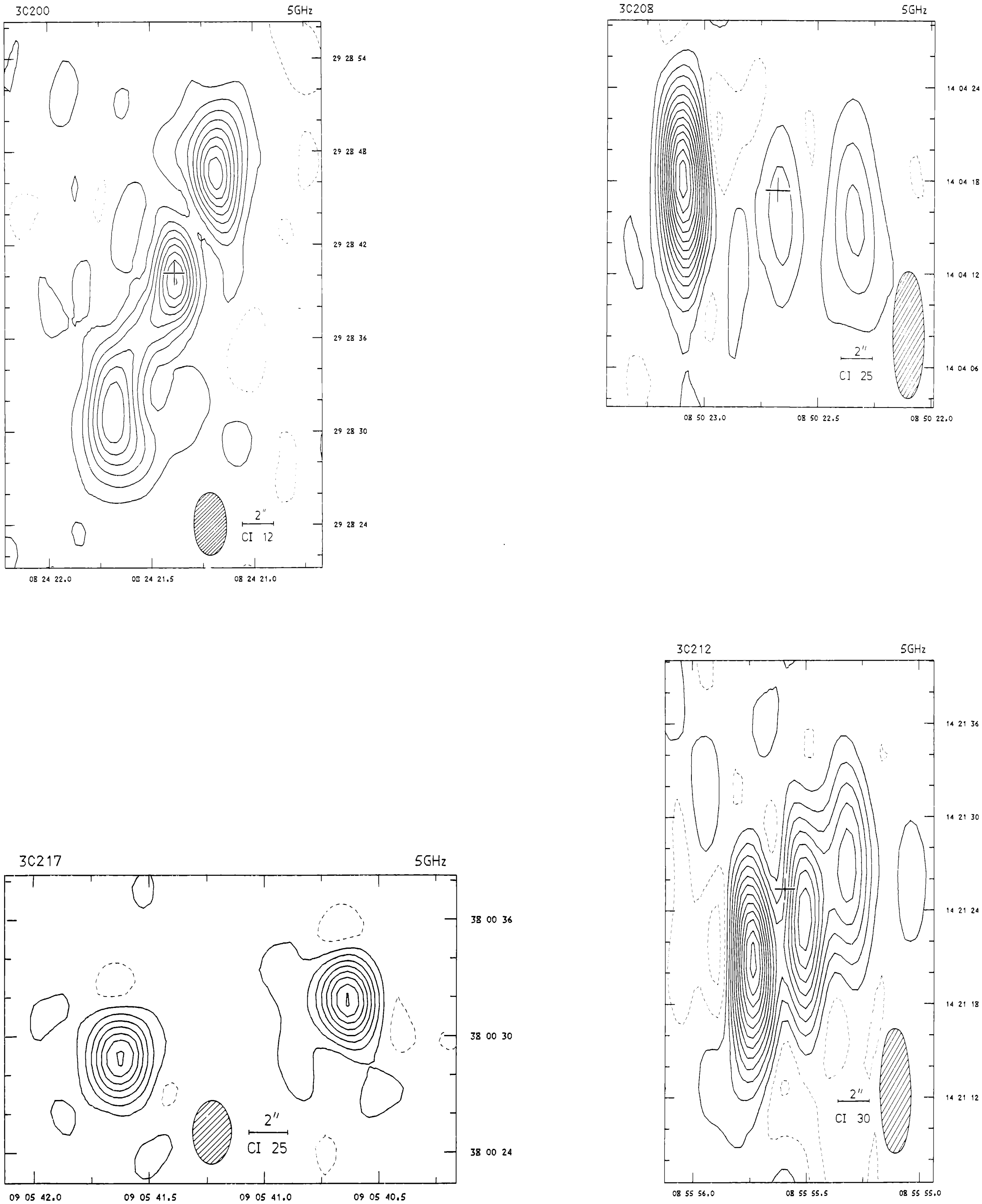

Figure 10. *3C 200.* The cross marks the position of a 20 mag red object.
3C 208. The object marked is a 17 mag quasar.
3C 212. The object marked is a 19 mag quasar.
3C 217. This source is unidentified.

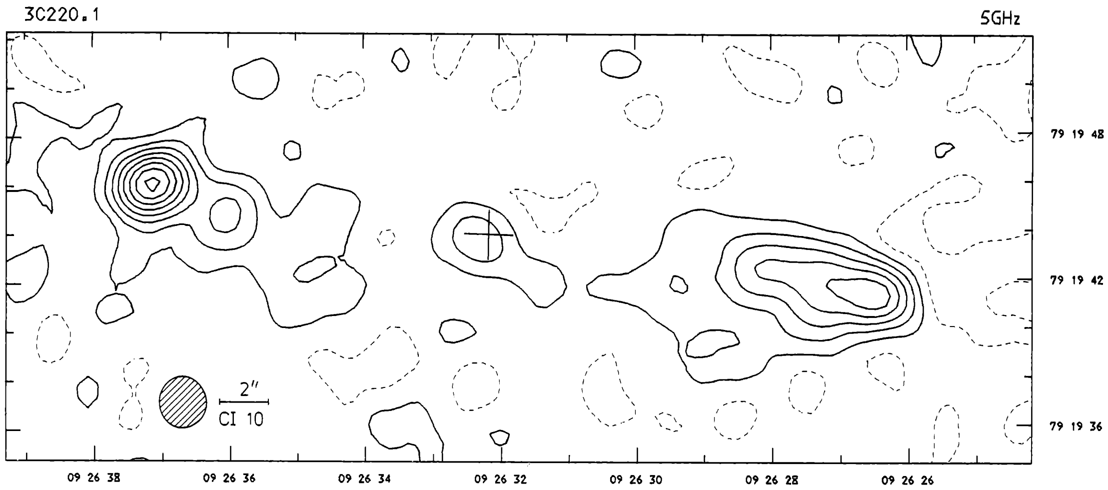

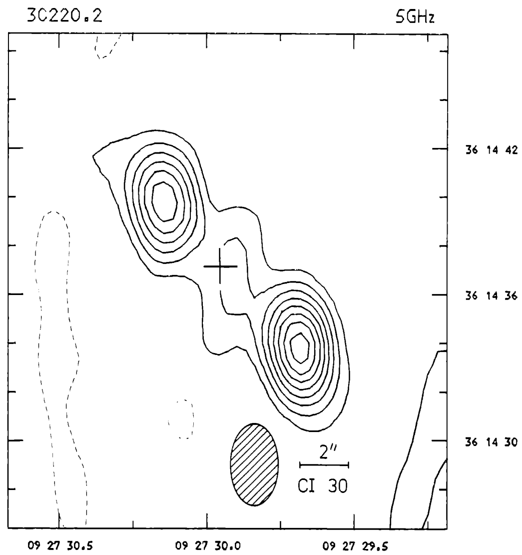

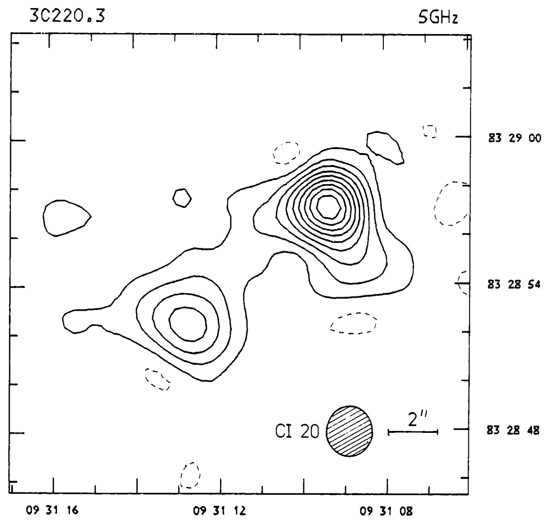

Figure 11. *3C 220.1.* The object marked is at the limit of the red PSS print and not visible on the blue print.
3C 220.2. The cross marks the position of a 19 mag quasar.
3C 220.3. The optical positions listed in Table 1 are of a 19 mag red object, a 17.5 mag neutral stellar object and a 19 mag red object respectively; none of these appears to be related to the source.

Figure 12. *3C 225 A.* The cross marks the position of a 19 mag galaxy, which has also been measured by KSK.
3C 225 B. This source is identified with a very faint galaxy (KSK), not visible on the PSS prints; the position of this galaxy as estimated by KSK is marked.
3C 226. The cross marks the position of a 19 mag red object; it seems likely that this is not related to the source.
3C 228. This source is not identified.

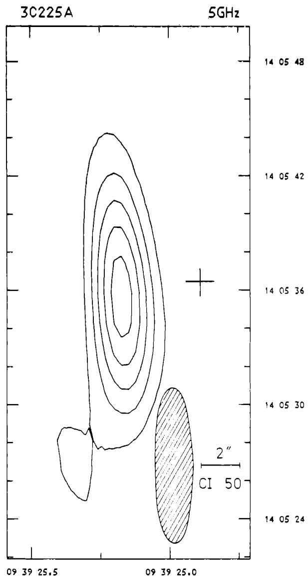
3C225A
5GHz
14 05 48
14 05 42
14 05 36
14 05 30
14 05 24
2″
CI 50
09 39 25.5
09 39 25.0

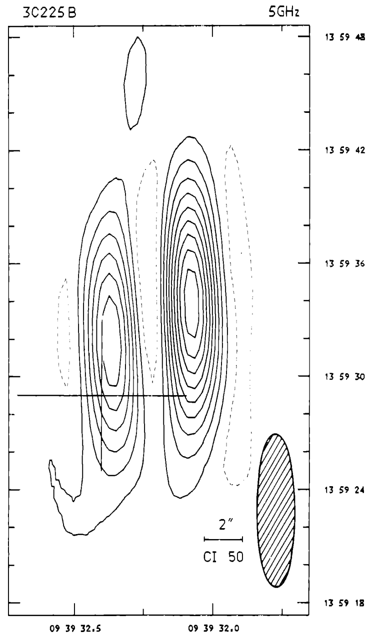
3C225B
5GHz
13 59 48
13 59 42
13 59 36
13 59 30
13 59 24
13 59 18
2″
CI 50
09 39 32.5
09 39 32.0

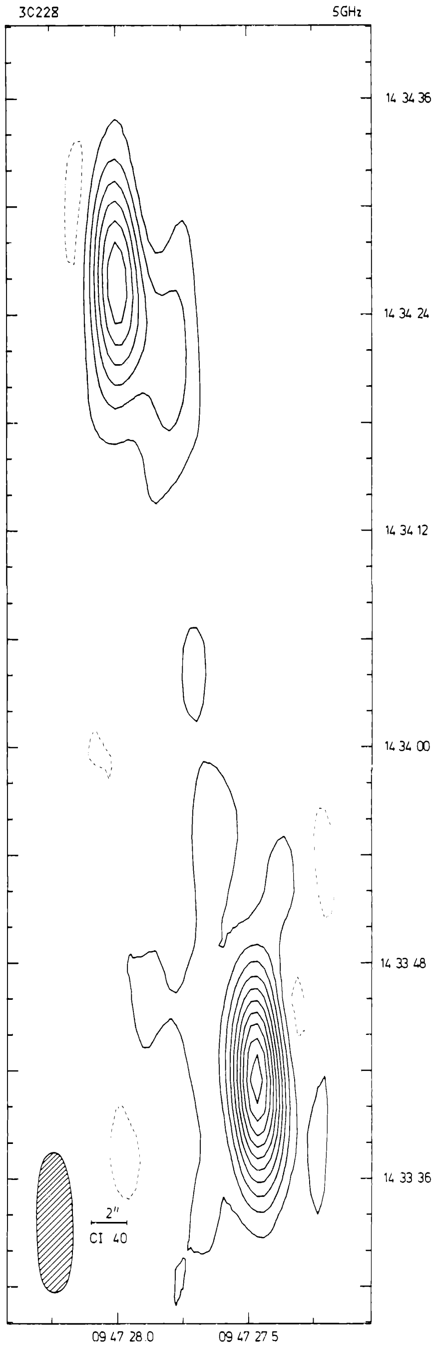
3C228
5GHz
14 34 36
14 34 24
14 34 12
14 34 00
14 33 48
14 33 36
2″
CI 40
09 47 28.0
09 47 27.5

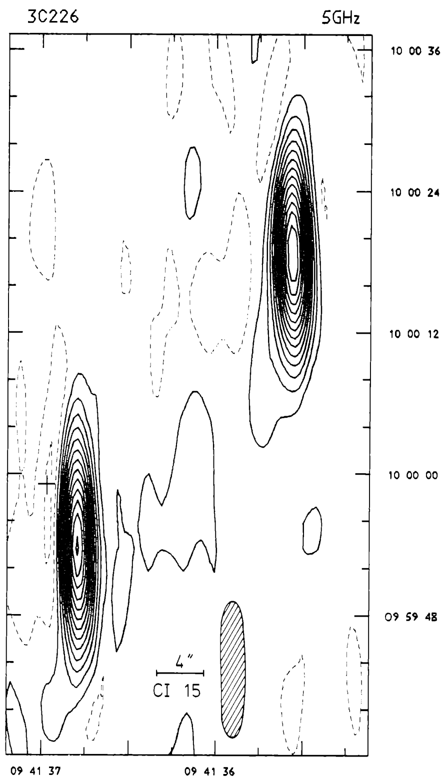
3C226
5GHz
10 00 36
10 00 24
10 00 12
10 00 00
09 59 48
4″
CI 15
09 41 37
09 41 36

Figure 12

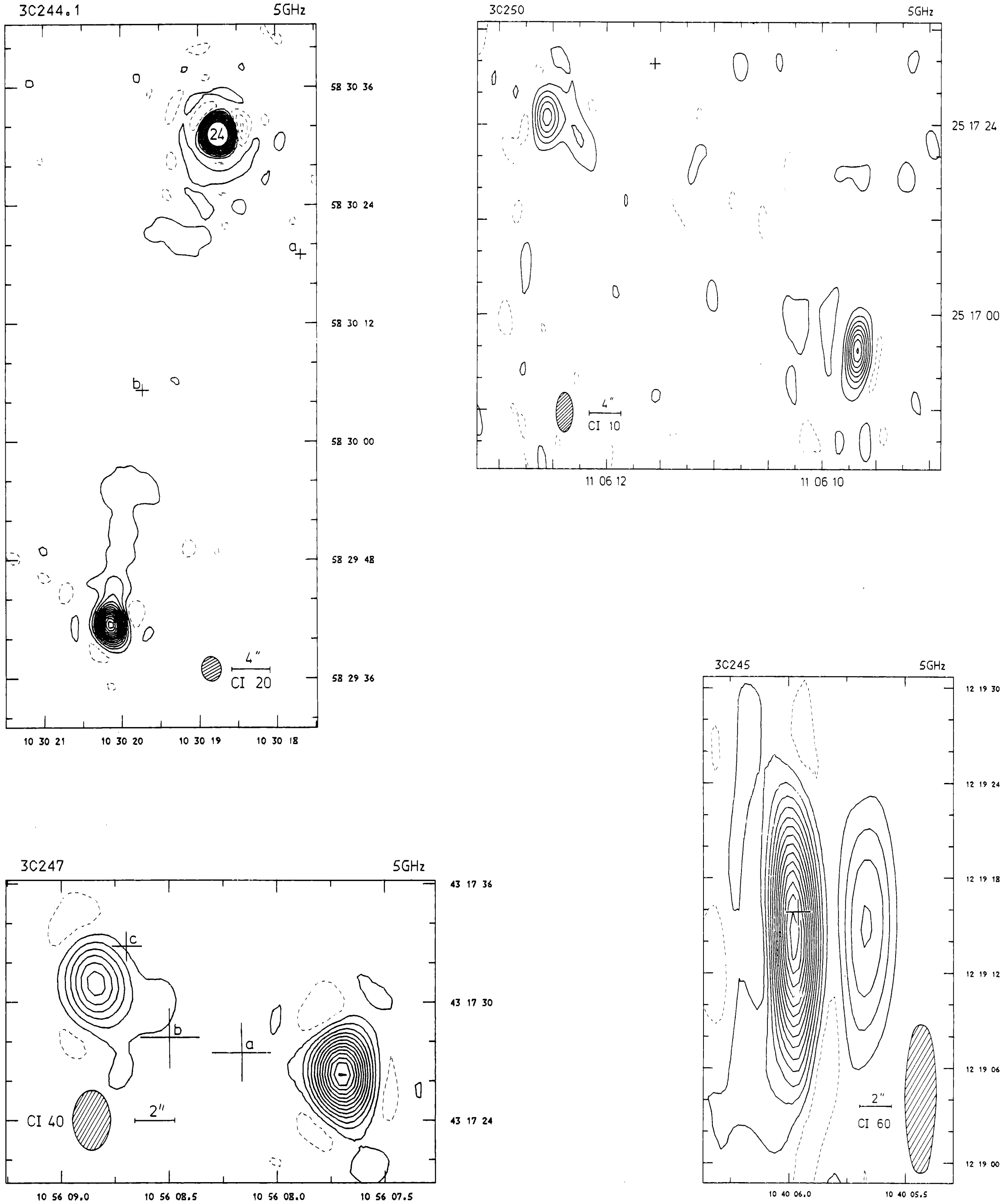

Figure 13. *3C 244.1.* The crosses mark the positions of (a) 19 mag red object and (b) 19 mag red galaxy.
3C 245. The object marked is a 17 mag quasar.
3C 247. The crosses mark the positions of (a) and (b) objects at the limit of the red PSS print and (c) a 19 mag blue star.
3C 250. The object marked is only visible on the red PSS print and seems unlikely to be related to the source; there are no other objects in the field (KSK).

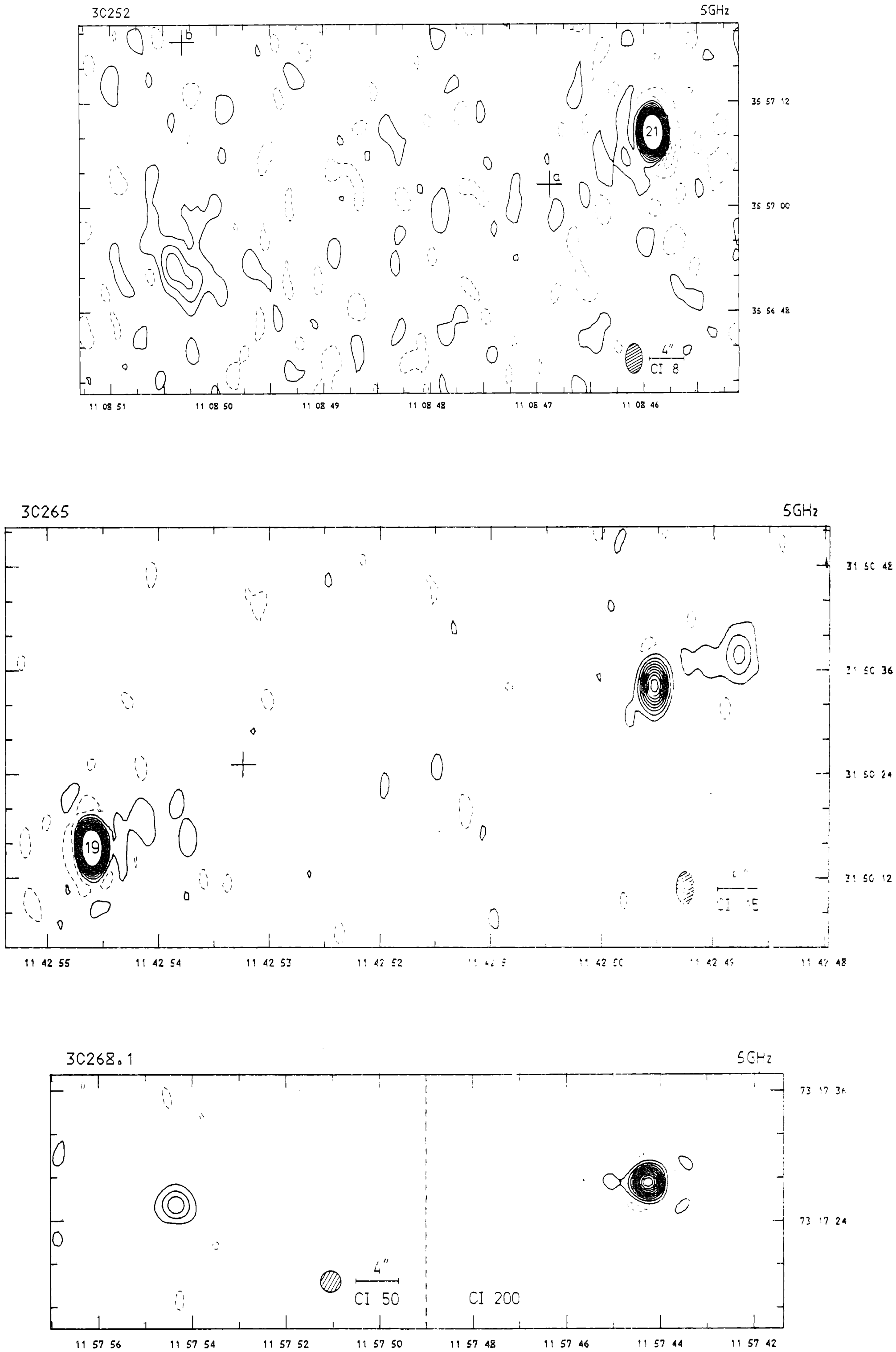

Figure 14. *3C 252.* Objects a and b are at the limit of the red PSS print and not visible on the blue.
3C 265. The cross marks the position of a 20 mag red object.
3C 268.1. There are two different contour intervals on this map. The objects measured are lettered c, g and E by KSK; none of these appears related to the source.

13*

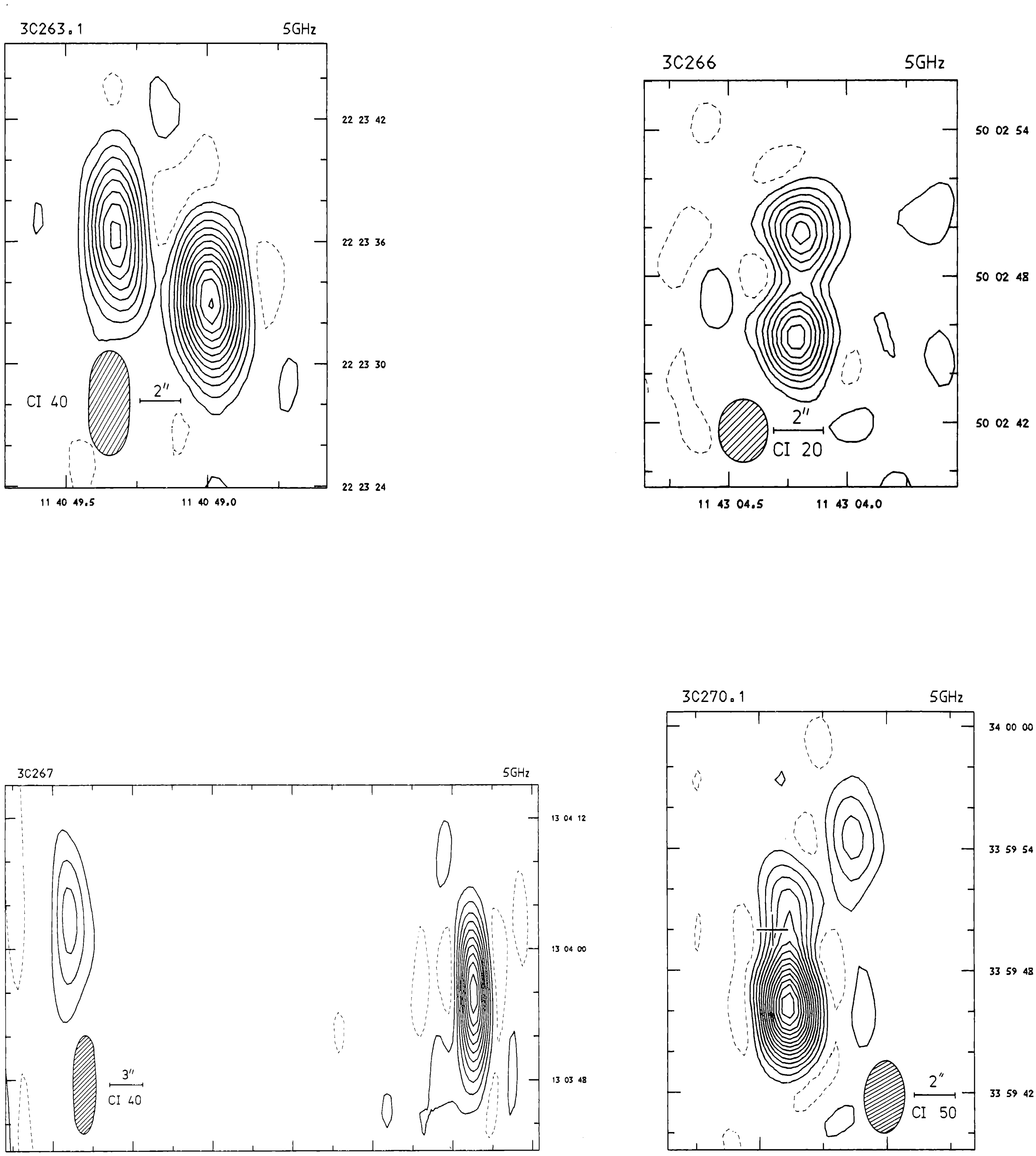

Figure 15. *3C 263.1.* KSK have found a faint red object in the field of this source; no position is given.
3C 266. The optical object marked by Wyndham has been measured and appears unrelated to the source.
3C 267. This source has not been identified.
3C 270.1. The cross marks the position of an 18.6 mag quasar.

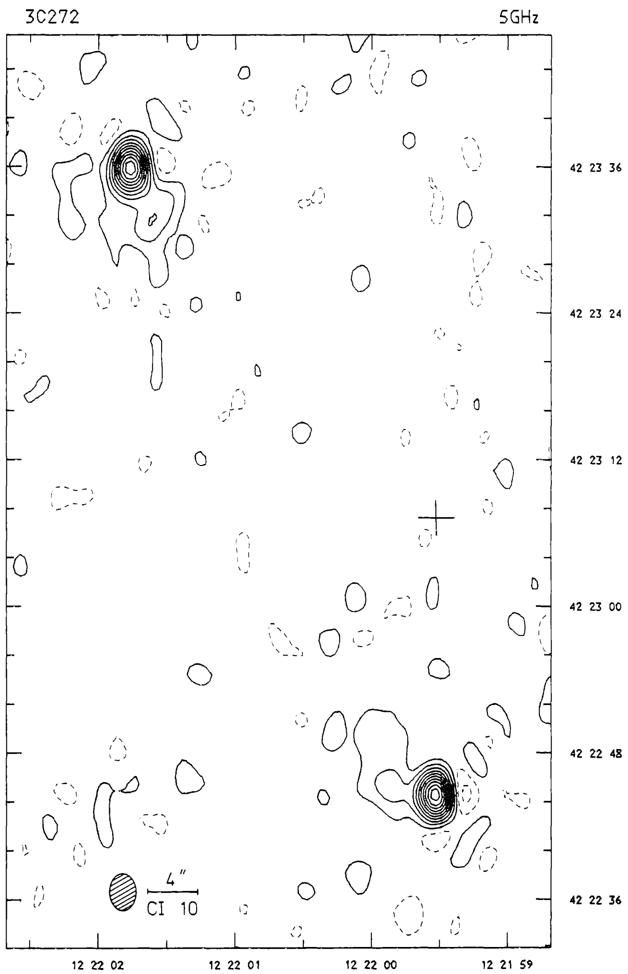

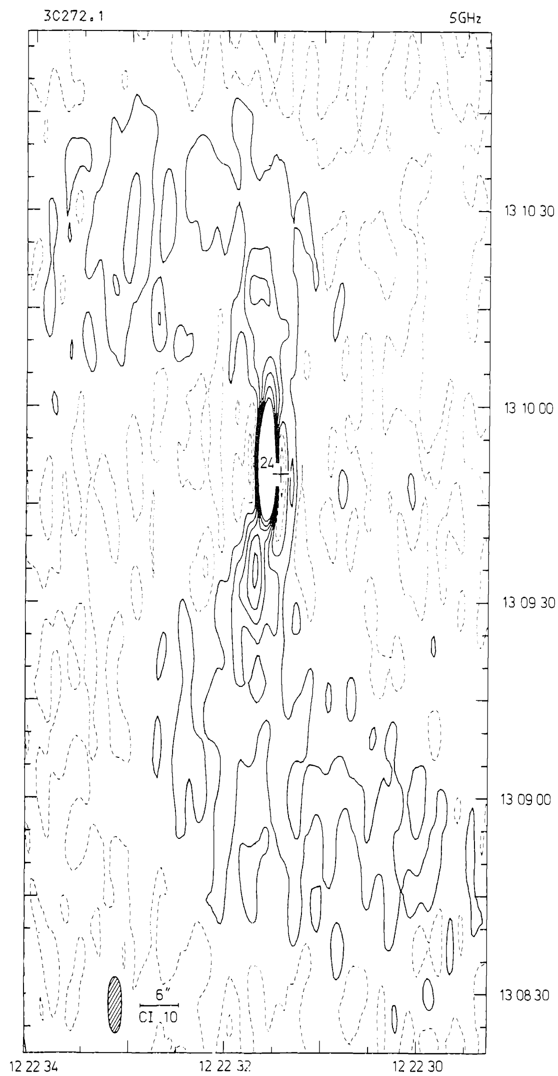

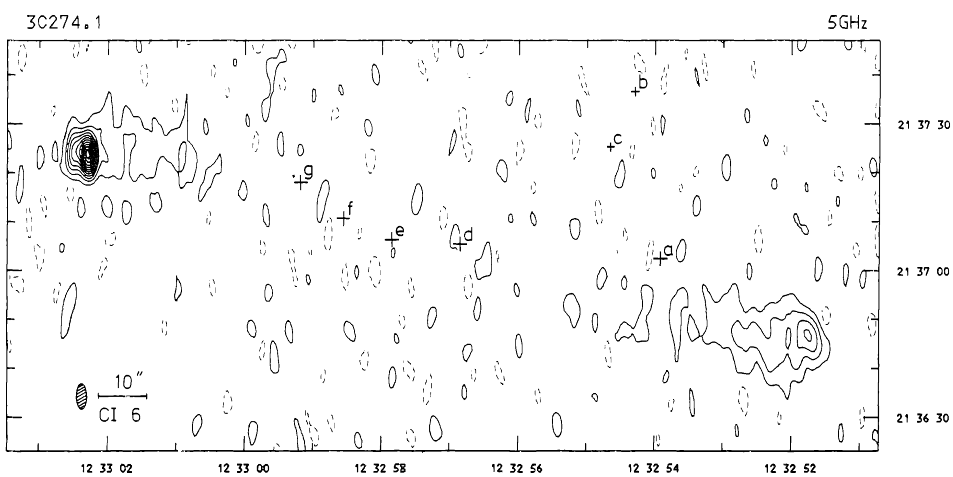

Figure 16. *3C 272.* The cross marks the position of an object at the limit of the blue PSS print, presumably the same object as found by KSK.

3C 272.1. The cross marks the centre of the E2 galaxy M84 in the Virgo cluster; the radio source lies within the galaxy.

3C 274.1. The crosses mark the positions of (a), (d), (e), (f) and (g) objects at the limit of the red PSS print and not visible on the blue print, (b) 19.5 mag red object and (c) 18.5 mag neutral object.

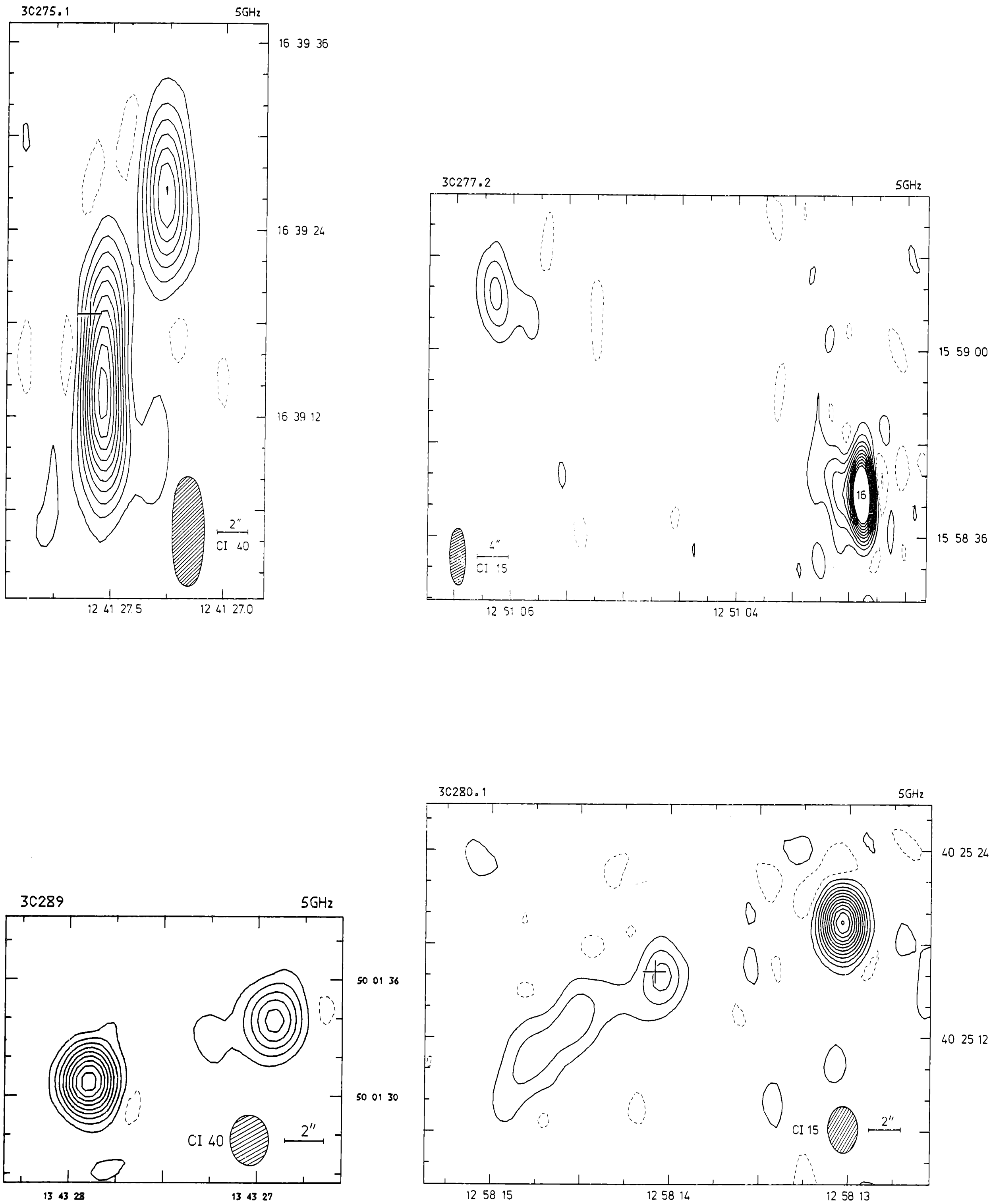

Figure 17. *3C 275.1.* The cross marks the position of a 19 mag quasar.
3C 277.2. This source has not been identified.
3C 280.1. The cross marks the position of a 19 mag quasar.
3C 289. This source has not been identified (KSK).

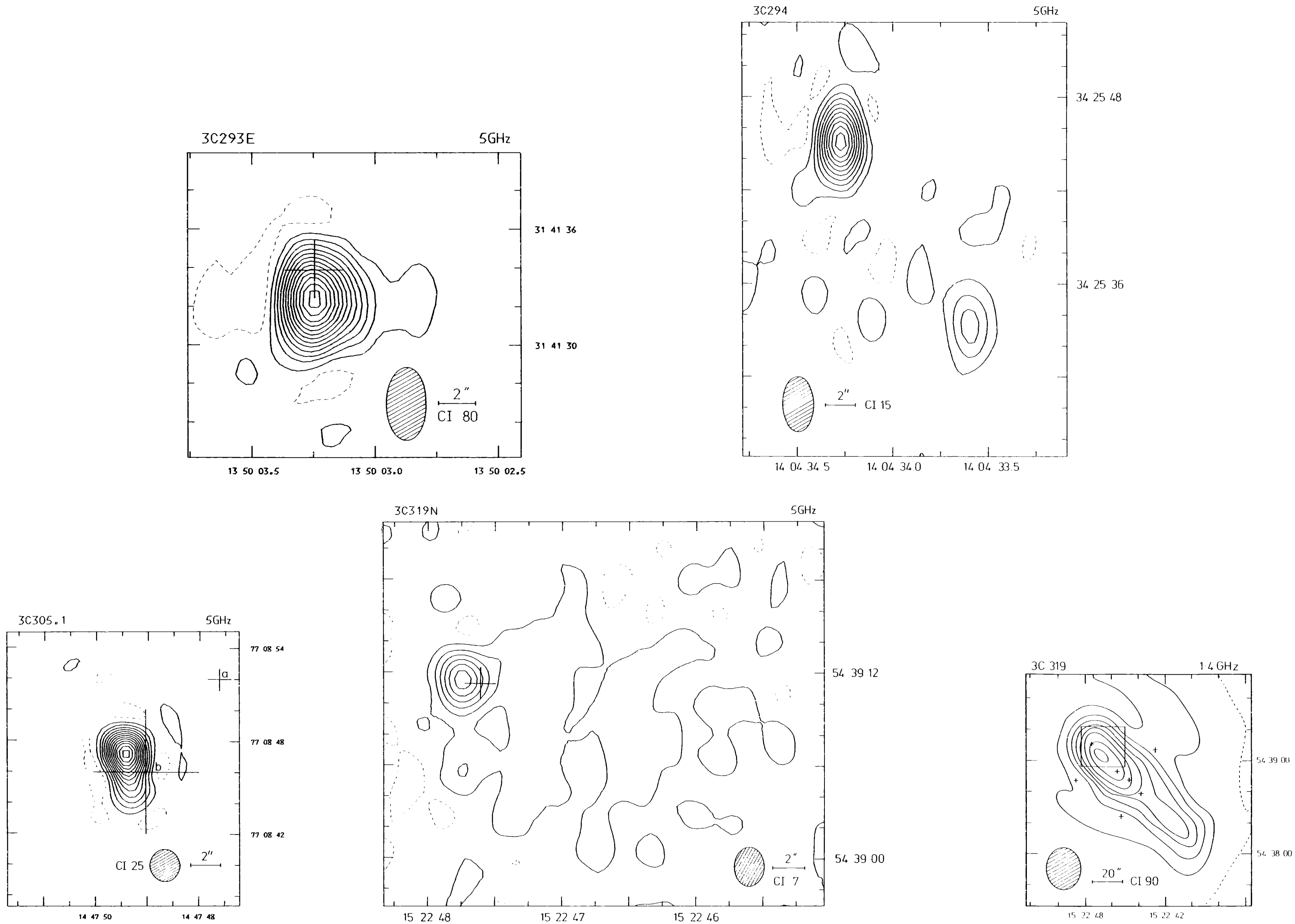

Figure 18. *3C293.* The cross marks the centre of a 14.5 mag galaxy; there is another weak radio component to the north-west (BEPR).
3C294. This source has not been identified (KSK).
3C305.1. Object a is a 19 mag red object; object b is a very faint object (KSK) which is not visible on the PSS prints.
3C319. The overall structure of the source is shown on the 1.4-GHz map from MKN; the crosses mark the positions of 18.5–19.5 mag red objects. The high-resolution map of the northern component is shown separately; there is no other unresolved structure brighter than 10 mJy.

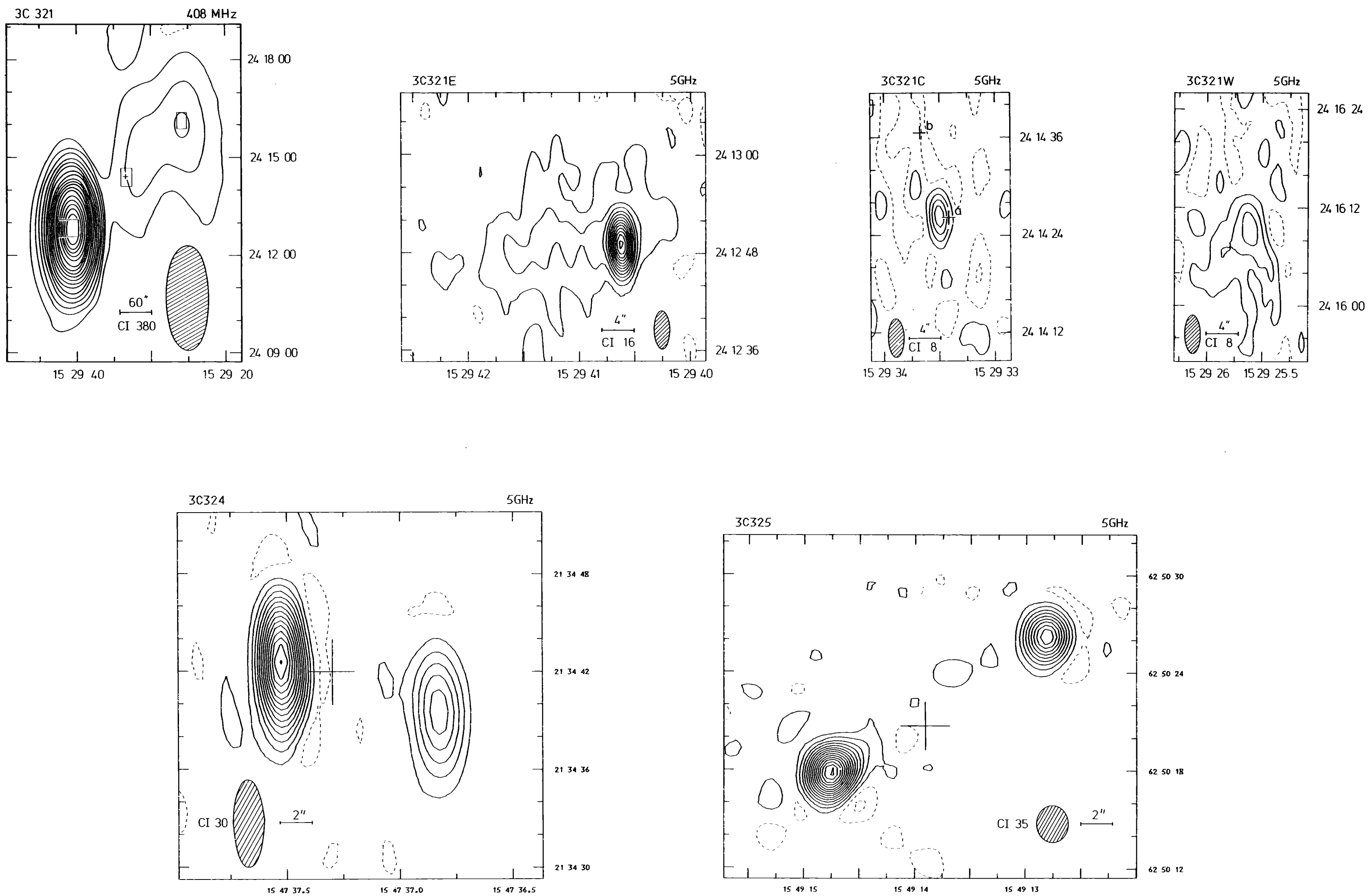

Figure 19. *3C321.* The low-resolution map was made with the One-Mile telescope at 408 MHz; this is discussed further in the notes to Table 1. The 5-GHz maps of the outer components and the central component are shown separately; the crosses mark the positions of (a) a 16 mag galaxy with a redshift of 0.096 and (b) a 16.5 mag stellar object (star D of KSK).
3C324. This source is identified with a very faint galaxy in a cluster (KSK), not visible on the PSS prints; the position of this galaxy as estimated by KSK is marked.
3C325. The cross marks the position of a very faint object at the limit of the red PSS print.

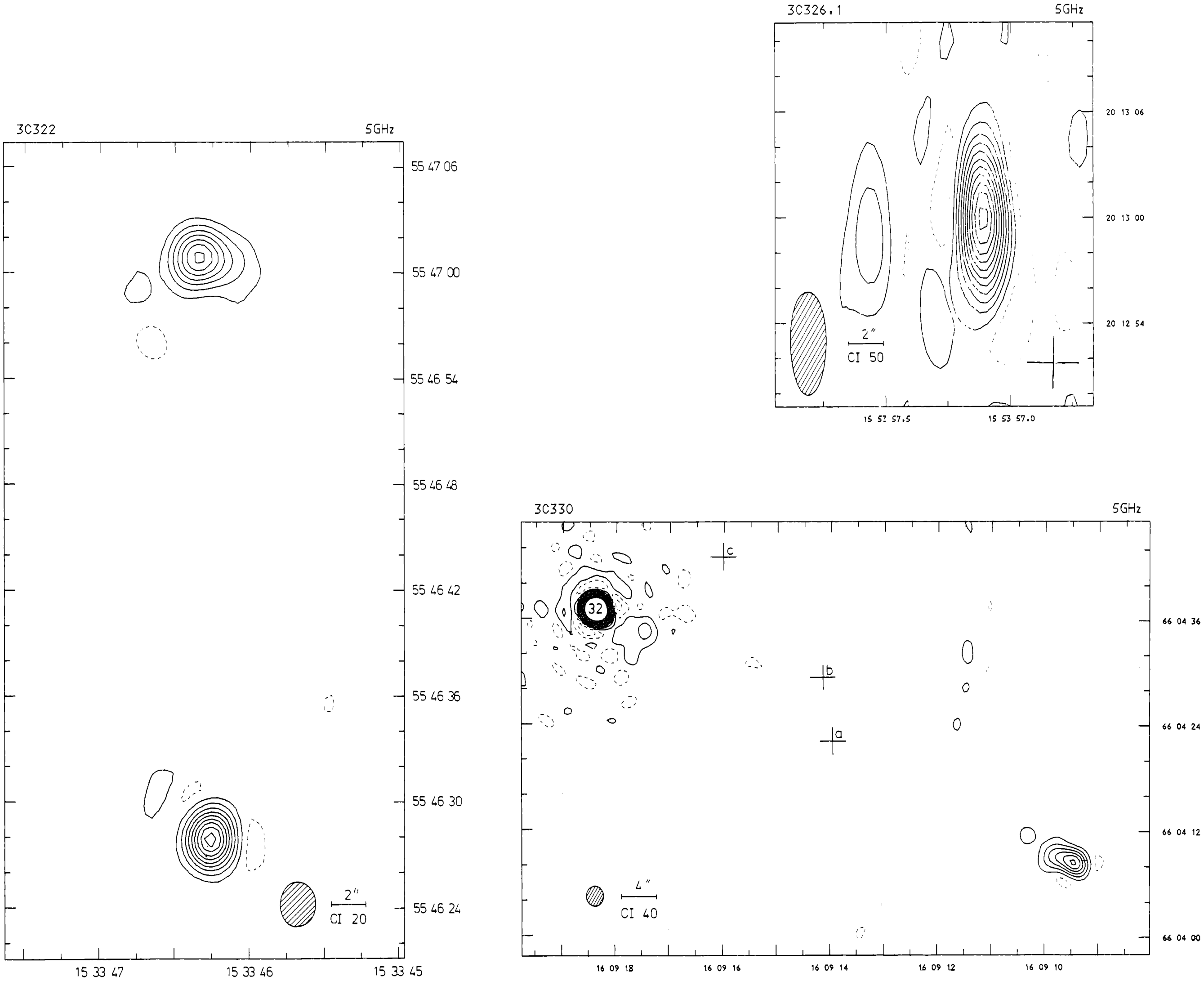

Figure 20. *3C 322.* The optical object marked by Wyndham has been measured and appears unrelated to the source.
3C 326.1. The cross marks the position of a very faint red object (object a of KSK).
3C 330. This source is identified with a faint cluster of galaxies (KSK). The positions of the objects marked were measured on a print of the plate taken by KSK; they are the galaxies marked by KSK.

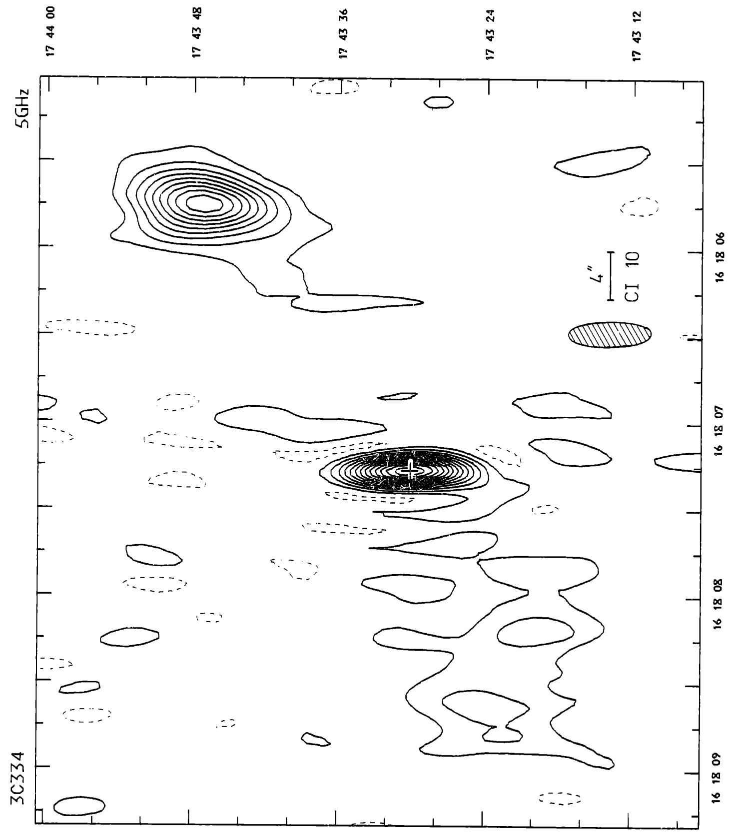

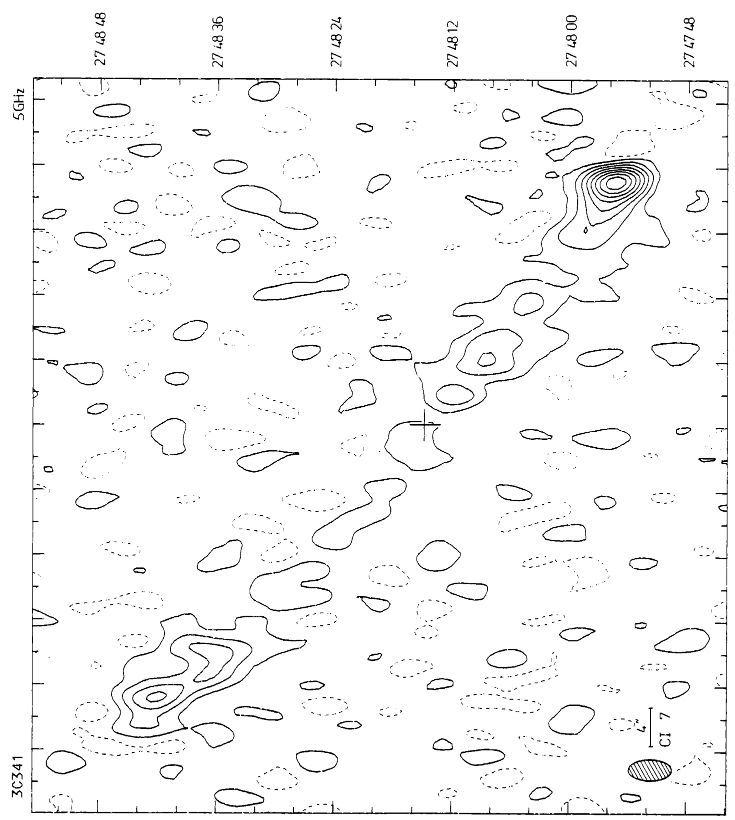

Figure 21. *3C 334.* The cross marks the position of a 16 mag quasar.
3C 341. The cross marks the position of a 20 mag object.

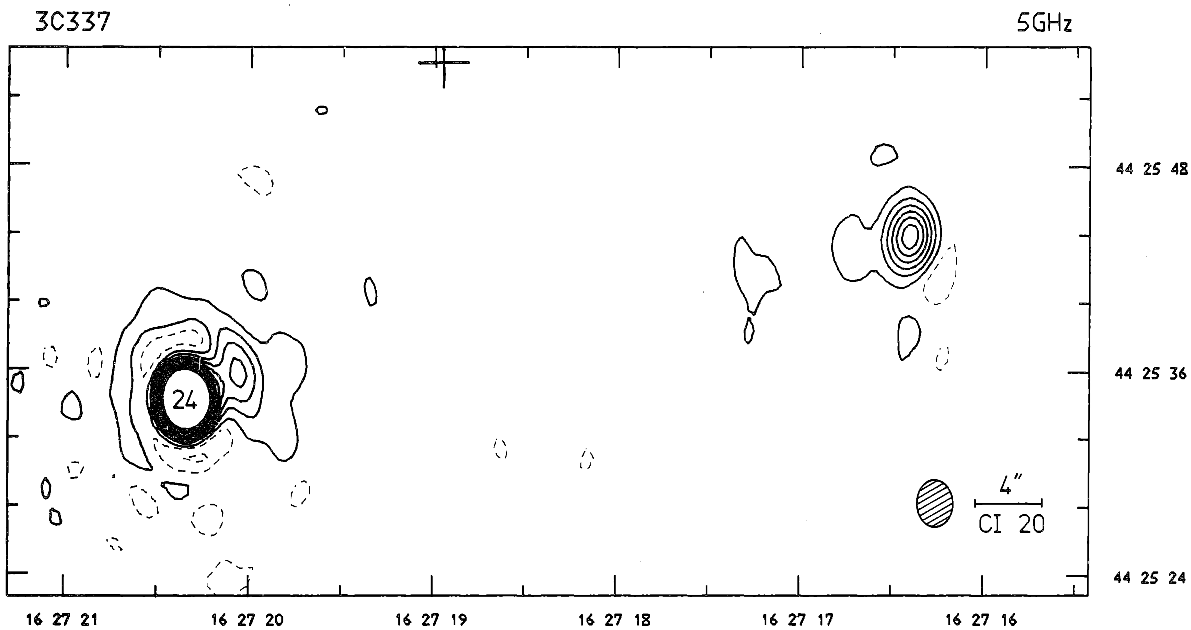

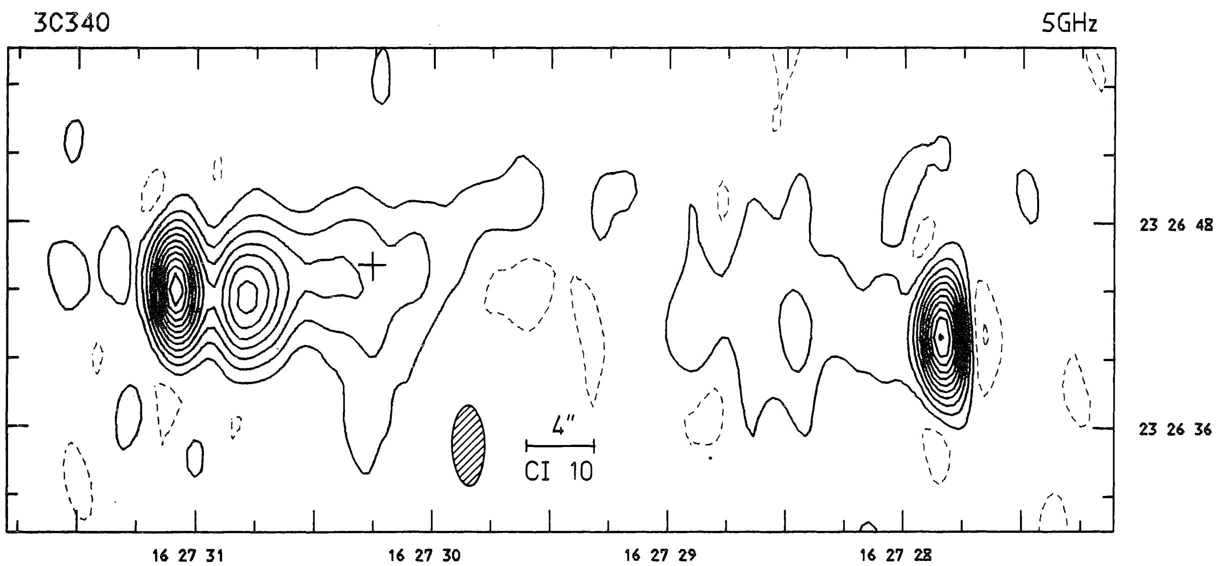

Figure 22. *3C 337.* The cross marks the position of a very faint blue object (object a of KSK). The source has been identified by KSK with a very faint group of galaxies lying on the line between the components.
3C 340. The cross marks the position of a 19 mag reddish object.

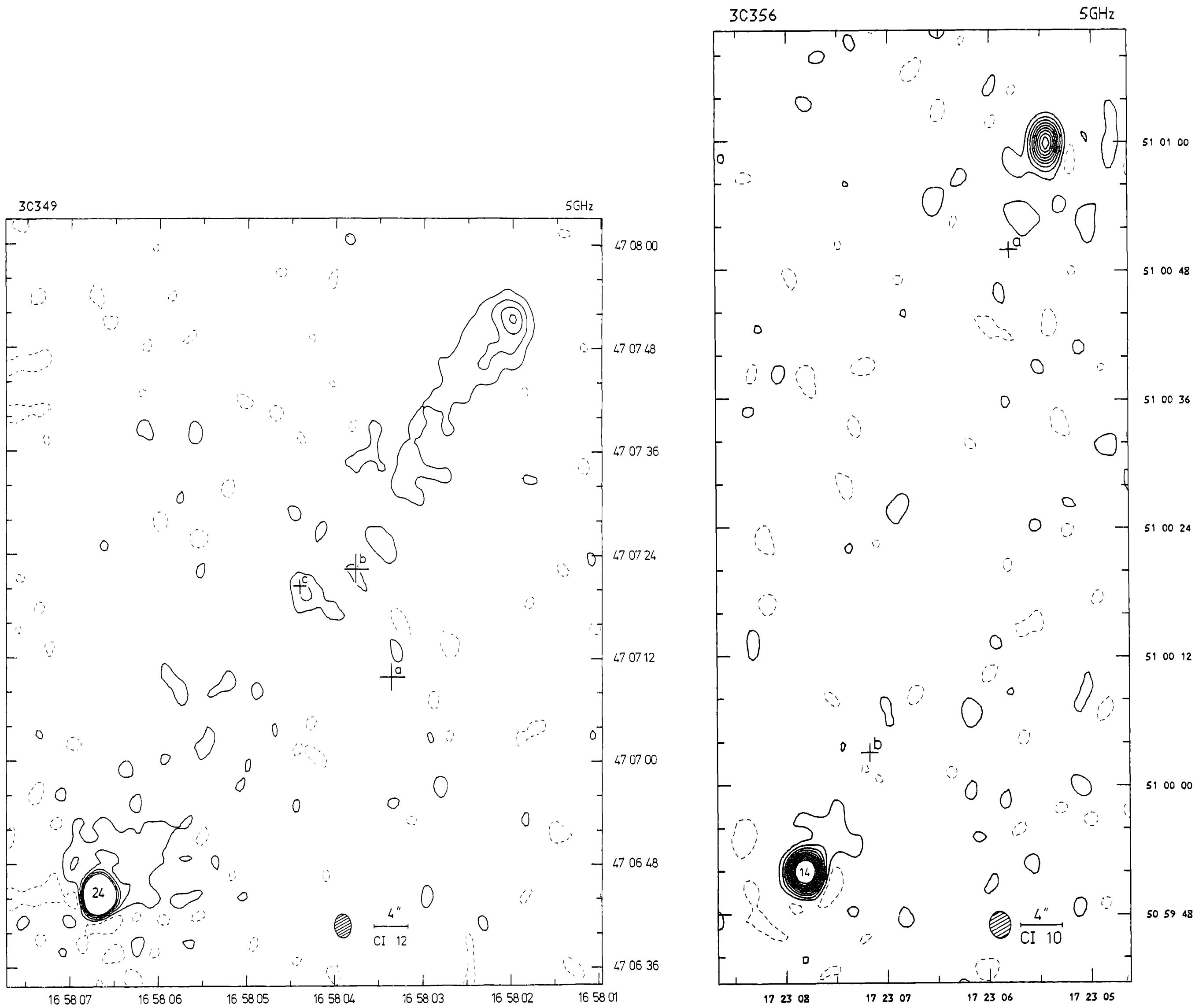

Figure 23. *3C 349.* The crosses mark the positions of (a) a 20 mag object (b) a 19.5 mag object and (c) a 19 mag galaxy with a redshift of 0.205.
3C 356. Objects a and b are 18 and 15 mag stars respectively (objects M and N of KSK); there are no other objects lying between the two radio components (KSK).

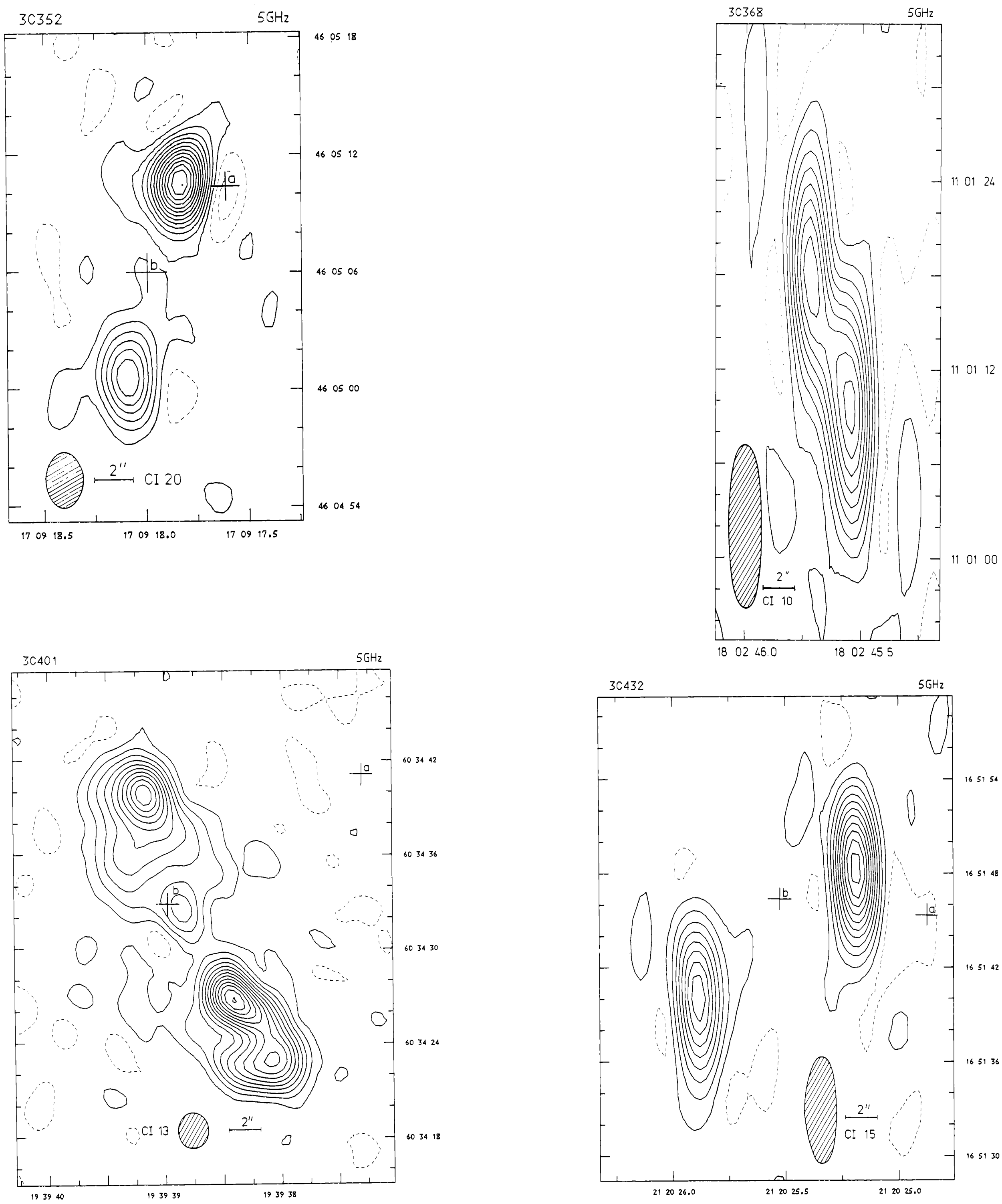

Figure 24. *3C 352.* This source is identified with a very faint diffuse object (KSK), not visible on the Sky Survey prints; the cross b marks the position of this object given by KSK. Object a is a 16 mag star.
3C 368. This source is unidentified.
3C 401. Object a is a 19 mag galaxy; object b is an 18 mag galaxy with a redshift of 0.201.
3C 432. This source is identified with an 18 mag quasar (object b); object a is a 19 mag stellar object.

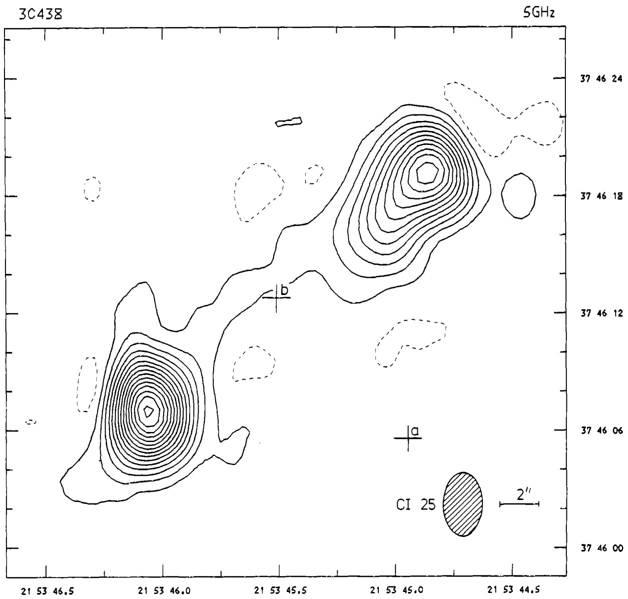

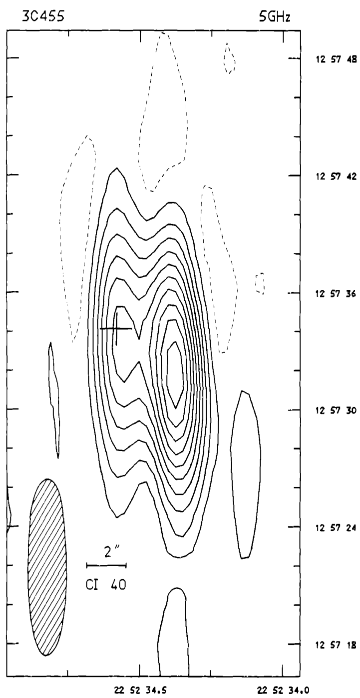

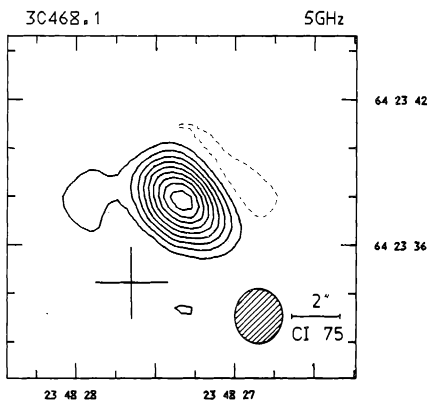

Figure 25. *3C438.* The source is identified with a 20 mag galaxy (object b), the brightest in a rich cluster (LG); object a is an 18 mag star.
3C455. The cross marks the position of a 19.5 mag quasar.
3C468.1. The cross marks the position of an object at the limit of the red PSS print; it is probably unrelated to the source.

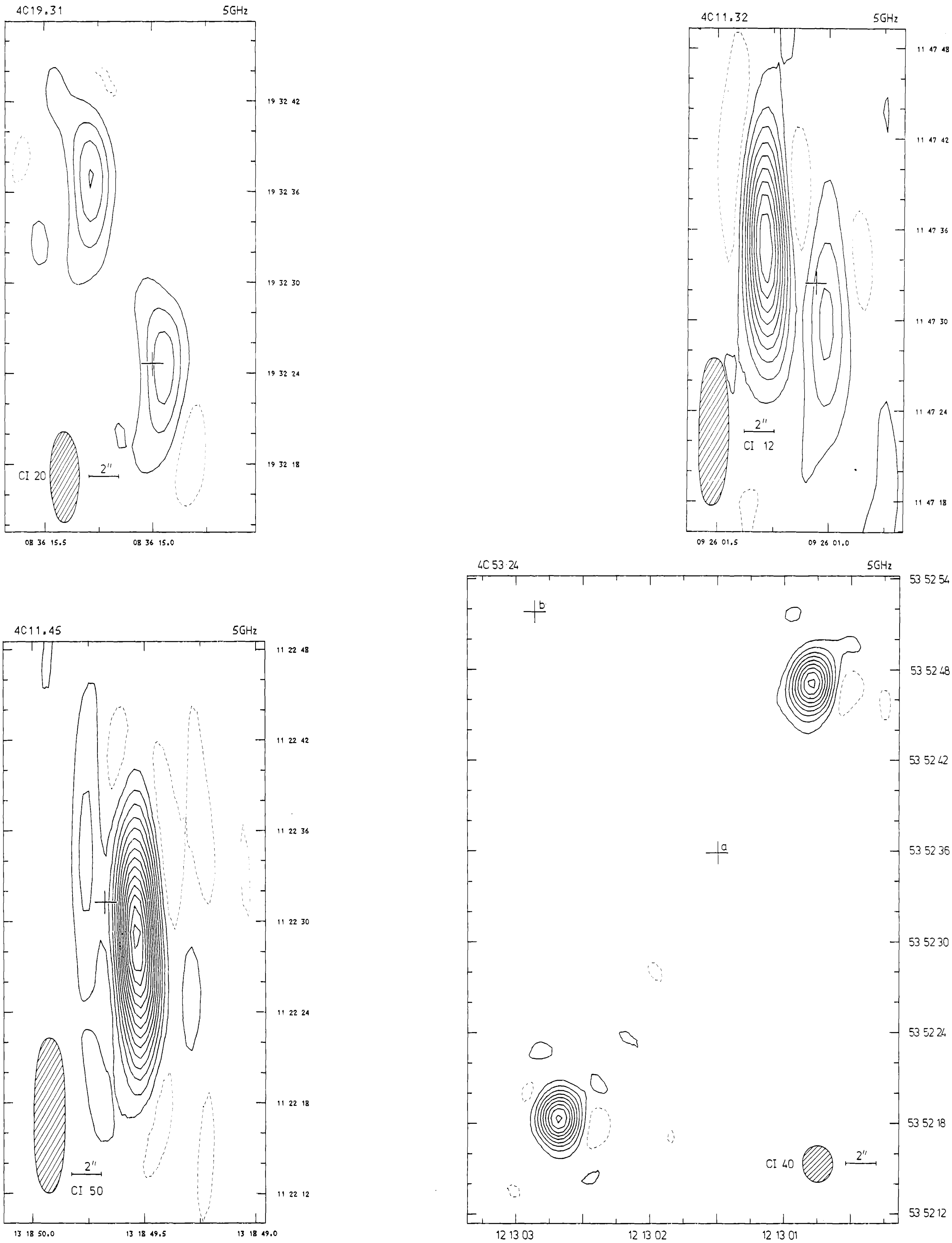

Figure 26. *4C 19.31.* The cross marks the position of a 17.7 mag quasar.
4C 11.32. The cross marks the position of a 19 mag quasar.
4C 53.24. The crosses mark the positions of (a) a 17 mag neutral stellar object and (b) a 19.5 mag red stellar object.
4C 11.45. The cross marks the position of a 19 mag quasar.

Table 1.

Source 3C	N	RA h m s	± s	dec ° ′ ″	± ″	Component pa °	ω_1 ″	ω_2 ″	Flux density mJy	±	θ ″	Integrated flux density mJy	±	z	Distance Mpc	Total size kpc
13	16	00 31 32.36	0.03	39 07 53.5	0.5	-	< 1.0	< 1.5	390	40	28	520	80	-	-	-
		33.76	0.03	30.7	0.5	-	< 1.0	1.9	120	20						
14	16	00 33 29.27	0.02	18 21 36.6	1.0	-	2.6	4.5	370	40	24	640	100	-	-	-
		29.53	0.02	13.6	1.0	-	< 1.1	4.5	190	20						
16	16	00 35 08.10	-	13 03 22.1	-	60	∼ 9	∼ 7	570	100	-	570	100	-	-	-
19	16	00 38 13.70	0.02	32 53 37.2	0.4	-	< 1.0	2.5	530	50	9.6	1280	100	-	-	-
		13.91	0.02	42.2	0.4	-	< 1.0	< 2.0	750	80						
20	32	00 40 17.40	0.03	51 47 16.0	0.4	-	1.7	2.0	1400	150	53	3900	200	-	-	-
		22.42	0.03	05.6	0.4	-	< 1.0	1.7	250	30						
		22.58	0.03	00.2	0.4	-	2.2	1.7	560	60						
Optical		(19.02	0.10	22.3	0.9)											
		20.04	0.10	10.8	0.9											
		20.39	0.10	08.2	0.9											
		21.37	0.10	08.8	0.9											
		(22.92	0.10	46 50.7	0.9)											
22	16	00 48 03.32	0.02	50 55 47.5	0.3	-	< 1.0	1.3	320	30	24	700	100	-	-	-
		05.84	0.02	42.0	0.3	-	< 1.0	1.3	420	40						
Optical		05.51	0.07	46.2	0.7											
31	16	01 04 39.17	0.02	32 08 44.3	0.6	-	< 1.0	< 1.7	140	15	≈ 1000	-	-	0.0169	100	480
Optical		(29.91	0.08	15 12.0	1.0)											
		(31.76	0.08	12 57.2	1.0)											
		(32.21	0.06	09 26.8	0.7)											
		(38.05	0.06	08 13.0	0.7)											
		39.16	0.08	08 43.6	1.0											
		(39.25	0.08	01 32.8	1.0)											
		(41.40	0.08	03 10.9	1.0)											
		(45.52	0.06	05 42.1	0.7)											
		(47.23	0.06	07 26.5	0.7)											
33.1	16	01 06 19.21	-	72 56 59.1	-	-	4.0	2.5	200	50	216	-	-	0.173	920	820
Optical		(05 58.36	0.15	55 48.1	0.7)											
		(06 01.78	0.15	55 37.4	0.7)											
		(04.53	0.20	55 52.0	1.0)											
		(04.57	0.20	56 05.8	1.0)											
		06.48	0.15	55 59.2	0.7											
34	32	01 07 30.82	-	31 31 20.9	-	-	12	4	160	30	48	430	100	-	-	-
		34.39	0.02	25.1	0.6	-	1.7	2.3	150	15						
35*	16	- - -	-	- - -	-	-	-	-	-	-	560	-	-	0.0677	390	980
Optical		01 09 05.00	0.07	49 12 39.2	0.7											
		(05.45	0.07	49.0	0.7)											
36	16	01 15 03.41	0.03	45 20 31.8	0.4	-	< 1.4	< 1.8	200	20	9	390	50	-	-	-
		03.59	0.05	36.7	0.7	-	< 1.0	< 1.8	80	20						
		03.69	0.05	39.8	0.7	-	< 1.0	< 1.8	80	20						
Optical		(03.01	0.09	40.9	1.0)											
42	16	01 25 41.89	0.02	28 47 40.0	0.6	-	1.3	2.8	290	30	28	960	100	0.3952	1800	180
		43.50	0.02	21.6	0.6	322	2.9	2.5	440	50						
Optical		(42.57	0.11	23.8	1.5)											
		42.68	0.11	30.4	1.5											
		(42.69	0.11	18.1	1.5)											
43*	16	01 27 15.048	0.007	23 22 52.2	0.2	-	< 0.5	< 1.5	1150	50	-	1150	50	-	-	-
Optical		15.04	0.05	51.5	0.7											
46	16	01 32 28.7	-	37 38 26	-	-	-	-	90	30	168	400	100	-	-	-
		40.8	-	39 24	-	-	-	-	75	30						
Optical		(33.84	0.07	39 01.4	0.8)											
		34.09	0.07	38 47.0	0.8											
		(34.50	0.09	38 27.5	1.0)											

1977MNRAS..84...61J

Table 1 – *continued*

Source 3C	N	RA h m s	± s	dec ° ′ ″	± ″	Component pa °	ω_1 ″	ω_2 ″	Flux density mJy	±	θ ″	Integrated flux density mJy	±	z	Distance Mpc	Total size kpc
49*	16	01 38 28.49	0.04	13 38 19	2	–	< 1.0	< 5.0	900	50	–	900	50	–	–	–
55	32	01 54 16.38	0.02	28 37 06.3	0.4	–	< 1.0	< 2.0	190	20	72	640	100	–	–	–
		20.93	0.04	36 59.1	1.0	–	1.8	4.6	80	20						
		21.61	0.02	37 01.4	0.4	61	4.5	2.1	340	30						
Optical		19.50	0.11	37 04.8	1.5											
68.1	32	02 29 26.95	0.02	34 10 55.7	0.4	–	1.5	1.4	700	70	46	800	80	1.237	4000	400
Optical		27.24	0.08	34.1	1.0											
76.1*	16	– – –	–	– –	–	–	–	–	–	–	45	–	–	0.0328	190	40
Optical		03 00 27.28	0.05	16 14 36.1	0.7											
		(27.56	0.05	12.2	0.7)											
98	64	03 56 06.52	–	10 15 07.5	–	–	–	–	2900	300	295	4500	300	0.0306	180	250
		14.46	–	19 25.2	–	–	–	–	2200	200						
Optical		10.25	0.05	17 32.9	0.8											
111	64	04 14 55.29	–	37 53 40.6	–	–	–	–	1000	100	216	7700	500	0.05	290	290
		15 00.61	0.02	54 19.4	0.4	–	< 1.0	< 1.0	3300	100						
		09.73	0.02	55 14.8	0.4	–	1.4	1.8	900	50						
Optical		00.61	0.08	54 19.0	0.7											
132	16	04 53 41.63	0.02	22 44 50.0	0.5	–	1.4	< 2.0	90	10	23	1200	100	0.214	1110	102
		41.99	0.05	45.8	1.3	–	4.5	4.0	460	50						
		42.74	0.02	36.8	0.5	117	7.7	3.0	780	80						
Optical		42.18	0.05	43.9	0.7											
		(42.63	0.05	41.8	0.7)											
133	16	04 59 53.84	0.02	25 12 12.7	0.7	–	< 1.0	< 2.7	600	60	11.8	2100	100	–	–	–
		54.25	0.02	11.5	0.7	–	< 1.0	< 3.0	410	40						
		54.67	0.02	09.2	0.7	148	3.3	2.9	940	90						
Optical		(52.64	0.06	35.7	1.0)											
		(53.88	0.06	30.2	1.0)											
		(54.19	0.06	01.0	1.0)											
173.1	32	07 02 45.12	0.10	74 53 46.4	0.4	–	2.5	1.8	280	60	60	900	100	0.292	1400	320
		49.74	0.12	54 41.5	0.5	22	3.6	2.4	200	40						
Optical		48.05	0.17	54 16.9	0.7											
175	32	07 10 13.86	0.01	11 51 06.9	1.0	–	3.0	8.0	320	50	48	670	70	0.768	3000	390
		15.38	0.01	23.1	1.0	–	< 2.0	< 5.0	40	8						
		16.61	0.01	33.7	1.0	–	< 2.0	< 7.0	390	40						
Optical		15.44	0.05	23.7	0.7											
		(15.83	0.05	23.0	0.7)											
		(15.91	0.05	31.3	0.7)											
175.1	16	07 11 14.16	0.01	14 41 30.8	0.8	–	< 1	< 4	280	30	7	550	50	–	–	–
		14.60	0.01	33.7	0.8	–	< 1	< 4	200	20						
Optical		(14.30	0.05	28.8	0.8)											
184	16	07 33 58.41	0.06	70 30 02.0	0.3	–	< 1	< 1	300	30	4.4	590	60	–	–	–
		59.25	0.06	00.8	0.3	–	< 1	< 1	320	30						
190*	16	07 58 45.00	0.02	14 23 03.2	1.2	–	2	< 4	830	80	–	830	80	–	–	–
Optical		45.00	0.10	04.5	1.5											
191*	16	08 02 03.77	0.04	10 23 56.5	4.0	–	< 0.8	< 4.0	590	60	–	590	60	1.95	5000	< 7
Optical		03.77	0.06	57.0	0.8											
192	16	08 02 29.21	0.03	24 19 22.9	1.0	–	3.3	< 4.0	170	20	190	–	–	0.0597	340	300
Optical		35.41	0.06	18 26.9	0.9											
		(36.40	0.06	20.5	0.9)											

Table 1 – *continued*

Source 3C	N	RA h m s	± s	dec ° ′ ″	± ″	Component pa °	ω₁ ″	ω₂ ″	Flux density mJy	±	θ ″	Integrated flux density mJy	±	z	Distance Mpc	Total size kpc
200	16	08 24 21.18	0.02	29 28 46.6	0.6	25	3.7	1.7	240	25	17	610	60	-	-	-
		21.38	0.02	39.8	0.6	-	< 1.0	< 2.0	88	15						
		21.68	0.02	30.9	0.6	-	6.0	2.0	270	40						
Optical		21.39	0.06	40.3	0.8											
208	16	08 50 22.34	0.03	14 04 15.4	2.0	-	1.7	5.5	110	10	11	580	60	1.109	3700	94
		22.66	0.03	15.7	2.0	-	< 1.0	< 4.0	54	5						
		23.09	0.01	18.0	0.8	-	< 1.0	5.0	410	40						
Optical		22.68	0.05	17.3	0.7											
212	16	08 55 55.32	0.03	14 21 26.8	1.6	-	< 1.5	< 6.0	190	30	9	980	100	1.063	3600	77
		55.51	0.03	23.5	1.6	-	< 1.5	< 6.0	310	50						
		55.73	0.02	21.0	1.2	-	< 1.5	< 6.0	440	40						
Optical		55.59	0.05	25.3	0.7											
216*	16	09 06 17.260	0.007	43 05 59.36	0.11	-	-	-	-	-	0.8	1810	100	0.67	2710	6
Optical		17.07	0.20	58.6	2.0											
217	16	09 05 40.64	0.02	38 00 31.8	0.3	-	1.5	< 1.6	250	25	12	430	40	-	-	-
		41.63	0.02	28.9	0.3	-	1.5	< 1.6	220	20						
220.1	16	09 26 26.56	0.20	79 19 41.4	0.5	78	7	1	280	40	30	540	50	-	-	-
		32.34	0.20	43.8	0.5	-	< 1	< 1	25	5						
		36.06	0.15	44.8	0.4	-	2	< 1 }	360	40						
		37.13	0.07	46.2	0.2	-	< 1	2 }								
Optical		32.2	0.4	43.8	1.0											
220.2	16	09 27 29.69	0.03	36 14 33.7	0.7	-	1.3	< 2.0	340	30	8	640	60	1.157	3800	69
		29.91	0.04	36.7	0.8	-	< 1	< 3	60	15						
		30.15	0.03	39.7	0.7	-	1.0	< 2.0	230	20						
Optical		29.95	0.06	36.9	0.7											
220.3	16	09 31 09.5	0.2	83 28 57.1	0.3	-	2	2	340	35	7.4	580	60	-	-	-
		12.6	0.2	52.4	0.3	-	2.6	2.3	300	30						
Optical	(	13.6	0.4	37.2	0.7)											
	(	19.0	0.4	29 10.2	0.7)											
	(	22.8	0.4	28 21.4	0.7)											
225A	16	09 39 25.17	0.01	14 05 35.9	0.8	15	4.4	< 3	380	40	-	380	40	-	-	-
Optical	(	24.89	0.05	36.4	0.7)											
225B	16	09 39 32.08	0.01	13 59 33.9	0.8	-	< 1	< 4	500	50	4.6	930	90	-	-	-
		32.37	0.01	31.6	0.8	-	< 1	< 4	330	30						
226	16	09 41 35.56	0.01	10 00 18.5	1.2	-	< 1.5	< 5.0	240	25	35	620	60	-	-	-
		36.79	0.01	09 59 53.7	1.2	-	< 1.0	< 5.0	210	20						
Optical	(	36.97	0.05	59.2	0.7)											
228	16	09 47 27.47	0.01	14 33 41.6	0.8	-	1	5.5	540	80	45	1200	100	-	-	-
		28.00	0.03	34 25.8	1.7	32	5	-	680	100						
241*	16	10 19 09.356	0.007	22 14 39.5	0.3	-	< 1.0	< 2.0	380	40	-	380	40	-	-	-
243*	16	10 23 55.34	0.01	06 43 00	10	-	-	-	220	40	-	220	40	1.699	4700	-
Optical		55.15	0.05	42 50.7	0.7											
244.1	32	10 30 18.75	0.03	58 30 31.2	0.2	-	1.0	1.2	580	60	53	1250	100	-	-	-
		20.15	0.03	29 41.4	0.2	-	1.0	2.0	400	60						
Optical	(	17.65	0.09	30 18.9	0.7)											
		19.75	0.09	05.2	0.7											

Table 1 – *continued*

Source 3C	*N*	RA h m s	± s	dec ° ′ ″	± ″	Component pa °	ω_1 ″	ω_2 ″	Flux density mJy	±	θ ″	Integrated flux density mJy	±	*z*	Distance Mpc	Total size kpc
245	16	10 40 05.67	0.02	12 19 15.0	1.4	–	1.7	< 6.0	350	40	4.6	1600	100	1.029	3600	39
		05.98	0.02	14.5	1.4	–	< 1.0	< 7.0	1200	100						
Optical		05.96	0.05	15.9	0.7											
247	16	10 56 07.70	0.03	43 17 26.3	0.4	–	< 1	< 2.0	670	70	13	930	90	–	–	–
		08.84	0.03	30.9	0.4	–	1.3	< 2.0	340	35						
Optical		08.17	0.14	27.4	1.5											
		08.51	0.14	28.1	1.5											
		(08.70	0.06	32.8	0.7)											
250	32	11 06 09.67	0.01	25 16 55.5	0.5	–	< 1.0	4.0	110	10	49	300	60	–	–	–
		12.56	0.02	17 25.0	0.7	–	1.8	< 2.0	70	10						
Optical		(11.55	0.05	31.7	0.7)											
252	32	11 08 45.91	0.02	35 57 08.4	0.4	–	< 1.0	1.7	200	20	60	350	80	–	–	–
		50.41	0.08	56 53.4	1.5	42	6	1.8	140	30						
Optical		46.89	0.12	57 02.6	1.5											
		(50.33	0.12	57 19.0	1.5)											
263.1	16	11 40 48.99	0.02	22 23 32.9	0.8	–	1.5	< 2.5	630	60	5.8	960	90	–	–	–
		49.33	0.02	36.3	0.8	–	< 1.0	2.5	370	40						
264*	16	11 42 29.58	0.02	19 53 02.7	0.4	–	< 2.6	< 3.3	400	50	55	–	–	0.0206	120	32
Optical		(28.46	0.06	54.2	0.8)											
		29.56	0.06	02.8	0.8											
265	32	11 42 48.74	0.03	31 50 37.8	0.8	–	2.2	3	50	10	78	720	80	–	–	–
		49.54	0.01	34.3	0.4	–	1.5	2.2	210	20						
		54.61	0.01	15.6	0.4	–	1.1	2.1	380	40						
Optical		53.24	0.12	25.1	1.5											
266	16	11 43 04.20	0.02	50 02 49.8	0.4	–	< 1	< 1	170	20	4.3	370	50	–	–	–
		04.21	0.02	45.5	0.4	–	< 1.0	1.3	200	20						
Optical		(06.7	0.04	48.4	0.8)											
267	16	11 47 20.87	0.01	13 03 55.7	0.9	–	< 1.0	7.0	400	40	38	700	70	–	–	–
		23.40	0.03	04 02.5	1.8	–	1.2	< 5.0	140	15						
268.1	32	11 57 44.26	0.05	73 17 27.6	0.2	–	< 1	< 1	2400	200	46	2800	100	–	–	–
		54.33	0.05	25.4	0.2	–	< 1	< 1	230	20						
Optical		(44.3	0.2	08.7	0.8)											
		(47.9	0.2	55.3	0.8)											
		(55.8	0.2	38.8	0.8)											
270.1	16	12 18 03.64	0.02	33 59 54.5	0.6	–	< 1	< 2	130	20	12	1120	50	1.519	4400	100
		03.89	0.02	46.2	0.6	0	4	< 1	1100	100						
Optical		03.95	0.06	50.0	0.7											
272	32	12 21 59.53	0.03	42 22 44.5	0.4	–	1.3	< 1.4	120	15	59	450	50	–	–	–
		22 01.77	0.03	23 36.0	0.4	–	1.3	1.9	140	15						
Optical		21 59.53	0.13	23 07.2	1.5											
272.1	16	12 22 31.58	0.02	13 09 50.7	1.5	–	< 1	< 4	350	35	120	–	–	0.0029	17	10
Optical		31.45	0.10	49.6	1.5											
274.1	64	12 32 51.73	0.07	21 36 46	2	–	–	–	310	60	150	720	60	–	–	–
		33 02.28	0.02	37 23.4	0.8	–	3.0	< 4.0	360	60						
Optical		32 53.91	0.11	02.5	1.5											
		(54.30	0.07	36.4	1.0)											
		(54.61	0.07	24.6	1.0)											
		56.86	0.11	05.5	1.5											
		57.85	0.11	06.2	1.5											
		58.55	0.11	11.1	1.5											
		59.20	0.11	18.1	1.5											

Table 1 – *continued*

Source 3C	N	RA h m s	± s	dec ° ′ ″	± ″	Component pa °	ω_1 ″	ω_2 ″	Flux density mJy	±	θ ″	Integrated flux density mJy	±	z	Distance Mpc	Total size kpc
275.1	16	12 41 27.26	0.02	16 39 26.1	1.0	–	< 1.0	< 3.5	260	25	14	1050	50	0.557	2400	100
		27.53	0.02	13.3	1.5	–	< 1.0	10	680	70						
Optical		27.62	0.05	18.6	0.7											
277.2	32	12 51 02.89	0.02	15 58 41.6	1.0	–	1.5	4.5	350	40	58	530	50	–	–	–
		06.16	0.02	59 07.2	1.0	57	3.4	3.2	60	15						
280.1	16	12 58 13.04	0.02	40 25 19.4	0.4	–	< 1.0	< 1.5	210	20	22	450	50	1.659	4600	190
		14.04	0.03	15.9	0.6	–	< 1.0	< 1.5	55	10						
		14.6	–	12.0	–	134	8.5	< 1.5	210	40						
Optical		14.09	0.04	16.2	0.7											
282*	16	13 06 31.359	0.010	66 00 13.76	0.10	–	–	–	–	–	1.1	710	70	–	–	–
Optical		(28.9	0.2	19.2	1.5)											
285*	16	– – –	–	– – –	–	–	–	–	–	–	134	–	–	0.0797	450	270
Optical		13 19 05.29	0.07	42 50 56.1	0.7											
289	16	13 43 26.91	0.02	50 01 33.9	0.3	–	< 1	< 1	260	30	10	760	80	–	–	–
		27.90	0.02	30.7	0.3	–	1.2	1.1	500	50						
293	16	13 50 03.24	0.02	31 41 32.2	0.6	90	2.2	< 2	1700	100	85	1700	100	0.0453	260	100
Optical		03.24	0.13	33.9	1.5											
294	16	14 04 33.60	0.05	34 25 33.4	0.8	–	< 1	< 2	60	15	15	300	40	–	–	–
		34.27	0.04	45.0	0.6	–	< 1	< 2	180	20						
303.1*	16	14 43 53.81	0.02	77 20 04.58	0.07	–	< 0.5	< 0.5	450	50	–	450	50	–	–	–
Optical		53.7	0.2	20 05.1	0.7											
		(56.6	0.2	19 52.0	0.7)											
305.1	16	14 47 49.39	0.09	77 08 47.3	0.3	9	1.8	< 1	480	50	–	480	50	–	–	–
Optical		(47.6	0.2	52.0	0.7)											
310*	16	15 02 46.88	0.02	26 12 35.4	0.7	–	< 1.0	< 2.0	90	20	250	–	–	0.0543	310	360
Optical		(45.79	0.07	31.3	0.9)											
		46.84	0.07	34.4	0.9											
		(48.07	0.07	27.3	0.9)											
		(50.97	0.07	37.3	0.9)											
314.1*	16	– – –	–	– – –	–	–	–	–	–	–	180	–	–	–	–	–
Optical		15 09 57.88	0.15	70 57 58.8	0.8											
		15 10 11.41	0.15	09.3	0.8											
315*		15 11 30.81	0.02	26 18 39.4	0.4	–	< 1.5	< 4.5	180	20	200	–	–	0.1086	600	530
Optical		(30.70	0.05	32.1	0.7)											
		30.72	0.05	38.8	0.7											
319	32	15 22 47.75	0.05	54 39 11.6	0.5	–	1.7	< 1.4	70	10	64	700	70	–	–	–
Optical		(42.85	0.10	39 06.9	1.0)											
		43.83	0.10	38 38.7	1.0											
		44.70	0.10	38 47.5	1.0											
		(45.37	0.10	38 24.3	1.0)											
		45.56	0.10	38 52.9	1.0											
		47.61	0.10	39 11.2	1.0											
		(48.68	0.10	38 46.7	1.0)											
321*	16	15 29 25.55	0.07	24 16 08	2	30	4.5	2.3	100	20	290	–	–	0.096	540	690
		33.50	0.03	14 26.5	1.0	–	< 1.0	< 2.5	30	5						
		40.63	0.02	12 49.0	0.7	–	1.7	3.3	270	30						
Optical		33.42	0.06	14 26.2	0.8											
		(33.70	0.06	14 36.6	0.8)											

Table 1 – *continued*

Source 3C	N	RA h m s	± s	dec ° ′ ″	± ″	Component pa °	ω_1 ″	ω_2 ″	Flux density mJy	±	θ ″	Integrated flux density mJy	±	z	Dis-tance Mpc	Total size kpc
322	16	15 33 46.25	0.02	55 46 27.8	0.3	–	1.1	1.6	260	25	33	480	50	–	–	–
		46.34	0.02	47 00.9	0.3	–	1.8	< 1.0	200	20						
324	16	15 47 36.82	0.02	21 34 39.6	0.8	–	< 1.0	< 3.0	180	20	10	690	70	–	–	–
		37.53	0.01	42.5	0.6	–	< 1.0	< 3.0	480	50						
325	16	15 49 12.81	0.04	62 50 26.2	0.3	–	< 1.0	1.7	410	40	16	1100	100	–	–	–
		14.76	0.04	17.8	0.3	136	1.8	< 1.1	780	80						
Optical		13.9	0.2	20.8	1.5											
326.1	16	15 53 57.11	0.02	20 13 00.0	0.9	–	< 1.0	< 3.0	570	60	6.6	720	70	–	–	–
		57.57	0.04	12 58.9	1.5	–	< 1.0	< 3.0	130	30						
Optical		(56.83	0.10	51.7	1.5)											
330	32	16 09 09.42	0.03	66 04 08.5	0.2	70	3.3	< 1.0	540	50	56	2180	150	0.549	2400	410
		18.37	0.03	37.1	0.2	–	1.1	< 1.0	1650	160						
Optical		13.9	0.2	22.3	1.5											
		14.1	0.2	29.8	1.5											
		(16.0	0.2	42.8	1.5)											
334	32	16 18 05.75	0.02	17 43 47.2	1.0	–	3.6	5.0	310	30	48	720	70	0.555	2400	350
		07.28	0.01	30.0	0.7	–	< 1.0	< 4.0	170	20						
		08.2	–	20	–	–	14	–	200	30						
Optical		07.28	0.05	30.1	0.7											
337	32	16 27 16.41	0.03	44 25 44.0	0.4	–	< 1.0	< 1.5	160	20	43	1060	100	–	–	–
		20.35	0.02	34.2	0.3	–	1.3	< 1.5	640	60						
Optical		(18.96	0.14	54.1	1.5)											
338*	16	16 26 55.33	0.02	39 39 36.4	0.3	–	< 1.0	< 1.5	150	20	41	400	100	0.0303	180	34
Optical		55.5	0.2	37	2											
340	32	16 27 27.84	0.02	23 26 41.4	0.8	–	< 1.2	< 3.0	150	15	47	800	80	–	–	–
		30.79	0.03	43.7	1.0	–	3.4	< 3.0	190	40						
		31.09	0.02	44.1	0.8	–	< 1.2	< 3.0	150	15						
Optical		30.26	0.05	45.4	0.7											
341	32	16 26 00.61	0.03	27 47 55.3	0.9	58	3.4	2.2	210	30	70	530	50	–	–	–
		04.6	–	48 42	–	36	11.5	2.6	190	40						
Optical		02.48	0.11	48 15.0	1.5											
349	32	16 58 02.00	0.04	47 07 51.7	0.5	142	10.0	2.9	360	50	82	1300	100	0.205	1100	350
		04.37	0.04	20.0	0.5	–	< 2.0	< 2.0	25	5						
		06.71	0.02	06 44.3	0.3	–	1.6	1.7	400	40						
Optical		(03.35	0.15	07 10.0	1.5)											
		(03.77	0.15	23.0	1.5)											
		04.44	0.07	20.3	0.7											
352	16	17 09 17.83	0.03	46 05 10.4	0.4	–	< 1.5	< 2.5	330	30	10	570	60	–	–	–
		18.09	0.05	00.6	0.7	–	< 1.5	< 2.5	180	20						
Optical		(17.60	0.08	10.4	0.8)											
356	32	17 23 05.44	0.03	51 00 59.8	0.4	–	< 1.0	1.9	140	15	75	350	50	–	–	–
		07.83	0.03	50 59 51.8	0.4	–	1.6	< 1.5	210	20						
Optical		(05.79	0.07	51 00 50.0	0.7)											
		(07.17	0.07	51 00 03.1	0.7)											
368	16	18 02 45.55	0.02	11 01 09.6	1.5	–	< 1	< 6	110	10	9	210	30	–	–	–
		45.72	0.02	17.9	1.5	–	< 1	< 5	100	10						
380*	16	18 28 13.473	0.007	48 42 40.46	0.13	–	< 0.7	< 1.0	5100	500	∿ 5	6200	300	0.691	2800	∿ 40
Optical		13.56	0.07	40.0	0.7											

Table 1 – *continued*

Source 3C/4C	N	RA h m s	± s	dec ° ′ ″	± ″	Component pa °	ω₁ ″	ω₂ ″	Flux density mJy	±	θ ″	Integrated flux density mJy	±	z	Distance Mpc	Total size kpc
386*	16	– – –	–	– – –	–	–	–	–	–	–	250	–	–	0.0177	100	120
Optical		18 36 12.87	0.10	17 09 06.9	1.5											
401	16	19 39 38.08	0.05	60 34 23.0	0.5	–	4.4	2.6	450	90	19	1700	100	0.201	1100	80
		38.40	0.02	26.8	0.2	48	2.9	1.5	570	100						
		38.84	0.05	32.6	0.5	–	< 2.0	< 2.0	40	10						
		39.18	0.05	39.9	0.5	22	3.9	2.5	850	150						
Optical		(37.29	0.09	41.1	0.7)											
		38.97	0.09	32.9	0.7											
432	16	21 20 25.19	0.02	16 51 48.2	1.0	–	< 1.0	< 3.0	200	20	13	440	50	1.805	4800	110
		25.89	0.02	40.1	1.0	–	1.2	4.0	160	15						
Optical		(24.87	0.05	45.3	0.7)											
		25.53	0.05	46.4	0.7											
438	16	21 53 44.86	0.03	37 46 19.1	0.7	129	4.5	2	880	100	19	1760	100	–	–	–
		46.07	0.02	07.1	0.4	–	2.2	3.2	950	100						
Optical		(44.95	0.06	05.7	0.7)											
		45.51	0.13	12.8	1.5											
442A*	16	– – –	–	– – –	–	–	–	–	–	–	270	–	–	0.0262	150	200
Optical		22 12 18.58	0.10	13 35 50.0	1.5											
		20.49	0.10	29.9	1.5											
		22.33	0.07	04.0	1.0											
449*	16	22 29 07.60	0.03	39 06 03.4	0.6	–	< 1.0	< 1.5	50	10	300	–	–	0.0181	110	150
Optical		07.68	0.13	04.6	1.5											
		(08.44	0.09	40.1	1.0)											
454*	16	22 49 07.697	0.005	18 32 43.5	0.2	–	< 0.4	< 1.3	930	50	–	930	50	1.757	4800	< 11
Optical		07.74	0.09	43.9	1.2											
455	16	22 52 34.38	0.02	12 57 31.8	1.4	–	< 1.3	< 5.4	630	60	3.2	840	50	0.543	2300	23
		34.56	0.02	33.5	1.4	–	< 1.0	< 4.0	300	30						
Optical		34.58	0.05	34.1	0.7											
468.1	16	23 48 27.34	0.05	64 23 37.8	0.3	55	2.4	< 1.1	1020	50	–	1020	50	–	–	–
Optical		(27.7	0.2	34.4	1.5)											
05.34*	16	08 05 19.22	0.01	04 41 36	8	–	< 1	–	340	40	–	340	40	2.877	5900	–
Optical		19.17	0.06	20.0	0.9											
19.31	16	08 36 14.95	0.03	19 32 24.6	1.5	–	< 1.0	< 4.0	100	20	18	260	40	1.691	4700	150
		15.28	0.03	36.8	1.5	–	< 1.0	< 4.0	110	20						
Optical		15.00	0.05	24.6	0.7											
13.39*	16	08 43 01.19	0.03	13 39 56.6	2.0	–	< 2.0	< 9.0	200	30	–	200	30	1.875	4900	< 74
Optical		01.27	0.05	57.8	0.7											
11.32	16	09 26 01.01	0.02	11 47 29.6	1.5	–	< 1.0	< 5.0	40	6	6.6	190	20	1.754	4800	55
		01.29	0.02	35.1	1.5	–	< 1.0	6.5	140	15						
Optical		01.06	0.05	32.4	0.7											
12.39*	16	11 16 20.78	0.01	12 51 06.2	0.5	–	< 0.5	< 2.5	1400	60	–	1400	60	2.118	5200	< 20
Optical		20.78	0.05	06.3	0.7											

1977MmRAS..84...61J

Table 1 – *continued*

Source 4C	*N*	RA h m s	± s	dec ° ′ ″	± ″	Component pa °	ω_1 ″	ω_2 ″	Flux density mJy	±	θ ″	Integrated flux density mJy	±	*z*	Distance Mpc	Total size kpc
53.24	16	12 13 00.80	0.02	53 52 47.0	0.2	-	< 1.0	2.0	490	50	33	950	100	-	-	-
		02.69	0.02	18.3	0.2	-	< 1.0	< 1.5	440	50						
Optical		01.49	0.08	35.9	0.7											
		(02.86	0.17	51.8	1.5)											
12.46*	16	13 07 04.34	0.01	12 10 21.5	0.5	-	< 0.5	< 2.5	1200	100	-	1200	100	-	-	-
Optical		04.27	0.05	22.0	0.7											
11.45	16	13 18 49.54	0.01	11 22 29.2	1.0	-	< 1.0	< 6.0	780	80	6.8	880	90	2.171	5300	54
		49.76	0.03	34.4	2.5	-	< 2.0	<10.0	100	30						
Optical		49.68	0.05	31.4	0.7											

Notes to Table 1:

3C 35. Low-resolution maps of this source at 408 MHz and 1.4 GHz are shown in Mackay (1969); there is no unresolved structure brighter than 10 mJy at 5 GHz in the region of the north component or in the region of the associated galaxy. The first optical object is a 14.5 mag galaxy with a redshift of 0.0677 and the second is a 17 mag neutral stellar object.

3C 43. The source is identified with a QSO of 20 mag on the PSS print; this QSO is optically variable (Sandage 1966).

3C 49. The source is identified with a 22 mag object, probably a galaxy (KSK, LG).

3C 76.1. There is no unresolved structure brighter than 10 mJy. The first optical object is a 15 mag DE3 galaxy of redshift 0.0328; the second is a 15.5 mag neutral stellar object. A low-resolution map at 1.4 GHz is shown in MKN.

3C 190. The source is identified with a 20 mag object.

3C 191. The source is identified with an 18 mag quasar.

3C 216. The angular size was derived from the visibility function on the assumption that the source is double; the derived pa is 62°. The source is identified with an 18 mag quasar.

3C 241. This source is not identified.

3C 243. Due to the low declination of this source no information can be obtained about its angular size in dec, nor can an accurate determination of its position in dec be made; the dec quoted is due to Wills & Bolton (1969). The source is identified with an 18.3 mag quasar; it is not in the revised 3C catalogue and is also called 4C 06.40.

3C 264. The structure of this large source has been discussed by Northover (1976); only the compact central radio component has been listed in the Table. The optical objects listed are (a) 14 mag elliptical galaxy and (b) 12.7 mag elliptical galaxy NGC 3862 with a redshift of 0.0206.

3C 282. The angular size was derived from the visibility function on the assumption that the source is double; the derived pa is 120°. The optical position in the Table is that of the 20 mag galaxy suggested as an identification by Wills (1967); it seems unlikely that this is related to the source. This source is not in the revised 3C catalogue; it is also known as 4C 65.14.

3C 285. A low-resolution map of this source at 1.4 GHz is shown in MKN. There is no unresolved structure at 5 GHz brighter than 10 mJy. The optical object is a 16 mag galaxy.

3C 303.1. The first optical position, which is in good agreement with the radio position, is that of a 19 mag red object; the second optical position is that of an 18 mag galaxy previously suggested as an identification by Wyndham.

3C 310. The first three optical objects lie in a common envelope; they are (a) a 16 mag galaxy, (b) a 15 mag galaxy (galaxy 1 of Griffin (1963)) which has a redshift of 0.053 and is coincident with the compact central radio component and (c) a 15 mag galaxy (galaxy 2 of Griffin). The fourth object is also a 15 mag galaxy. There is no unresolved structure other than the central component brighter than 20 mJy. A low-resolution map at 1.4 GHz is shown in Mackay (1969).

3C 314.1. There is no unresolved structure brighter than 10 mJy. The first optical object is an 18 mag red object, the second is a 17 mag galaxy. A low-resolution map at 1.4 GHz is shown in Mackay (1969).

3C 315. The structure of this large source has been discussed in detail by Northover (1976); only the compact central radio component has been listed in the Table. The optical objects listed are two 17 mag galaxies; the northern galaxy has a redshift of 0.1086.

3C 321. Observations were made with the Cambridge One-Mile telescope (Elsmore, Kenderdine & Ryle 1966) at 408 MHz. Four interferometer spacings were used in the synthesis and the response was a pencil beam with half-power beamwidths of 80 arcsec in RA and 200 arcsec in dec. The details of the components are listed below using the same notation as for Table 1.

RA h m s	± s	dec ° ′ ″	± ″	Component pa °	ω_1 ″	ω_2 ″	Flux density mJy	±
15 29 25.9	0.5	24 16 00	20	130	180	<100	2000	200
15 29 40.7	0.5	24 12 50	20	–	<40	<100	6500	600

3C 338. The optical position is the centre of the 12.6 mag cD galaxy NGC 6166, measured on the PSS print; this galaxy has four nuclei which cannot be distinguished on the PSS prints, but whose positions are given by Griffin (1963). The compact central radio component is coincident with nucleus 1 of Griffin; there is no other unresolved structure brighter than 15 mJy. A low-resolution map of this source is shown in MKN.

3C 380. The visibility function indicates that about 18 per cent of the flux originates in low-brightness structure on a scale of a few arcsec. The associated object is a 17 mag quasar.

3C 386. There is no unresolved structure brighter than 20 mJy. The associated object is a 12 mag galaxy. A low-resolution map at 1.4 GHz is shown in Mackay (1969).

3C 442A. There is no unresolved structure brighter than 10 mJy within a region of radius 135 arcsec centred on the associated galaxies. The optical objects are (a) 13.8 mag galaxy NGC 7236 with redshift 0.0262, (b) 14.5 mag galaxy NGC 7237 and (c) 16.5 mag galaxy. A low-resolution map at 408 MHz is shown in Mackay (1969).

3C 449. Thre is no other unresolved structure brighter than 10 mJy. The optical objects are (a) 12.5 mag galaxy with redshift 0.0181 and (b) 15 mag galaxy. Low-resolution maps at 408 and 1407 MHz are shown in Mackay (1969).

3C 454. The source is identified with an 18.4 mag quasar.

4C 05.34. Due to the low declination of this source, no information can be obtained about its angular size in dec, nor can an accurate determination of its position in dec be made; the dec quoted is due to Wills & Bolton (1969). The source is identified with an 18 mag quasar.

4C 13.39. This source is identified with a 17.5 mag quasar.

4C 12.39. This source is identified with a 19.2 mag quasar.

4C 12.46. This source is identified with a 19 mag blue object with a featureless spectrum.

the angular scale being shown by a horizontal bar and the half-power beam shape by a shaded ellipse. The contour interval for each source is indicated by the number beside the letters CI; this is the flux density in mJy of an unresolved source which would produce a change of one contour. The brightness temperature (K) corresponding to one contour on a map having a resolution 2 × 2 cosec δ arcsec is found by multiplying this number by 25 sin δ. For several of the very intense compact components the contours above a certain level have been omitted but the peak level is indicated. The positions of the optical objects in the fields of the sources are shown by crosses, the extent of each cross indicating the uncertainty in position. In most cases these are the positions measured from the PSS prints using the method described in Section 4, but when the object is too faint to be seen on the

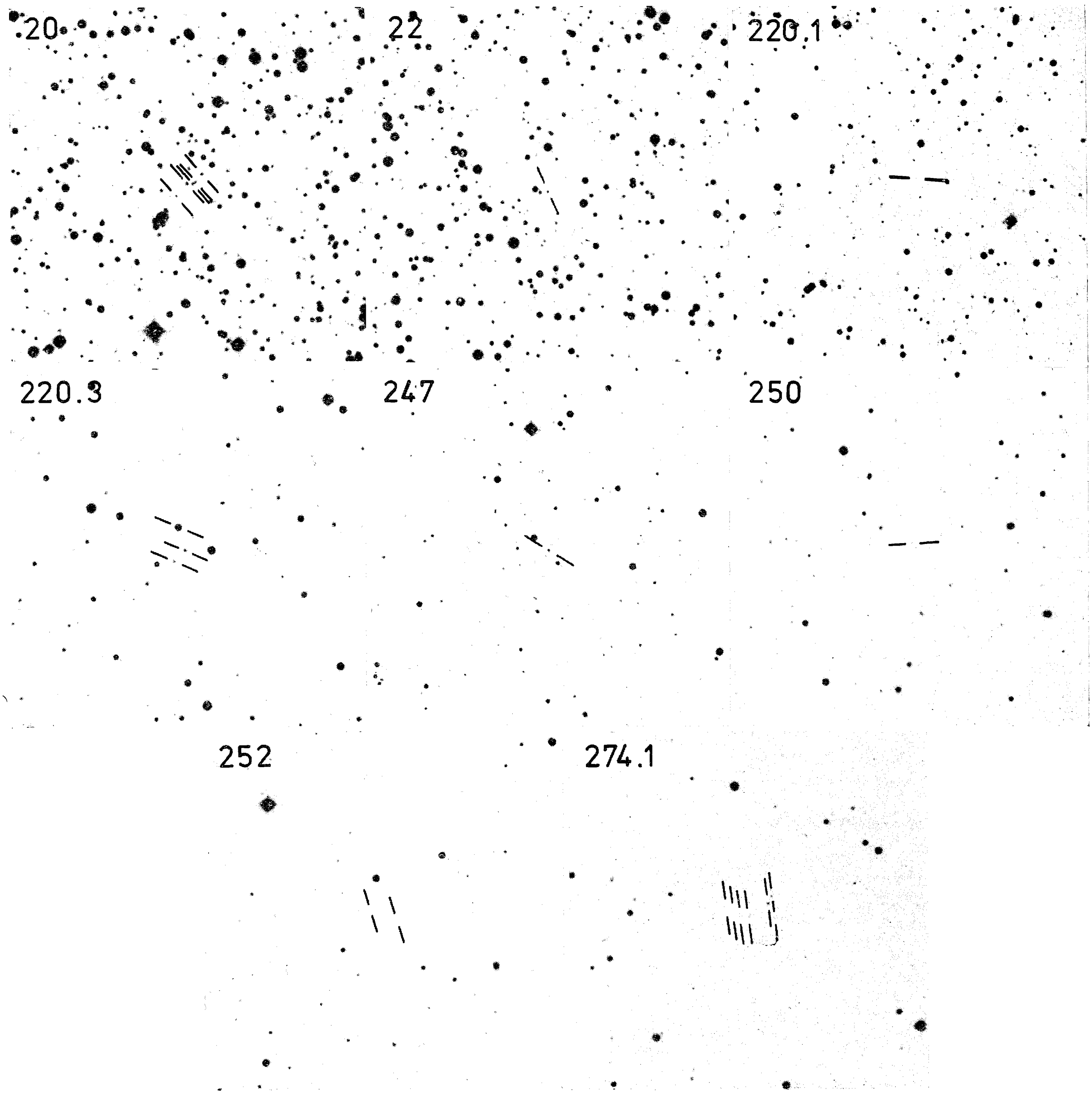

Plates 1 and 2. Finding charts taken from the red prints of the Sky Survey; the fields are approximately 8.5 × 8.5 arcmin. North is to the top and east to the left. (© 1957 National Geographic Society – Palomar Observatory Sky Survey.)

[*facing page* 96]

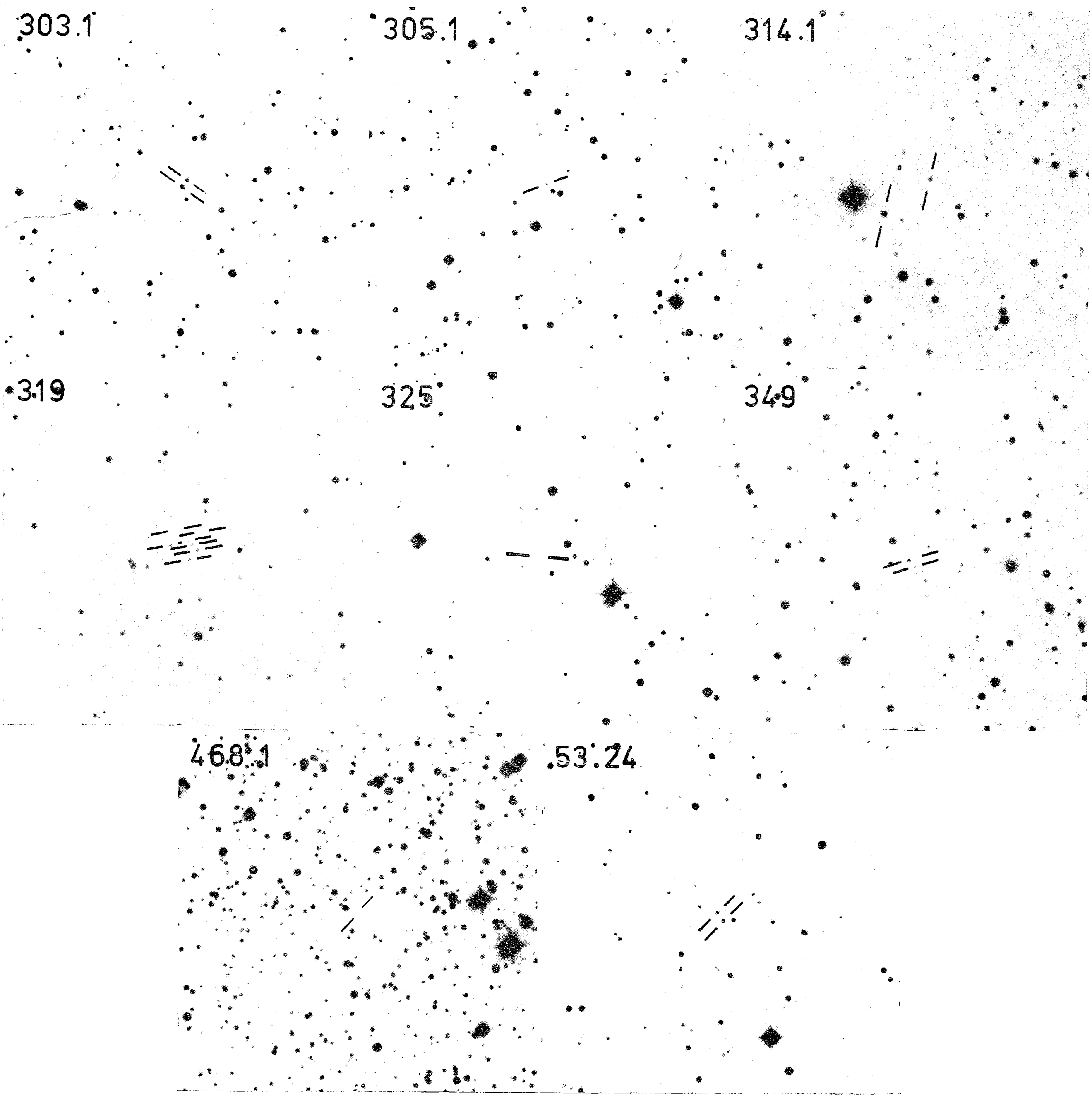
303.1
305.1
314.1
319
325
349
468.1
53.24

Sky Survey prints the position given by Kristian, Sandage & Katem (1974, hereafter KSK) is used, or the 200-in plates of Longair & Gunn (1975, hereafter LG) were measured directly as described in Section 4.

For several sources, maps at a resolution of 2 × 2 cosec δ arcsec are only given for the regions of highest brightness. In each case a lower resolution map has also been included to show the structure of low brightness and to indicate the areas covered by the detailed maps. Maps are not presented for several sources of large extent in which the only compact structure observed was the central component, or in which there is no compact structure, or for sources of small angular size which are unresolved or only very slightly resolved in the present observations. There are notes on all these sources following Table 1. Further details of the remaining sources are given in the figure captions. References to the original identification, magnitude or redshift are not necessarily given but may be found in Smith, Spinrad & Smith (1976). The magnitudes quoted here are either V magnitudes from that compilation, or rough estimates from the prints of the Sky Survey.

The data for each source are presented in Table 1 and, in general, only the details of the more compact regions are quoted. The details of the more extensive regions may be obtained from the maps, and their flux densities by subtraction of the flux densities of the high brightness regions from the integrated flux densities.

The details in Table 1 are as follows:

(1) Source number from the 3C or 4C catalogues; an asterisk indicates that there are notes following Table 1.
(2) The number of spacings, N, used in the synthesis (see Section 2).
(3), (4) 1950.0 coordinates of the peaks of emission, with estimated errors; no error is quoted if the component has no well-defined peak. The figures preceded by the word 'optical' and all subsequent figures are coordinates of the optical objects measured as described in Section 4; those in brackets are unlikely to be related to the radio source.
(5) The position angle of the major axis of the component, if well defined.
(6), (7) The angular extents of each component parallel and perpendicular to its major axis; if no position angle is given in (5), the quoted angular sizes are in RA and dec. When the component is barely resolved, a Gaussian brightness distribution is assumed in estimating its angular extent. For more complex components the quoted sizes are only approximate.
(8) The flux density of each component at 5 GHz with the estimated error.
(9) The overall angular extent of the source. This is usually the separation of the outermost peaks of a multiple source.
(10) The integrated flux density of the source at 5 GHz with estimated error. This is the maximum amplitude on the smallest interferometer spacing used in the observations. For 3C sources the values measured in this way agree well with those given by Kellermann, Pauliny-Toth & Williams (1969).
(11) Redshift of the associated object.
(12) Distance derived from the redshift given in column 11; an Einstein–de Sitter model has been used, assuming H_0 = 50 km/(s Mpc), Ω = 1 and q_0 = 0.5.
(13) Total linear size of the source if the angular size is that given in column 9.

4 Optical measurements

The positions of the optical objects in the fields of all the sources have been measured on the PSS prints with reference to stars in the Smithsonian Catalogue. An x–y measuring machine, a Coradograph, at the Institute of Astronomy, Cambridge, was used and the data were analysed by means of a programme due to A. N. Argue. An attempt has been made to measure the positions of all objects within the area of each map although in some cases where the source is of very large angular extent or the identification is well confirmed this has not been done. In the cases of 3C 42 and 3C 55 the suggested identifications due to LG have been measured directly from the 200-in. plates relative to secondary reference stars measured on the PSS prints. Where necessary, finding charts for the measured objects are shown in Plates 1 and 2. Finding charts for the other 3C sources may be found in Griffin (1963), Wyndham (1966) and references therein, LG and KSK. Finding charts for the 4C sources are in Wills & Bolton (1969) and references therein.

5 The complete sample

A complete sample of 3CR sources has now been observed with the 5-km telescope at 5 GHz. The sample was selected according to the following criteria:

(a) The flux density of each individual source at 178 MHz is greater than or equal to 10 Jy according to the compilation given by Kellermann *et al.* (1969).

(b) $\delta \geqslant 10°$.

(c) $|b| \geqslant 10°$.

There are 166 sources in this sample of which one, 3C 326, was not observed as it was originally thought to be galactic. Since it now seems likely to be extragalactic we have included it in the sample.

Table 2.

3C	S_{178}	Ref	3C	S_{178}	Ref	3C	S_{178}	Ref
6.1	17.3	PH	207	13.6	PH	303.1	12.4	JPR
9	17.8	PH	208	18.5	JPR	305	15.7	PH
13	12.0	JPR	212	15.1	JPR	305.1	12.4	JPR
14	10.4	JPR	215	11.4	PH	309.1	22.7	ER
16	11.2	JPR	216	20.2	JPR	310	56.0	JPR
19	12.1	JPR	217	11.3	JPR	314.1	10.6	JPR
20	42.9	JPR	219	41.2	T2	315	18.9	N
22	12.1	JPR	220.1	15.8	JPR	318	12.3	ER
28	16.3	RP	220.3	15.7	JPR	319	15.3	JPR
31	16.8	JPR	223	14.7	RP	321	13.5	JPR
33	54.4	HM	225B	20.0	JPR	322	10.1	JPR
33.1	13.0	JPR	226	15.0	JPR	324	15.8	JPR
34	11.9	JPR	228	21.8	JPR	325	15.6	JPR
35	10.5	JPR	231	14.6	H	326	12.1	-
41	10.6	L	234	31.4	RP	330	27.8	JPR
42	12.0	JPR	236	11.3	PH	334	10.9	JPR
43	11.6	JPR	239	13.2	PH	336	11.5	PH
46	10.2	JPR	241	11.6	JPR	337	11.8	JPR
47	26.4	PH	244.1	20.3	JPR	338	46.9	JPR
48	55.0	ER	245	14.4	JPR	340	10.1	JPR
49	10.3	JPR	247	16.8	JPR	341	10.8	JPR
55	22.7	JPR	249.1	12.5	PH	343	12.4	ER
61.1	31.2	HM	250	11.9	JPR	343.1	11.5	ER
65	15.2	L	252	11.0	JPR	345	10.8	ER
66B	30.0	N	254	19.9	PH	346	10.9	PH
67	10.0	PH	263	15.2	PH	349	13.3	JPR
68.1	12.8	JPR	263.1	18.2	JPR	351	13.7	RP
68.2	13.0	PH	264	26.0	N	352	11.3	JPR
76.1	12.2	JPR	265	19.5	JPR	356	11.3	JPR
79	30.5	RP	266	11.1	JPR	368	13.8	JPR
83.1B	26.0	RP	267	14.6	JPR	380	59.4	JPR
84	62.6	ER	268.1	21.4	JPR	381	16.6	RP
98	47.2	JPR	268.3	10.7	PH	382	19.9	RB
109	21.6	RP	268.4	10.3	PH	386	23.9	JPR
123	189.0	PH	270.1	13.6	JPR	388	24.6	PH
132	13.7	JPR	272	10.3	JPR	390.3	47.5	HM
133	22.3	JPR	272.1	19.5	JPR	401	20.9	JPR
138	22.2	ER	274	1050.0	T1	427.1	26.6	PH
147	60.5	ER	274.1	16.5	JPR	432	11.0	JPR
153	15.3	PH	275.1	18.3	JPR	433	56.2	PH
171	19.5	PH	277.2	12.0	JPR	436	17.8	RP
172	15.1	JS	277.3	12.4	PH	437	14.6	L
173.1	15.4	JPR	280	23.7	PH	438	44.7	JPR
175	17.6	JPR	280.1	11.9	JPR	441	12.6	L
175.1	11.4	JPR	284	11.4	RP	442A	17.0	JPR
181	14.5	PH	285	11.4	JPR	449	11.5	JPR
184	13.2	JPR	286	24.0	ER	452	54.4	RP
184.1	13.0	RP	287	16.0	ER	454	11.6	JPR
186	14.1	RP	288	18.9	PH	454.3	13.0	ER
190	15.0	JPR	289	12.0	JPR	455	12.8	JPR
191	13.0	JPR	293	12.7	JPR	460	10.3	PH
192	21.0	JPR	294	10.3	JPR	465	37.8	RB
196	68.2	PH	295	83.5	PH	469.1	12.4	L
200	14.0	JPR	299	11.8	RP	470	10.1	RP
204	10.5	PH	300	17.9	RP			
205	12.6	PH	303	11.2	PH			

The sample is listed in Table 2 whose details are as follows:

(1) Source number from the 3CR catalogue.
(2) Flux density at 178 MHz on the scale of Kellermann *et al.* (1969).
(3) Reference to the 5 GHz, 5-km telescope observations as follows:
ER Elsmore & Ryle 1976
H Hargrave 1974
HM Hargrave & McEllin 1975
JPR This paper
JS Jenkins & Scheuer 1976
L Longair 1975
N Northover 1973
PH Pooley & Henbest 1974
RB Riley & Branson 1973
RP Riley & Pooley 1976
T1 Turland 1975a
T2 Turland 1975b

Acknowledgments

We thank the many members of staff of the Observatory for their work in the operation of the telescope, and Mr A. N. Argue for the use of the $x-y$ measuring machine. We are grateful to Dr J. R. Shakeshaft for his work in keeping up-to-date bibliographies on all the 3C sources which has greatly facilitated this research. C.J.J. thanks the SRC for a research studentship.

References

Branson, N. J. B. A., Elsmore, B., Pooley, G. G. & Ryle, M., 1972. *Mon. Not. R. astr. Soc.*, **156**, 377.
Burch, S. F., 1977. *Mon. Not. R. astr. Soc.*, in press.
Elsmore, B. & Ryle, M., 1976. *Mon Not. R. astr. Soc.*, **174**, 411.
Elsmore, B., Kenderdine, S. & Ryle, M., 1966. *Mon. Not. R. astr. Soc.*, **134**, 87.
Griffin, R. F., 1963. *Astr. J.*, **68**, 421.
Hargrave, P. J., 1974. *Mon. Not. R. astr. Soc.*, **168**, 491.
Hargrave, P. J. & McEllin, M., *Mon. Not. R. astr. Soc.*, **173**, 37.
Harris, A., 1973. *Mon. Not. R. astr. Soc.*, **163**, 19P.
Jenkins, C. J. & Scheuer, P. A. G., 1976. *Mon. Not. R. astr. Soc.*, **174**, 327.
Kellermann, K. I., Pauliny-Toth, I. I. K. & Williams, P. J. S., 1969. *Astrophys. J.*, **157**, 1.
Kristian, J., Sandage, A. & Katem, B., 1974. *Astrophys.* J., **191**, 43.
Longair, M. S., 1975. *Mon. Not. R. astr. Soc.*, **173**, 309.
Longair, M. S. & Gunn, J. E., 1975. *Mon. Not. R. astr. Soc.*, **170**, 121.
Lynds, R. & Wills, D., 1972. *Astrophys. J.*, **172**, 531.
Macdonald, G. H., Kenderdine, S. & Neville, A. C., 1968. *Mon. Not. R. astr. Soc.*, **138**, 259.
Mackay, C. D., 1969. *Mon. Not. R. astr. Soc.*, **145**, 31.
Northover, K. J. E., 1973. *Mon. Not. R. astr. Soc.*, **165**, 369.
Northover, K. J. E., 1976. *Mon. Not. R. astr. Soc.*, **177**, 307.
Pooley, G. G. & Henbest, S. N., 1974. *Mon. Not. R. astr. Soc.*, **169**, 477.
Riley, J. M. & Branson, N. J. B. A., 1973. *Mon. Not. R. astr. Soc.*, **164**, 271.
Riley, J. M. & Pooley, G. G., 1976. *Mem. R. astr. Soc.*, **80**, 105.
Ryle, M., 1972. *Nature*, **239**, 435.
Sandage, A., 1966. *Astrophys. J.*, **144**, 1234.
Smith, H. E., Burbidge, E. M. & Spinrad, H., 1976. *Astrophys. J.*, **210**, 627.
Smith, H. E., Spinrad, H. & Smith, E. O., 1976. *Publ. astr. Soc. Pacific*, **88**, 621.
Turland, B. D., 1975a. *Mon. Not. R. astr. Soc.*, **170**, 281.
Turland, B. D., 1975b. *Mon. Not. R. astr. Soc.*, **172**, 181.
Wills, D., 1967. *Mon. Not. R. astr. Soc.*, **135**, 339.
Wills, D. & Bolton, J. G., 1969. *Aust. J. Phys.*, **22**, 775.
Wyndham, J. D., 1966. *Astrophys. J.*, **144**, 459.